Electronic Supplementary Material (ESI) for Chemical Science.

SUPPORTING INFORMATION

Controlling the Optical and Catalytic Properties of Photo-Active Artificial Metalloenzymes Using Chemogenetic Engineering

Yasmine S. Zubi[†], Bingqing Liu[†], Yifan Gu, Dipankar Sahoo, and Jared C. Lewis[*]

[†]These authors contributed equally to this study
*To whom correspondence should be addressed

Table of Contents

Supplemental Figures and Tables

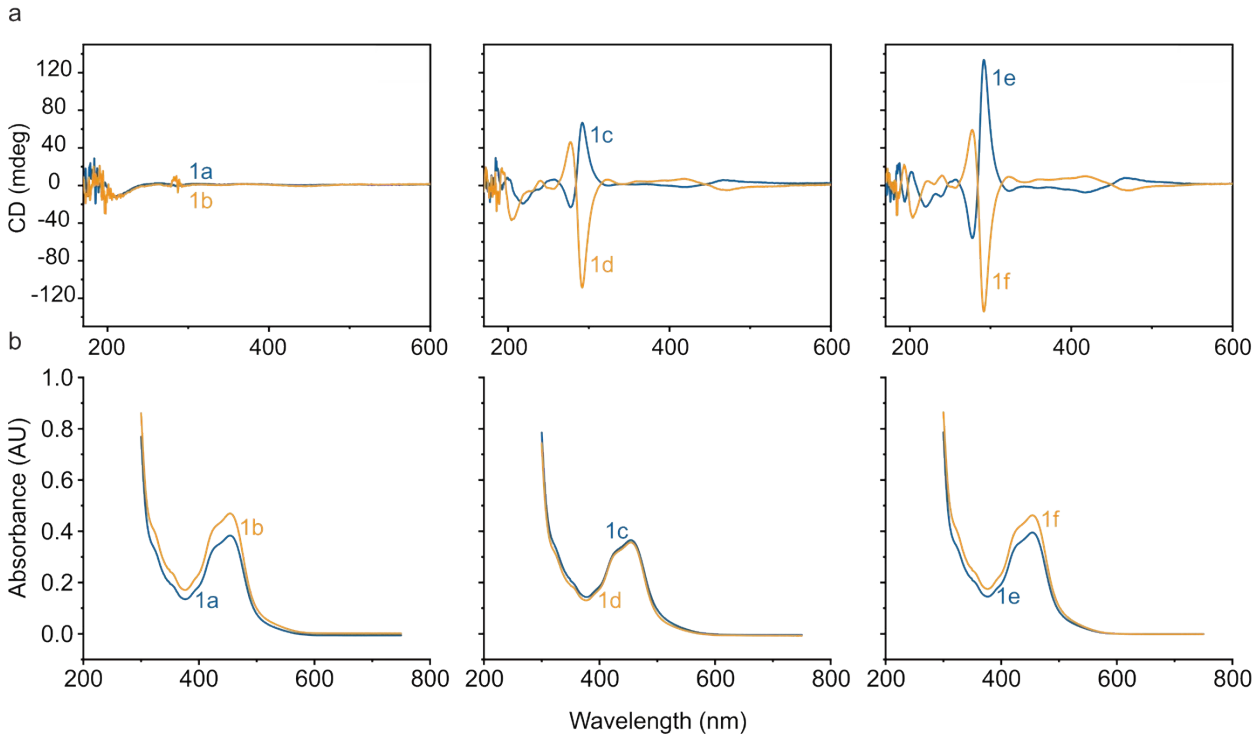

Supplementary Figure 1. Spectroscopic Characterization of Cofactors 1a-1f.
(a) CD of cofactors **1a-1f** (0.1 mg/mL) in ACN. **(b)** UV-Vis spectra of cofactors **1a-1f** (50 μM) in 5% ACN/MQ H_2O.

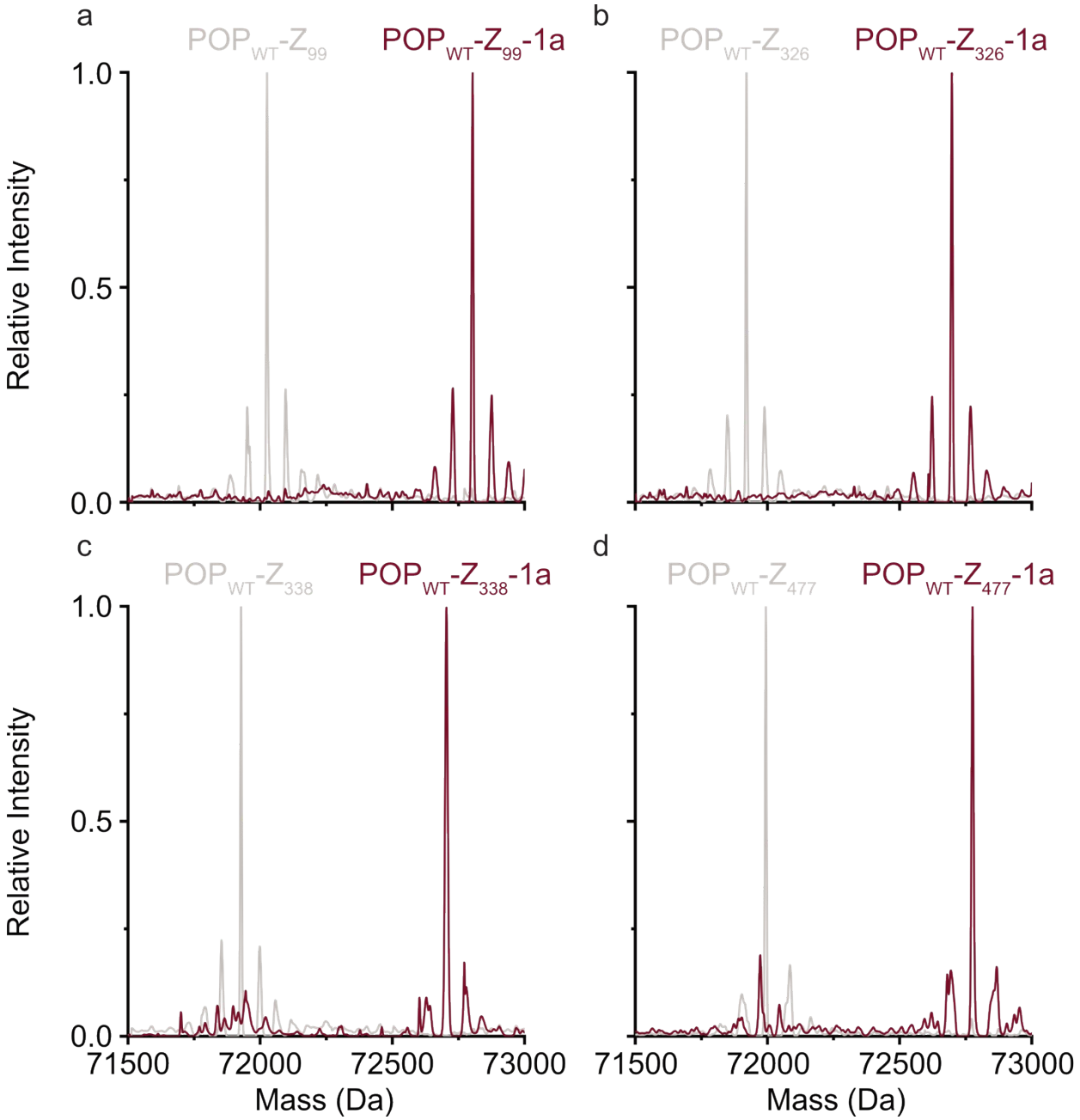

Supplementary Figure 2. Representative Protein MS showing Z Incorporation and Subsequent Bioconjugation with Cofactor 1a.

Azidophenylalanine (Z) was successfully incorporated into POP at residues **(a)** 99 (theoretical – 72,021 Da; observed – 72,026 Da), **(b)** 326 (theoretical – 71,915 Da; observed – 71,920 Da), **(c)** 338 (theoretical – 71,922 Da; observed – 71,928 Da), and **(d)** 477 (theoretical – 71,991 Da; observed – 71,994 Da). Subsequent bioconjugation with cofactor **3a** yielded the desired ArMs **(a)** POP$_{WT}$-Z$_{99}$ (theoretical – 72,797 Da; observed – 72,804 Da), **(b)** POP$_{WT}$-Z$_{326}$ (theoretical – 72,691 Da; observed – 72,697 Da), **(c)** POP$_{WT}$-Z$_{338}$ (theoretical – 72,698 Da; observed – 72,704 Da), and **(d)** POP$_{WT}$-Z$_{477}$ (theoretical – 72,767 Da; observed – 72,776 Da).

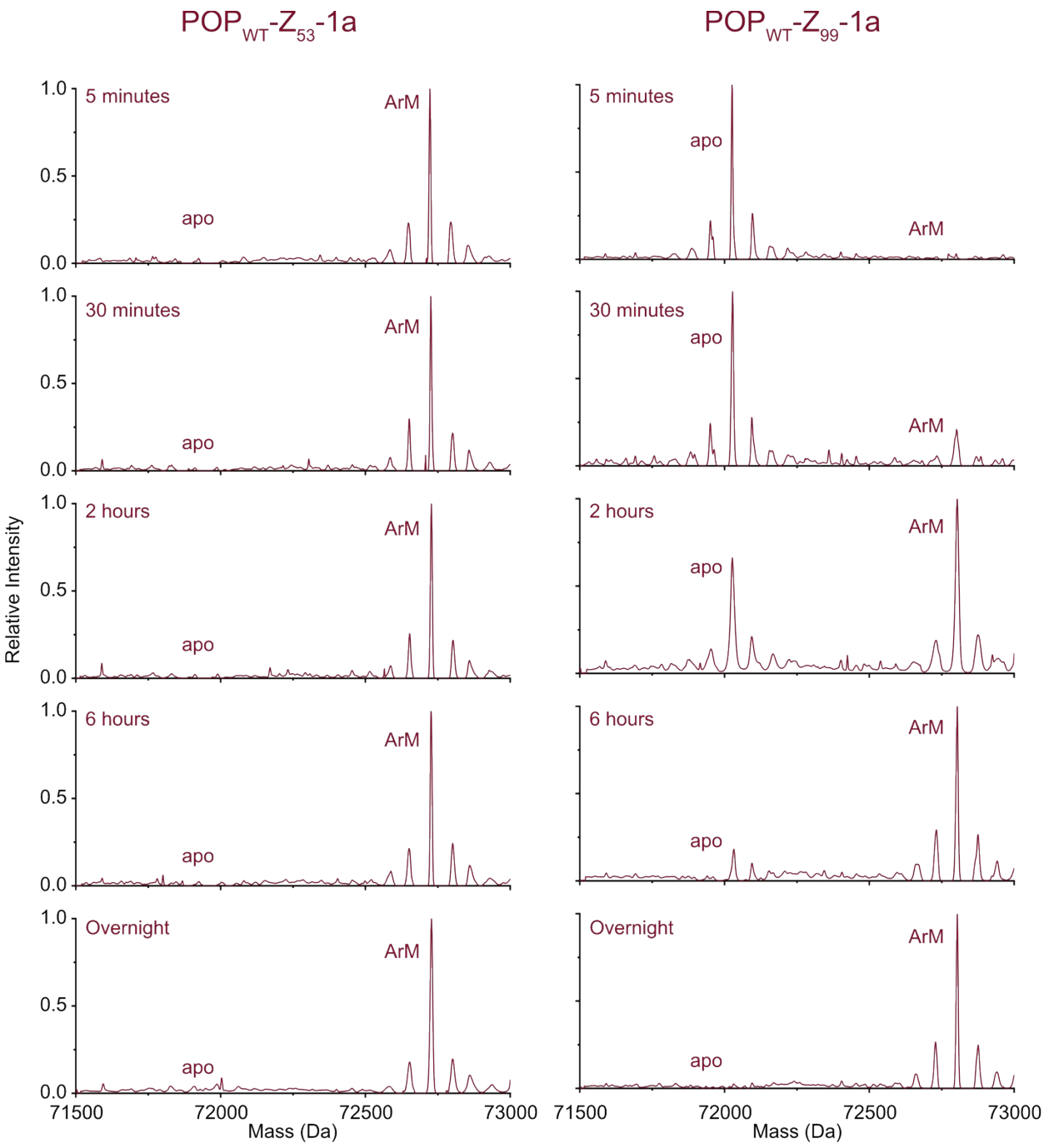
POP$_{WT}$-Z$_{53}$-1a
POP$_{WT}$-Z$_{99}$-1a
5 minutes
30 minutes
2 hours
6 hours
Overnight
ArM
apo
Relative Intensity
1.0
0.5
0.0
71500
72000
72500
73000
Mass (Da)

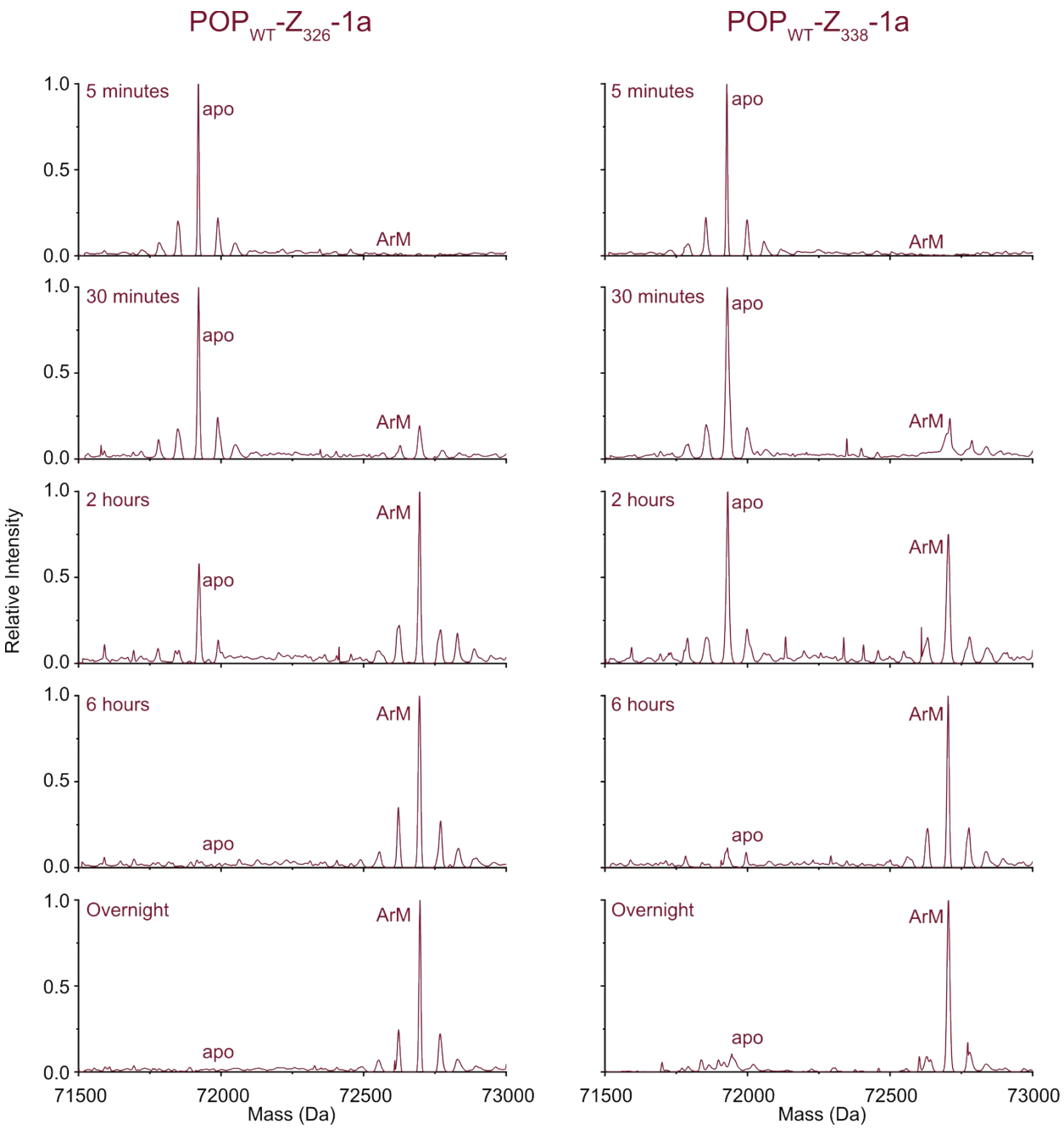
POP$_{WT}$-Z$_{326}$-1a
POP$_{WT}$-Z$_{338}$-1a
5 minutes
30 minutes
2 hours
6 hours
Overnight
apo
ArM
Relative Intensity
1.0
0.5
0.0
71500
72000
72500
73000
Mass (Da)

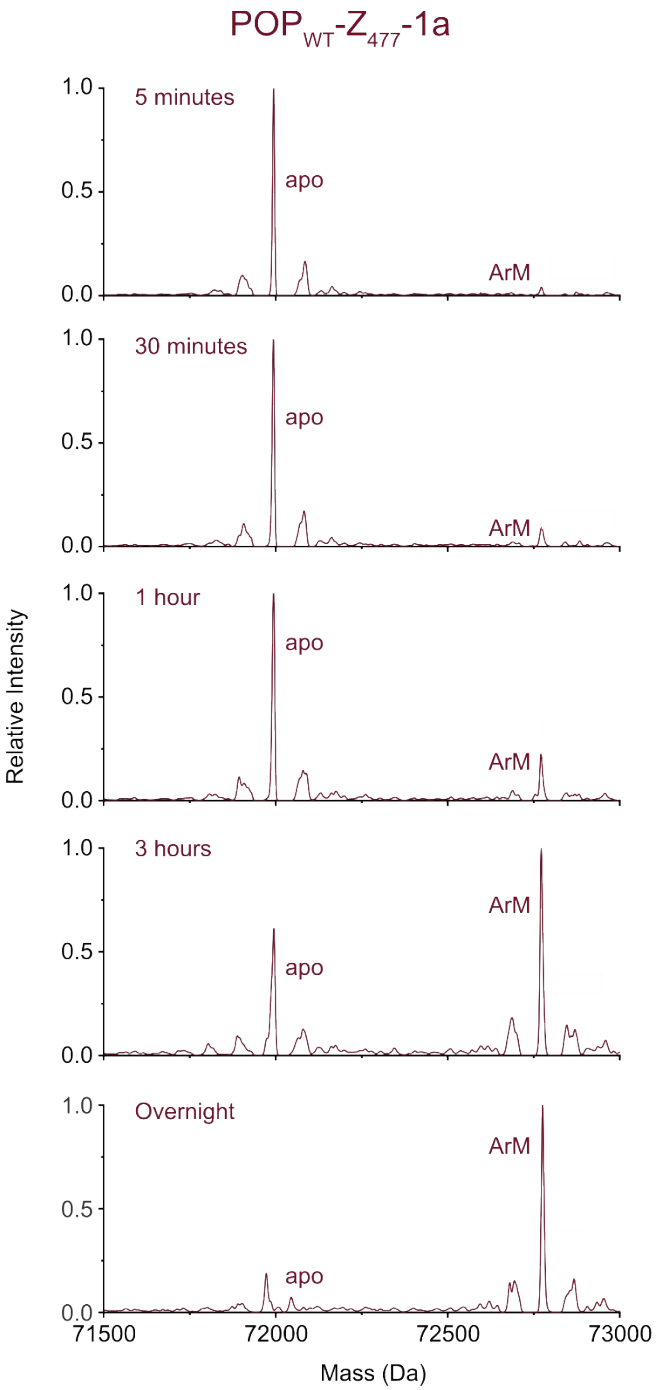

Supplementary Figure 3. Time-Course Protein MS Following Bioconjugation between Different Scaffolds and Cofactor 1a.

Intact protein MS was used to analyze samples during SPAAC reaction between different protein scaffolds (POP_{WT}-Z_{53}, POP_{WT}-Z_{99}, POP_{WT}-Z_{326}, POP_{WT}-Z_{338}, and POP_{WT}-Z_{477}) and an excess of cofactor **1a** (2.75 equivalents).

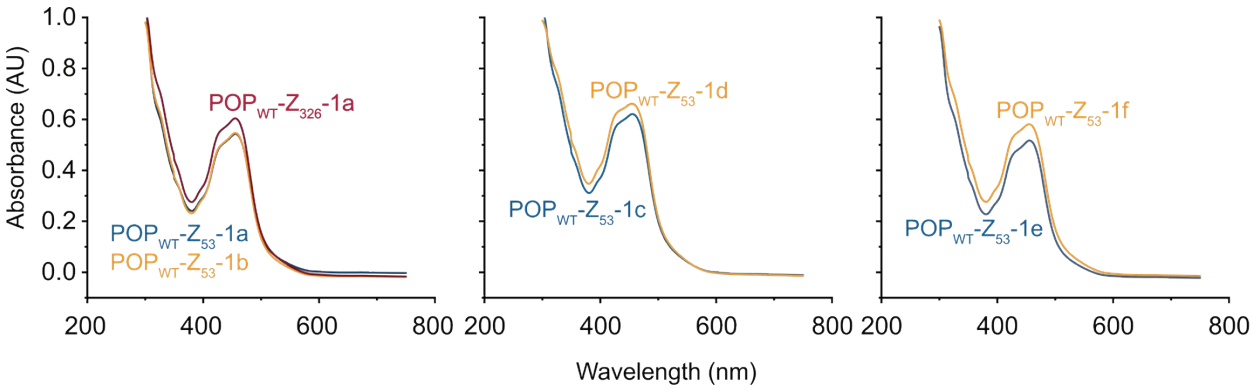

Supplementary Figure 4. UV-Vis Spectra of Representative ArMs.
UV-Vis spectra of POP$_{WT}$-Z$_{53}$-1a, POP$_{WT}$-Z$_{326}$-1a, POP$_{WT}$-Z$_{53}$-1b, POP$_{WT}$-Z$_{53}$-1c, POP$_{WT}$-Z$_{53}$-1d, POP$_{WT}$-Z$_{53}$-1e, and POP$_{WT}$-Z$_{53}$-1f (50 μM in MQ H_2O).

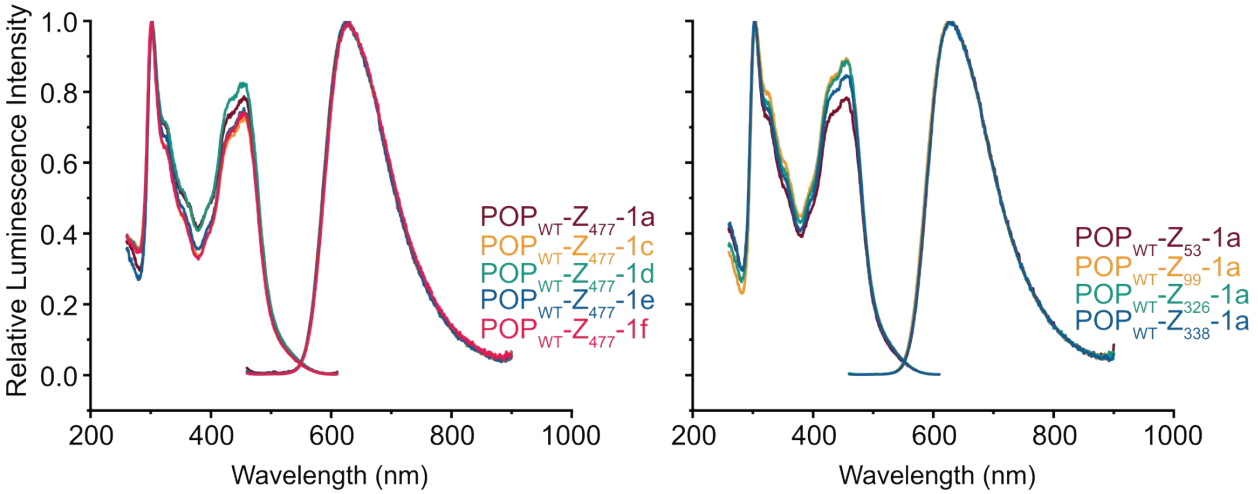

Supplementary Figure 5. Excitation and Emission Spectra of Representative ArMs. Excitation (λ_{em} = 620 nm) and emission (λ_{exc} = 450 nm) spectra of ArMs constructed with scaffold POP$_{WT}$-Z$_{477}$ and cofactors **1a-1f** (left) and with scaffolds POP$_{WT}$-Z$_{53}$, POP$_{WT}$-Z$_{99}$, POP$_{WT}$-Z$_{326}$, and POP$_{WT}$-Z$_{338}$ with cofactor **1a** (right). All samples were 50 μM ArM in MQ H_2O. Data is shown as relative luminescence intensity (normalized to 1.0).

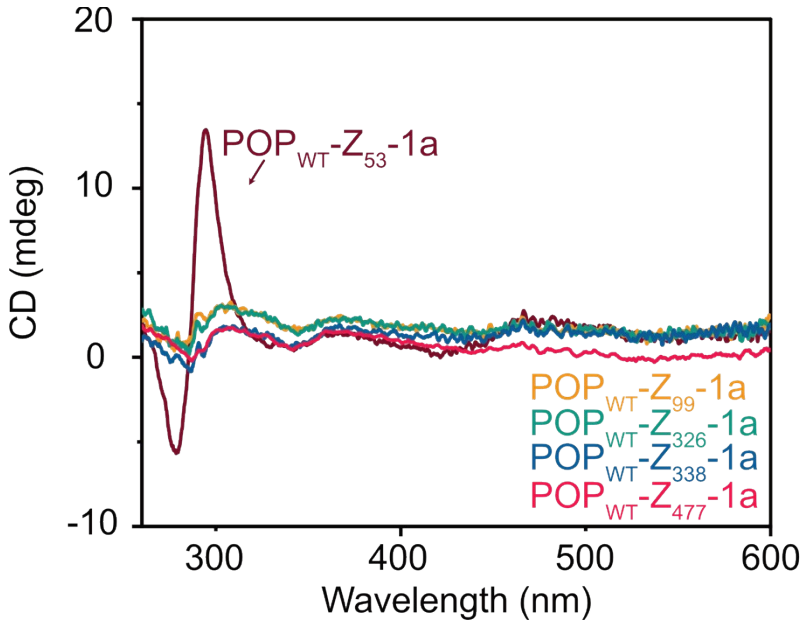

Supplementary Figure 6. CD Spectra of Representative ArMs.
CD spectra of POP$_{WT}$-Z$_{53}$-**1a**, POP$_{WT}$-Z$_{99}$-**1a**, POP$_{WT}$-Z$_{326}$-**1a**, POP$_{WT}$-Z$_{338}$-**1a**, and POP$_{WT}$-Z$_{477}$-**1a** (20 μM) in MQ H_2O. Only the ArM synthesized from scaffold POP$_{WT}$-Z$_{53}$ had significant signal around 300 nm, consistent with the π → π* intraligand transitions of the Ru(II) polypyridyl cofactor. This suggests preferential binding of the Λ isomer to POP$_{WT}$-Z$_{53}$, leading to enrichment of this ArM.

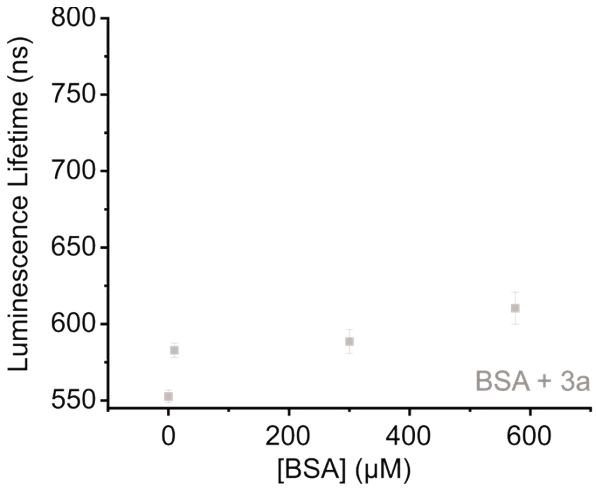

Supplementary Figure 7. Luminescence Lifetime of 3a vs. Increasing BSA Concentrations. Luminescence lifetime (λ_{exc} = 450 nm, λ_{em} = 620 nm) of cofactor **3a** (5 μM) with increasing concentrations of BSA in MQ H_2O. Plotted data points represent single measurements and error bars represent standard deviations resulting from single exponential tail fitting of decay data.

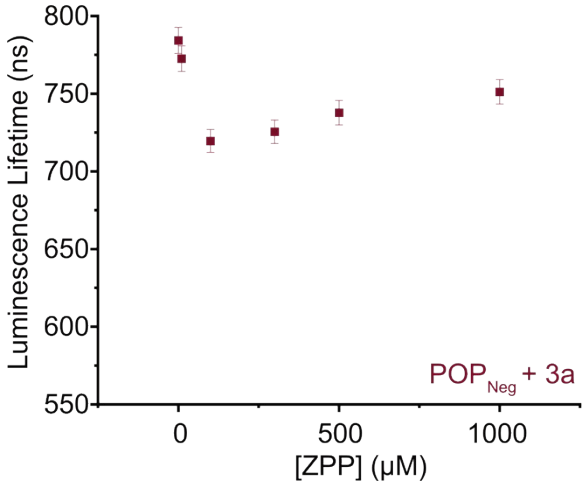

Supplementary Figure 8. Effects of ZPP on 3a Binding to POP_{Neg}.
Luminescence lifetime (λ_{exc} = 450 nm, λ_{em} = 620 nm) of cofactor **3a** (5 μM) preincubated with POP_{Neg} (300 μM) in response to increasing concentrations of the known covalent inhibitor, ZPP (0-1 mM) in 10% ACN/MQ H_2O. Plotted data points represent single measurements and error bars represent standard deviations resulting from single exponential tail fitting of decay data.

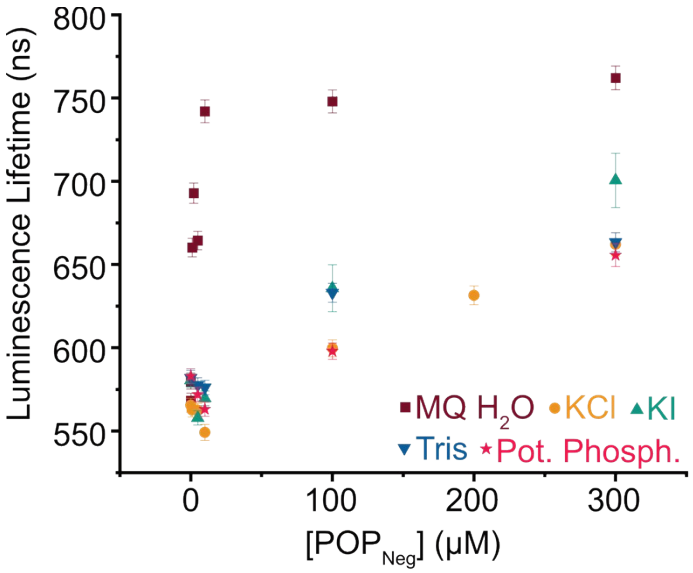

Supplementary Figure 9. Effects of Solvent on 3a Binding to POP$_{Neg}$.
Luminescence lifetime (λ_{exc} = 450 nm, λ_{em} = 620 nm) of cofactor **3a** (5 μM) with increasing concentrations of POP$_{Neg}$ (0-300 μM) in MQ H_2O, 50 mM KCl, 50 mM KI, 50 mM Tris (pH 7.4), or 50 mM potassium phosphate (pH 7.4). Plotted data points represent single measurements and error bars represent standard deviations resulting from single exponential tail fitting of decay data.

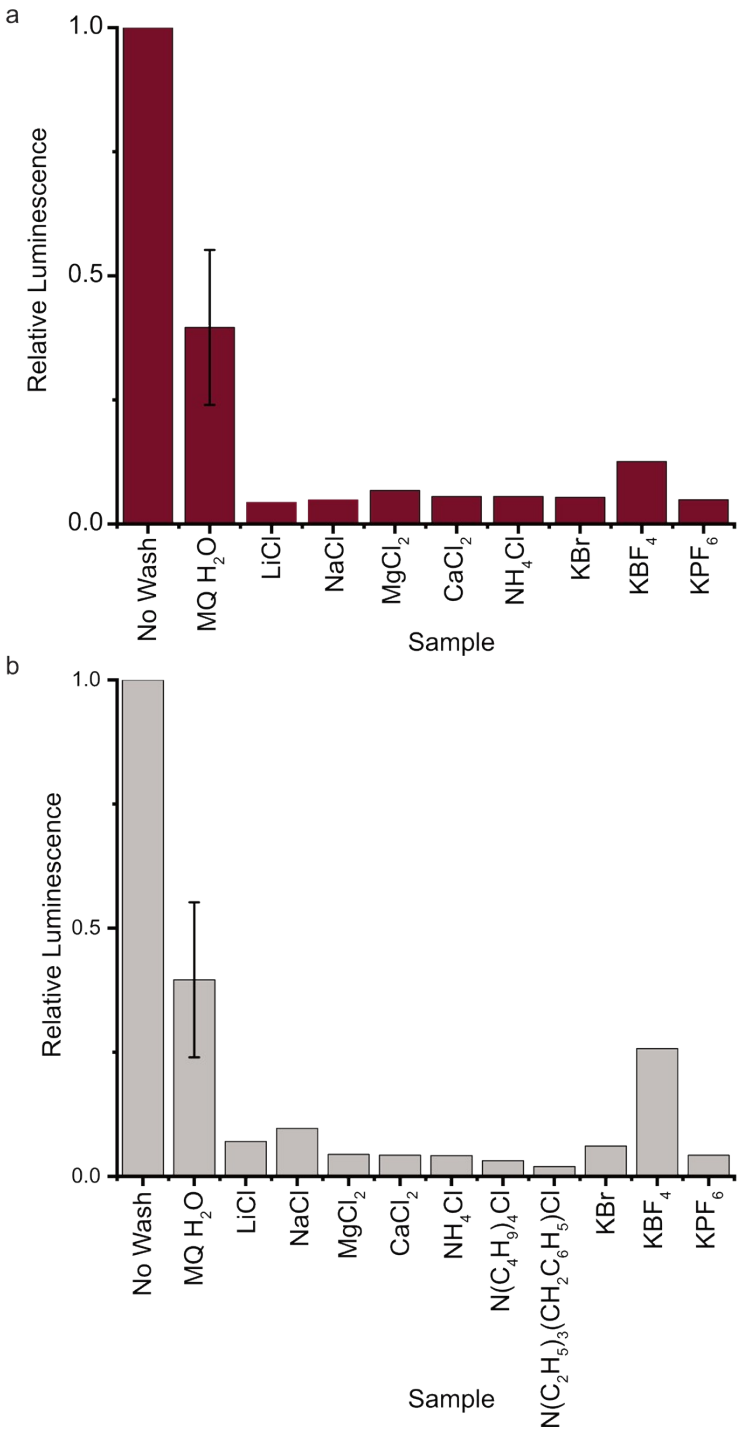

Supplementary Figure 10. Effects of Different Salts on 3a Binding to POP_{Neg}.
POP_{Neg} (95 µM) and cofactor **3a** (5 µM) were preincubated at room temperature in 400 µL of MQ H_2O. 10 mL of either **(a)** MQ H_2O/50 mM salt solution or **(b)** MQ H_2O/10 mM salt solution was added to the sample, and then concentrated to 1 mL in a 30 kDa MWCO spin filter. Luminescence intensity (λ_{exc} = 450 nm, λ_{em} = 620 nm) was measured to determine relative retention of cofactor after washing with water/salt solution and compared to samples that were not subjected to dilution/concentration. Bars represent single measurements, except for MQ H_2O sample, which was performed in triplicate (n=3) and error bars represent standard deviations.

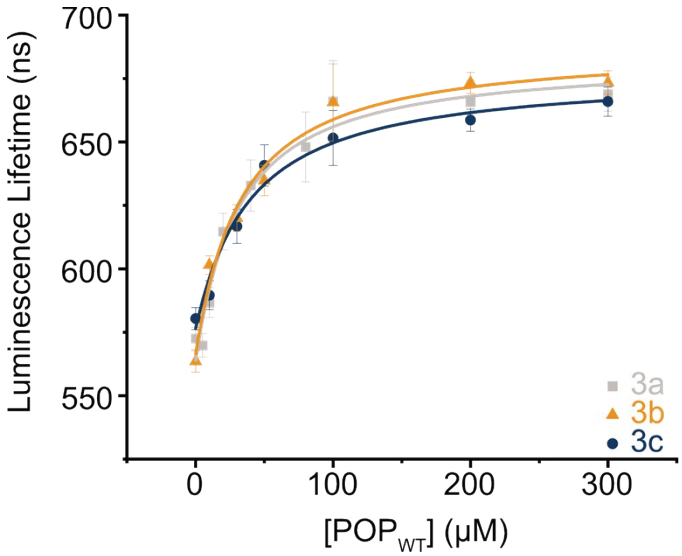

Supplementary Figure 11. Effects of Ru(Bpy)$_3^{2+}$ Chirality on Binding to POP$_{WT}$.
Luminescence lifetime (λ_{exc} = 450 nm, λ_{em} = 620 nm) of cofactor **3a**/**3b**/**3c** (5 μM) preincubated with increasing concentrations of POP$_{WT}$ (0-300 μM) in MQ H_2O. 0.5% ACN was added to increase solubility for samples containing **3b**/**3c**. Plotted data points represent single measurements and error bars represent standard deviations resulting from single exponential tail fitting of decay data. Data were fit with ***Eq. 1*** to determine K_d.

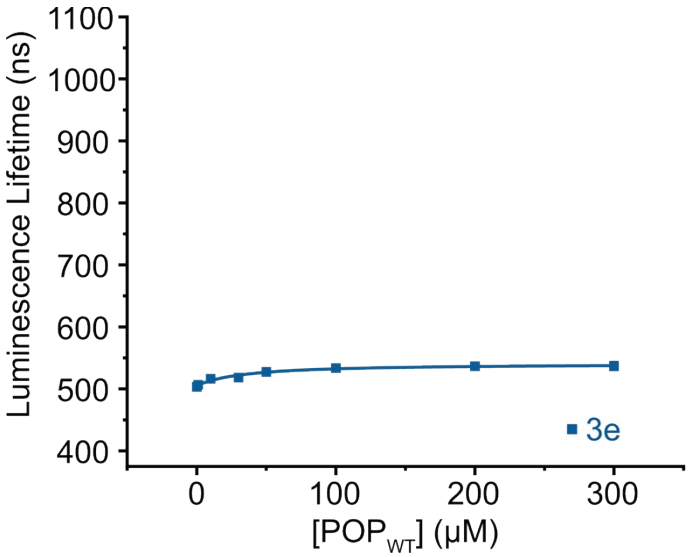

Supplementary Figure 12. 3e Binding to POP$_{WT}$.
Luminescence lifetime (λ_{exc} = 450 nm, λ_{em} = 630 nm) of cofactor **3e** (5 μM) preincubated with increasing concentrations of POP$_{WT}$ (0-300 μM) in MQ H_2O/0.5% ACN. Plotted data points represent single measurements and error bars represent standard deviations resulting from single exponential tail fitting of decay data. Data were fit with ***Eq. 1*** to determine K_d.

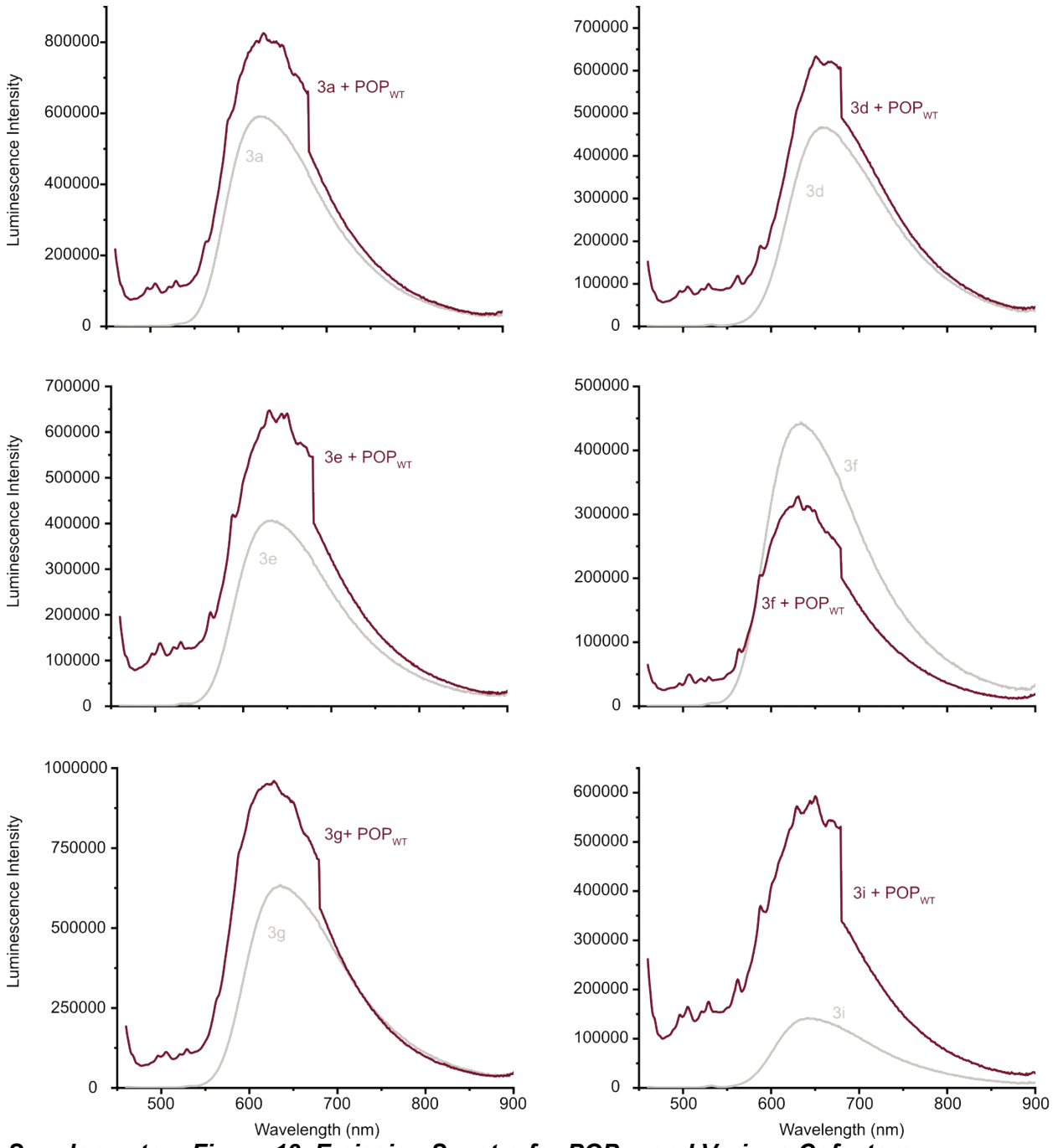

Supplementary Figure 13. Emission Spectra for POP$_{WT}$ and Various Cofactors.
Emission (λ_{exc} = 450 nm) spectra of non-covalent ArMs constructed with scaffold POP$_{WT}$ and ruthenium cofactors (**3a**, **3d**, **3e**, **3f**, **3g**, and **3i**). Samples contained 300 μM protein and 5 μM metal cofactor in MQ H_2O. 0.5% ACN was added to increase solubility of PF_6^- salts. Significant noise was observed in ArM samples, likely due to light scattering from the protein.

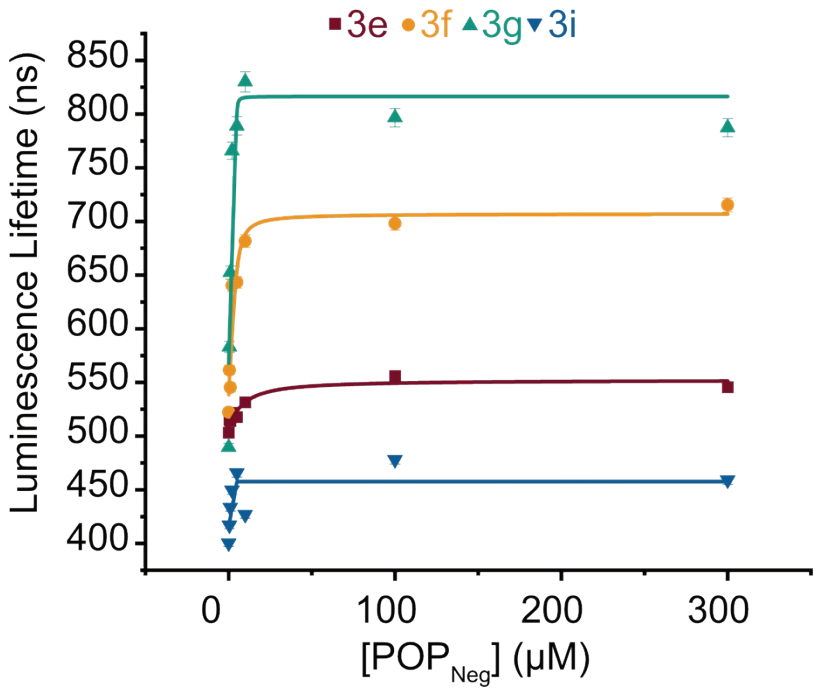

Supplementary Figure 14. Binding of Various Cofactors to POP$_{Neg}$.
Luminescence lifetime (λ_{exc} = 450 nm, λ_{em} = 620-650 nm) of cofactors **3e**, **3f**, **3g**, and **3i** (5 μM) preincubated with increasing concentrations of POP_{Neg} (0-300 μM) in MQ H_2O. 0.5% ACN was added to increase solubility of PF_6^- salts. Plotted data points represent single measurements and error bars represent standard deviations resulting from single exponential tail fitting of decay data. Data were fit with ***Eq. 1*** to determine K_d.

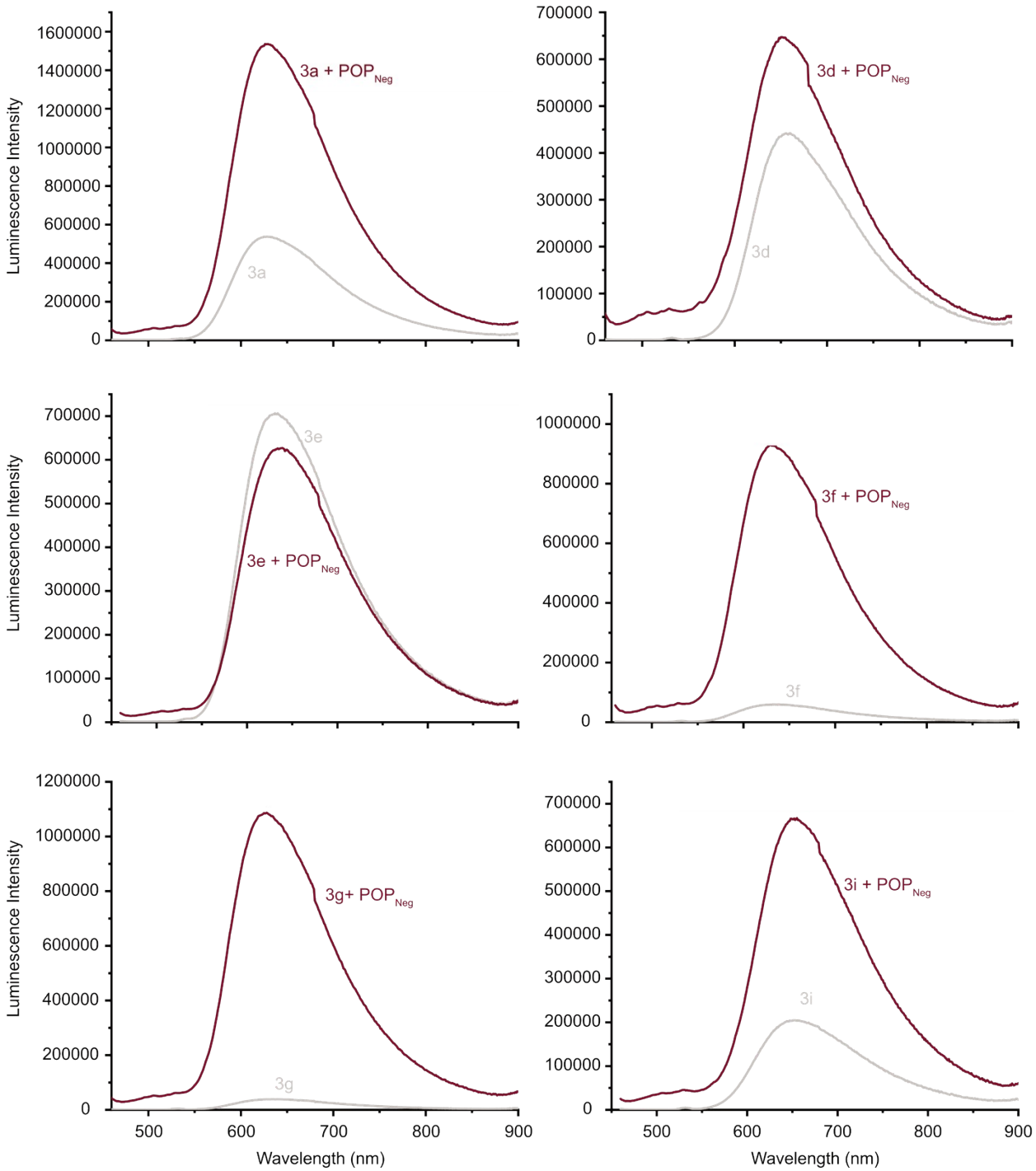

Supplementary Figure 15. Emission Spectra for POP_{Neg} and Various Cofactors.
Emission (λ_{exc} = 450 nm) spectra of non-covalent ArMs constructed with scaffold POP_{Neg} and ruthenium cofactors (**3a**, **3d**, **3e**, **3f**, **3g**, and **3i**). Samples contained 300 μM protein and 5 μM metal cofactor in MQ H_2O. 0.5% ACN was added to increase solubility of PF_6^- salts.

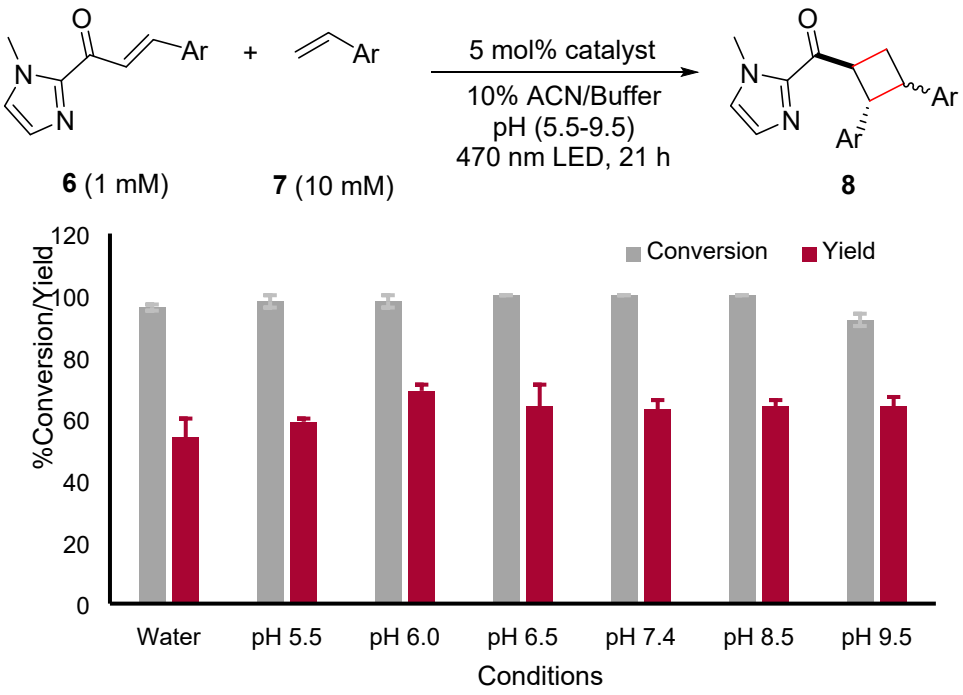

Supplementary Figure 16. pH Optimization for the Cycloaddition of 6 and 7.
Optimal pH and buffer conditions were screened for the [2+2] photocycloaddition between cinnamoyl imidazole **6** and styrene **7**. Reaction conditions were as follows: 1 mM **6**, 10 mM **7**, 5.0 mol% $Ru(Bpy)_3Cl_2$ (50 µM), and 10% ACN (v/v) in a total of 100 µL. The following buffer conditions were screened: MQ H_2O, 25 mM MES (pH 5.5), 25 mM MES (pH 6.0), 25 mM MES pH (6.5), 25 mM Tris (pH 7.4), 25 mM Tricine (pH 8.5), and 25 mM CHES (pH 9.5). Reactions were performed under anaerobic conditions in a wetbox in glass vials sealed with a screwcap. After irradiation for 21 hours, 100 µL of the internal standard (10 mM) 1,3,5-trimethoxybenzene (TMB) in ACN was added to the reactions. Samples were centrifuged to remove precipitation and then filtered through a 0.2 µm polypropylene filter plate prior to analysis by achiral UHPLC. Yields were determined by a calibration curve prepared using isolated authentic product **8** and TMB. Data represent average values obtained from triplicate reactions (n=3) and error bars represent standard deviations.

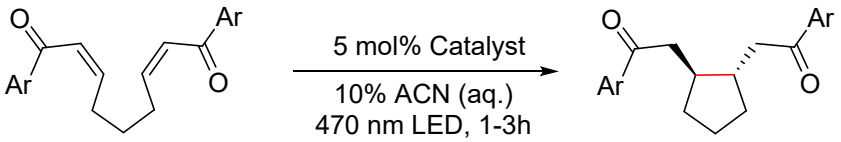

4 (25 μM) **5**

Supplementary Table 1. Reductant Screening for Reductive Cyclization of Dienone 4.

Index	Reductant	Solvent	[a]Condition	Yield **5** (%)
1	N/A	50 mM Tris (pH 7.4)	Aerobic	0
2	50 mM ascorbate	MQ H_2O	Aerobic	38
3	50 mM ascorbate	50 mM Tris (pH 7.4)	Aerobic	53
4	50 mM ascorbate	MQ H_2O	Anaerobic	71
5	50 mM DMAP	MQ H_2O	Aerobic	0
6	50 mM pyridine	MQ H_2O	Aerobic	0
7	50 mM triethylamine	MQ H_2O	Aerobic	11
8	50 mM piperidine	MQ H_2O	Aerobic	15
9	50 mM butylamine	MQ H_2O	Aerobic	1
10	50 mM morpholine	MQ H_2O	Aerobic	0
11	50 mM DBU	MQ H_2O	Aerobic	8
12	50 mM aniline	MQ H_2O	Anaerobic	0
13	39 mM 4-aminophenol	MQ H_2O	Anaerobic	79

[a]Aerobic reactions were irradiated for 3 hours and anaerobic reactions were irradiated for 1 hour under inert conditions in a wetbox; Reactions were performed in singlicate (n=1). Reaction conditions were as follows: 25 μM dienone substrate **4**, 5 mol% $Ru(Bpy)_3Cl_2$ (1.25 μM), and 10% ACN (v/v) in a total of 100 μL. After irradiation, 100 μL of the internal standard (3 mM) 1,3,5-trimethoxybenzene (TMB) in ACN was added to the reactions. Samples were filtered through a 0.2 μm filter plate prior to analysis by achiral UHPLC. Yields were determined by a calibration curve prepared using isolated authentic product **5** and TMB.

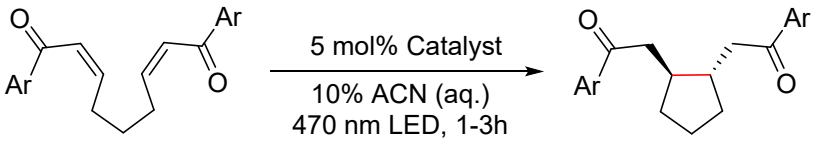

4 (25 μM) **5**

Supplementary Table 2. Ascorbate Concentration Screening for Reductive Cyclization of Dienone 4.

Index	Reductant	[a]Condition	Yield **5** (%)
1	50 mM ascorbate	Aerobic	32
2	10 mM ascorbate	Aerobic	8
3	5 mM ascorbate	Aerobic	0
4	1 mM ascorbate	Aerobic	0
5	0.5 mM ascorbate	Aerobic	0
6	0.25 mM ascorbate	Aerobic	0
7	0.1 mM ascorbate	Aerobic	0
8	0.05 mM ascorbate	Aerobic	0
9	0 mM ascorbate	Aerobic	0
10	50 mM ascorbate	Anaerobic	71
11	10 mM ascorbate	Anaerobic	71
12	5 mM ascorbate	Anaerobic	63
13	1 mM ascorbate	Anaerobic	22
14	0.5 mM ascorbate	Anaerobic	6
15	0.25 mM ascorbate	Anaerobic	0
16	0.1 mM ascorbate	Anaerobic	0
17	0.05 mM ascorbate	Anaerobic	0
18	0 mM ascorbate	Anaerobic	0

[a]Aerobic reactions were irradiated for 3 hours and anaerobic reactions were irradiated for 1 hour under inert conditions in a wetbox; Reactions were performed in singlicate (n=1). Reaction conditions were as follows: 25 μM dienone substrate **4**, 5 mol% $Ru(Bpy)_3Cl_2$ (1.25 μM), and 10% ACN (v/v) in a total of 100 μL. After irradiation, 100 μL of the internal standard (3 mM) 1,3,5-trimethoxybenzene (TMB) in ACN was added to the reactions. Samples were filtered through a 0.2 μm filter plate prior to analysis by achiral UHPLC. Yields were determined by a calibration curve prepared using isolated authentic product **5** and TMB.

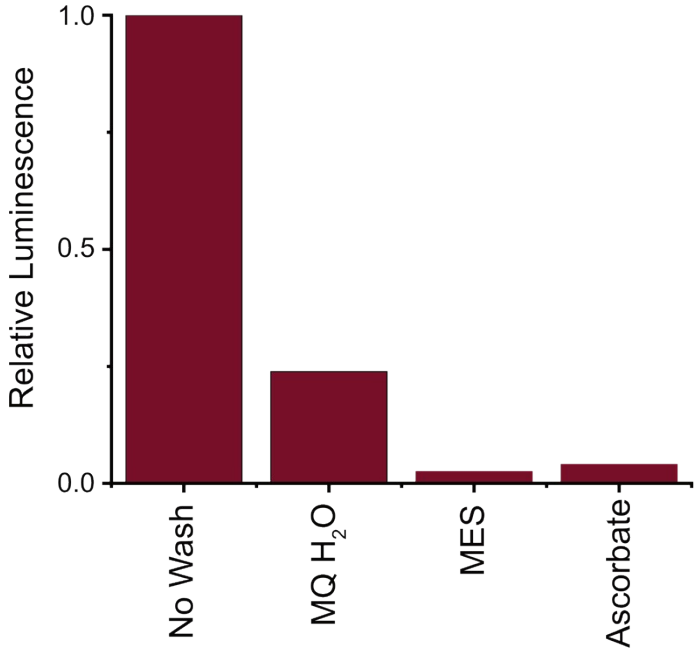

Supplementary Figure 17. Effects of Ascorbate and MES on 3a binding to POP_{Neg}.
POP_{Neg} (95 μM) and cofactor **3a** (5 μM) were preincubated at room temperature in 400 μL of MQ H_2O. 10 mL of either MQ H_2O, 25 mM MES (pH 6.0), or 50 mM sodium ascorbate was added to the sample, and then concentrated to 1 mL in a 30 kDa MWCO spin filter. Luminescence intensity (λ_{exc} = 450 nm, λ_{em} = 620 nm) was measured to determine relative retention of cofactor after washing with water/salt solution and compared to samples that were not subjected to dilution/concentration. Bars represent single measurements.

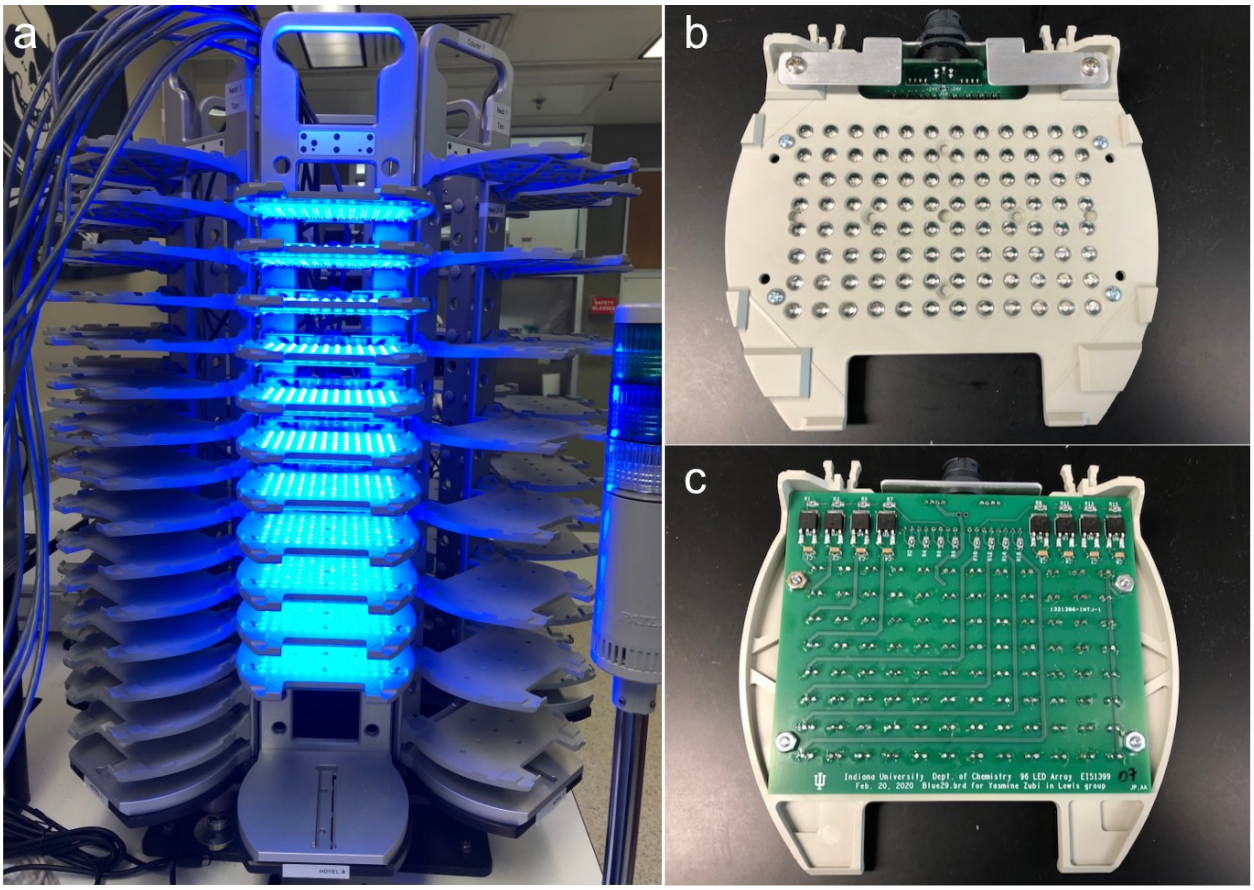

Supplementary Figure 18. LED Array Photoreactor.
(a) Custom 11-plate, 470 nm LED photoreactor mounted into a plate hotel (ThermoFisher custom dual RA hotel; CI01868) of an automation platform is capable of precisely illuminating 1056 reactions simultaneously. **(b)** Front and **(c)** back of a custom LED array. Individual LED plates can be removed from the hotel and transferred into an inert glovebox to facilitate irradiation of anerobic reactions with a smaller power supply. More information about the photoreactor's design is shown in Supplementary Figures 56-58 (*vide infra*).

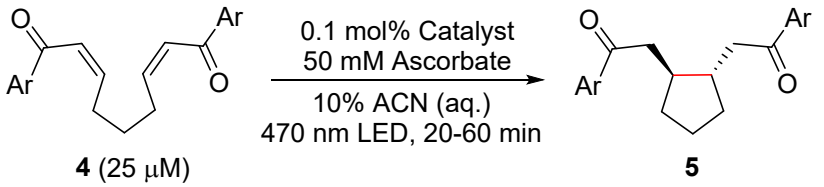

4 (25 μM) **5**

Supplementary Table 3. ArM Screening Reductive Cyclization Results.

Index	Cofactor	Protein Scaffold	[a]Yield **5** (%)	[b]Yield **5** (%)
1	3a	None	32 ± 3	79 ± 4
2	1a	POP_{Neq}-Z_{53}	47 ± 5	87 ± 3
3	1d	POP_{Neg}-Z_{53}	57 ± 1	89 ± 1
4	1f	POP_{Neg}-Z_{53}	58 ± 3	87 ± 1
5	1a	POP_{WT}-Z_{326}	46 ± 3	90 ± 2
6	1a	None	N/A	80 ± 4
7	1b	None	N/A	83 ± 4
8	1c	None	N/A	88 ± 4
9	1d	None	N/A	81 ± 6
10	1e	None	N/A	83 ± 10
12	1f	None	N/A	83 ± 3
13	3a	POP_{Neg}-Z_{53}	N/A	67 ± 5

[a]Irradiated for 20 minutes; [b]Irradiated for 1 hour; Reactions were performed in triplicate (n=3). Reaction conditions were as follows: 50 mM sodium ascorbate, 25 μM dienone substrate **4**, 0.1 mol% catalyst (0.025 μM), and 10% ACN (v/v) in a total of 100 μL. Reactions were performed under anaerobic conditions in the wetbox. After irradiation, 100 μL of the internal standard (3 mM) 1,3,5-trimethoxybenzene (TMB) in ACN was added to the reactions. Samples were filtered through a 0.2 μm filter plate prior to analysis by achiral UHPLC. Yields were determined by a calibration curve prepared using isolated authentic product **5** and TMB.

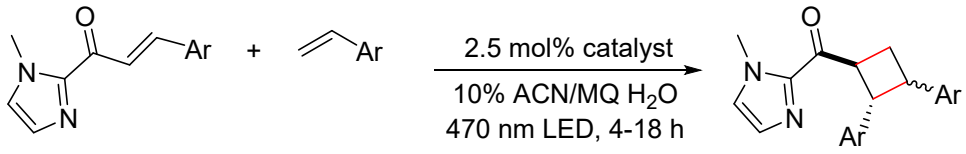

6 (1 mM) **7** (10 mM) **8**

Supplementary Table 4. ArM Screening Photocycloaddition Results.

Index	Cofactor	Protein Scaffold	[a]Yield **8** (%)	[b]Yield **8** (%)
1	3a	None	7	10
2	1a	POP_{WT}-Z_{99}	10	5
3	1a	POP_{WT}-Z_{326}	6	25
4	1a	POP_{WT}-Z_{338}	9	17
5	1a	POP_{WT}-Z_{399}	6	14
6	1a	POP_{WT}-Z_{401}	10	18
7	1a	POP_{WT}-Z_{411}	7	12
8	1a	POP_{WT}-Z_{413}	11	15
9	1a	POP_{1GSH}-Z_{477}	10	25
10	1a	POP_{2PL}-Z_{477}	6	16
11	1a	POP_{3H}-Z_{477}	11	16
12	1a	POP_{3L}-Z_{477}	10	15
13	1a	POP_{5G}-Z_{477}	N/A	23
14	1c	POP_{WT}-Z_{53}	12	25
15	1d	POP_{WT}-Z_{53}	N/A	31
16	1e	POP_{WT}-Z_{53}	10	21
17	1f	POP_{WT}-Z_{53}	11	17
18	1c	POP_{Neg}-Z_{53}	3	13
19	1d	POP_{Neg}-Z_{53}	9	21
20	1e	POP_{Neg}-Z_{53}	6	16
21	1f	POP_{Neg}-Z_{53}	8	21

[a]Irradiated for 4 hours; [b]Irradiated for 18 hours; Reactions were performed in singlicate (n=1) unless otherwise noted. Additionally, screening reactions were performed in microtiter plates, resulting in lower yields compared to final triplicate reactions that were performed in glass vials. Reaction conditions were as follows: 1 mM imidazole substrate **6**, 10 mM 4-methoxstyrene **7**, and 10% ACN (v/v) in a total of 100 µL. Reactions included 2.5 mol% catalyst (25 µM) except for reactions with POP_{3H}-Z_{477}-1a (0.7 mol%), POP_{5G}-Z_{477}-1a (0.9 mol%), POP_{WT}-Z_{401}-1a (2.43 mol%), and POP_{WT}-Z_{413}-1a (2.21 mol%). Reactions were performed under anaerobic conditions in the wetbox. After irradiation, 100 µL of the internal standard (10 mM) 1,3,5-trimethoxybenzene (TMB) in ACN was added to the reactions. Samples were centrifuged to remove precipitation and then filtered through a 0.2 µm filter plate prior to analysis by achiral UHPLC. Yields were determined by a calibration curve prepared using isolated authentic product **8** and TMB.

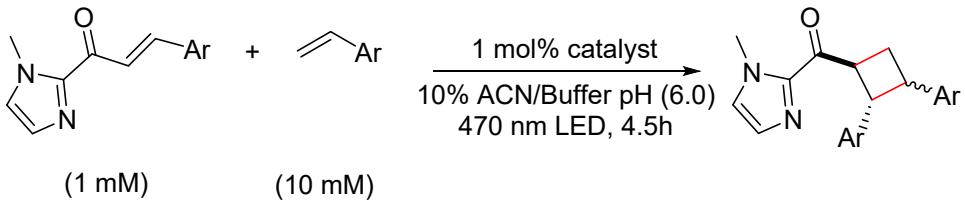

(1 mM) (10 mM)

Supplementary Table 5. Control Photocycloaddition Results.

Index	Cofactor	Protein Scaffold	Yield **8** (%)
1	**3a**	None	25 ± 1
2	**3a**	POP_{Neg}-Z_{53}	19 ± 4
3	**1a**	None	47 ± 3
4	**1b**	None	36 ± 4
5	**1c**	None	46 ± 5
6	**1d**	None	52 ± 3
7	**1e**	None	44 ± 10
8	**1f**	None	42 ± 7

Reactions were performed in triplicate (n=3) unless otherwise noted. Reaction conditions were as follows: 1 mM imidazole substrate **6**, 10 mM 4-methoxstyrene **7**, and 10% ACN (v/v) in a total of 100 µL. Reactions included 2.5 mol% catalyst (25 µM) except for reactions with POP_{3H}-Z_{477}-**1a** (0.7 mol%), POP_{5G}-Z_{477}-**1a** (0.9 mol%), POP_{WT}-Z_{401}-**1a** (2.43 mol%), and POP_{WT}-Z_{413}-**1a** (2.21 mol%). Reactions were performed under anaerobic conditions in the wetbox using glass vials. After irradiation, 100 µL of the internal standard (10 mM) 1,3,5-trimethoxybenzene (TMB) in ACN was added to the reactions. Samples were centrifuged to remove precipitation and then filtered through a 0.2 µm filter plate prior to analysis by achiral UHPLC. Yields were determined by a calibration curve prepared using isolated authentic product **8** and TMB.

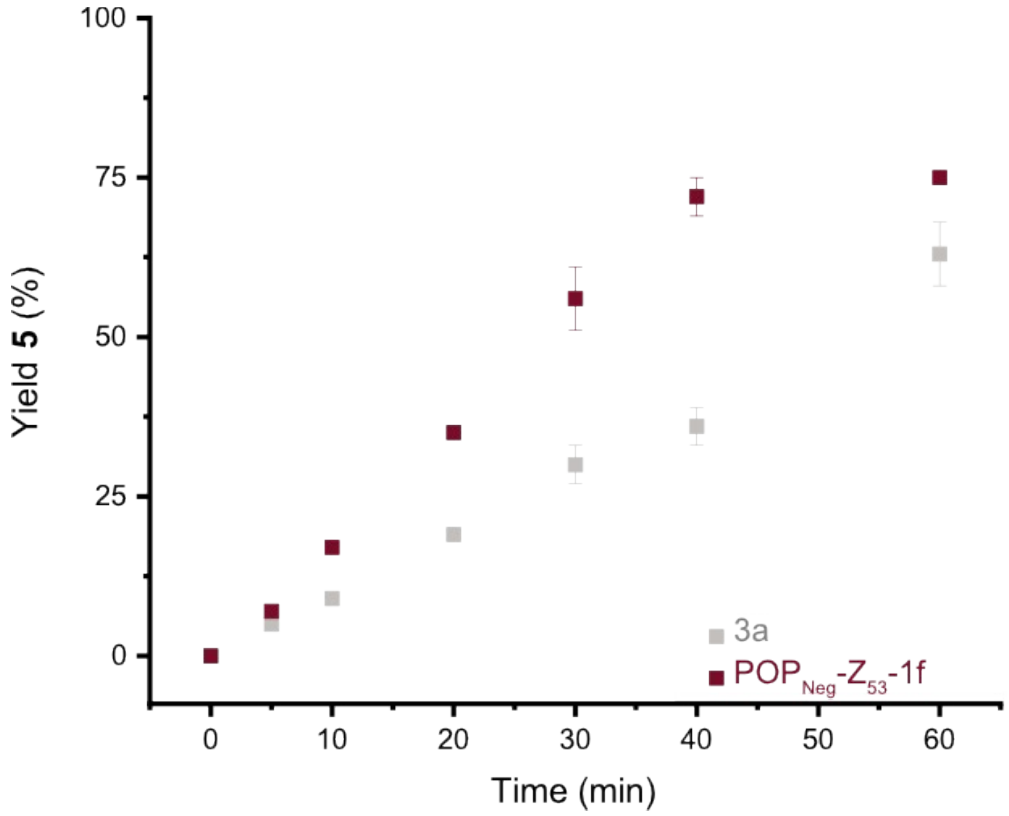

Supplementary Figure 19. Time Course Photoreductive Cyclization Reactions.
Time course reactions of the reductive cyclization of dienone **4** were performed with $Ru(Bpy)_3^{2+}$ (**3a**) and the ArM POP_{Neg}-Z_{53}-**1f**. Reaction conditions were as follows: 25 μM substrate **4**, 0.1 mol% catalyst (0.025 μM), and 10% ACN (v/v) in a total of 100 μL. Samples were prepared in black polystyrene well plates (transparent flat bottoms) and irradiated for either 0, 5, 10, 20, 30, 40, or 60 minutes in a wetbox (anaerobic). After irradiation, 100 μL of the internal standard (3 mM) 1,3,5-trimethoxybenzene (TMB) in ACN was added to the reactions. Samples were filtered through a 0.2 μm filter plate prior to analysis by achiral UHPLC. Yields were determined by a calibration curve prepared using isolated authentic product **5** and TMB. Data represent average values obtained from triplicate reactions (n=3) and error bars represent standard deviations.

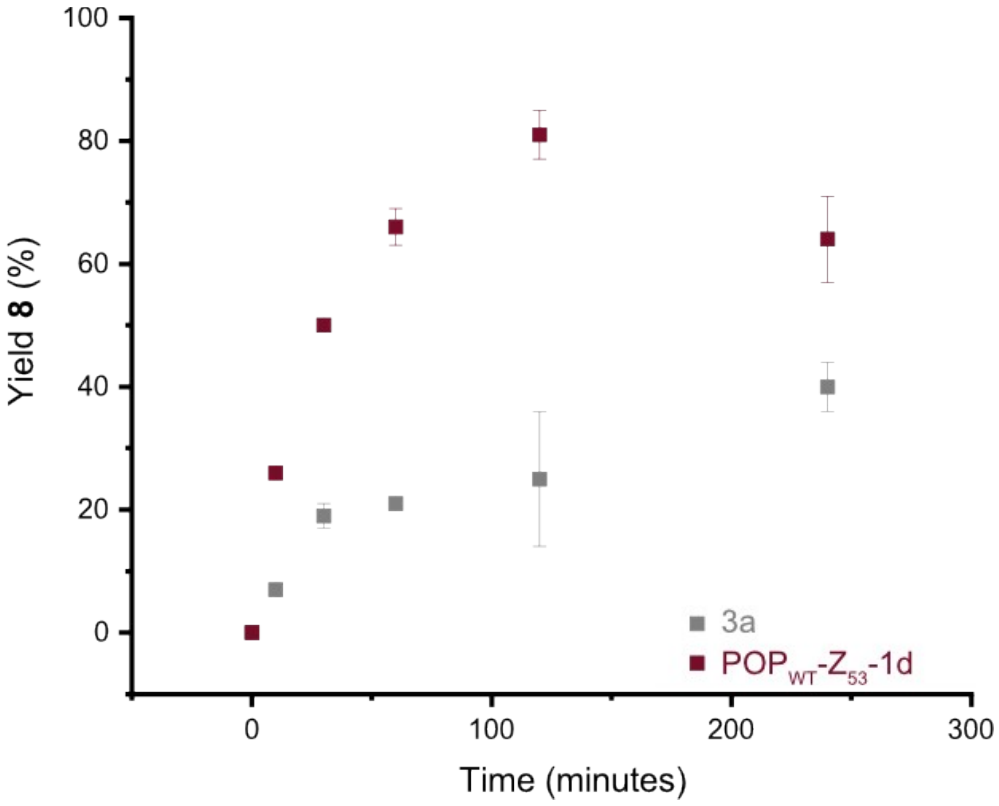

Supplementary Figure 20. Time Course [2+2] Photocycloaddition Reactions.
Time course reactions of the [2+2] photocycloaddition of *C*-cinnamoyl imidazole **6** and 4-methoxy styrene **7** were performed with $Ru(Bpy)_3^{2+}$ (**3a**) and the ArM POP_{WT}-Z_{53}-**1d**. Reaction conditions were as follows: 25 mM MES (pH 6.0), 1 mM substrate **6**, 10 mM styrene **7,** 1.0 mol% catalyst (10 μM), and 10% ACN (v/v) in a total of 100 μL. Samples were prepared in glass vials with a PE screw cap (12x35 mm) and irradiated for either 0, 10, 30, 60, 120, or 240 minutes in a wetbox (anaerobic). After irradiation, 100 μL of the internal standard (10 mM) 1,3,5-trimethoxybenzene (TMB) in ACN was added to the reactions. Samples were filtered through a 0.2 μm filter plate prior to analysis by achiral UHPLC. Yields were determined by a calibration curve prepared using isolated authentic product **8** and TMB. Data represent average values obtained from triplicate reactions (n=3) and error bars represent standard deviations.

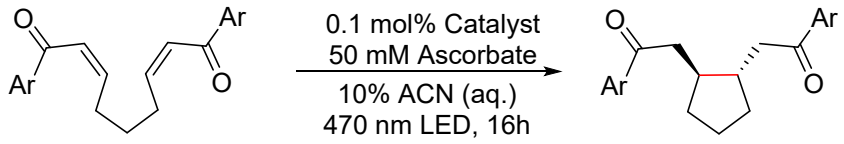

(25 μM)

Supplementary Table 6. Reductive Cyclization Reactions with Longer Irradiation

Index	Cofactor	Protein Scaffold	Yield **5** (%)
1	**3a**	None	94 ± 3
2	**1f**	POP_{Neg}-Z_{53}	94 ± 1

Reactions were performed in triplicate (n=3). Reaction conditions were as follows: 50 mM sodium ascorbate, 25 μM dienone substrate **4**, 0.1 mol% catalyst (0.025 μM), and 10% ACN (v/v) in a total of 100 μL. Reactions were performed under anaerobic conditions in the wetbox. After irradiation, 100 μL of the internal standard (3 mM) 1,3,5-trimethoxybenzene (TMB) in ACN was added to the reactions. Samples were filtered through a 0.2 μm filter plate prior to analysis by achiral UHPLC. Yields were determined by a calibration curve prepared using isolated authentic product **5** and TMB.

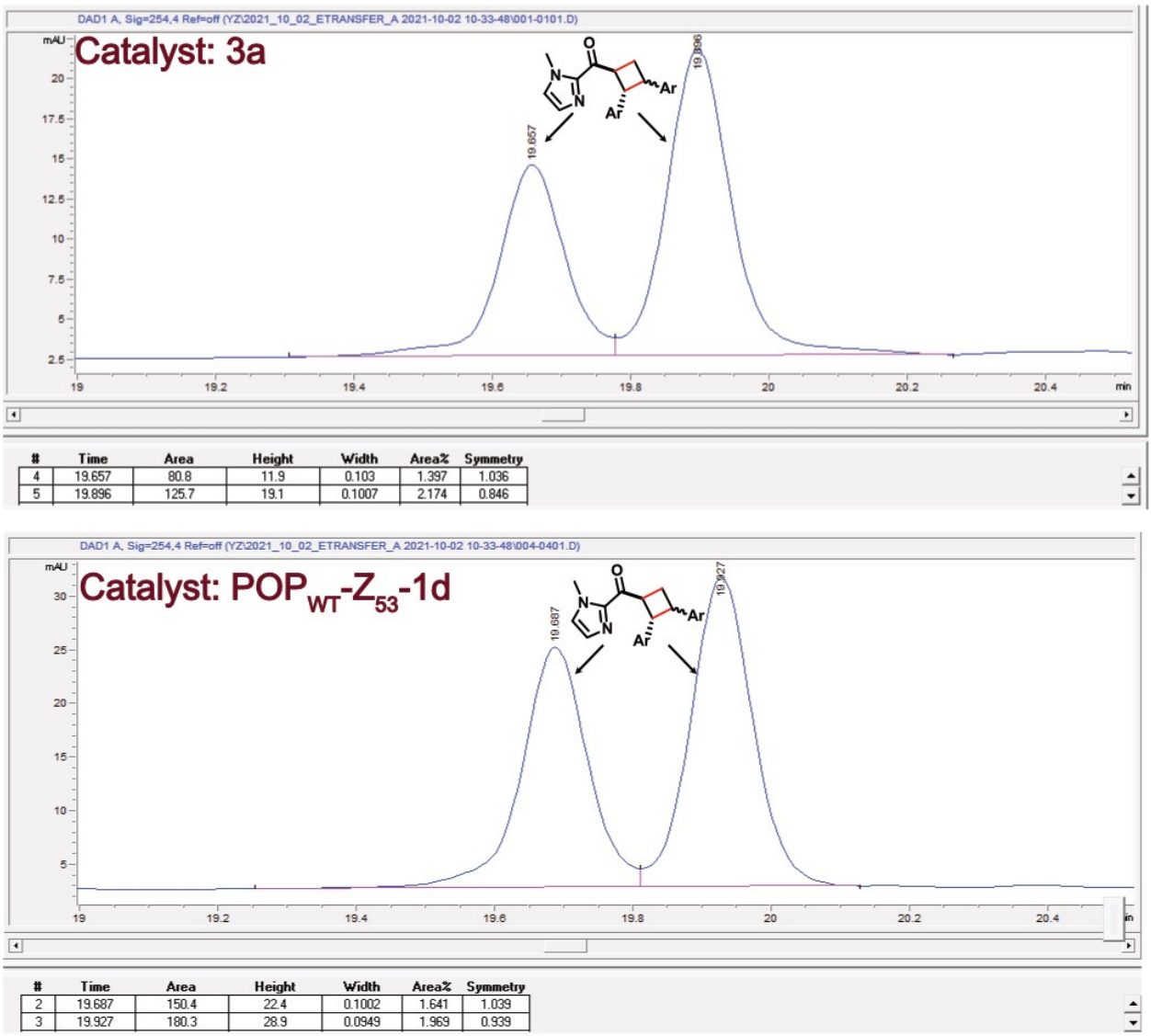

#	Time	Area	Height	Width	Area%	Symmetry
4	19.657	80.8	11.9	0.103	1.397	1.036
5	19.896	125.7	19.1	0.1007	2.174	0.846

#	Time	Area	Height	Width	Area%	Symmetry
2	19.687	150.4	22.4	0.1002	1.641	1.039
3	19.927	180.3	28.9	0.0949	1.969	0.939

Supplementary Figure 21. UHPLC Chromatograms Highlighting Changes in d.r. Observed for ArMs.

Representative chromatograms of [2+2] photocycloaddition of *C*-cinnamoyl imidazole **6** and 4-methoxy styrene **7** performed with $Ru(Bpy)_3^{2+}$ (**3a**) and the ArM POP_{WT}-Z_{53}-1d. Reaction conditions were as follows: 25 mM MES (pH 6.0), 1 mM substrate **6**, 10 mM styrene **7,** 1.0 mol% catalyst (10 µM), and 10% ACN (v/v) in a total of 100 µL. Samples were prepared in glass vials with a PE screw cap (12x35 mm) and irradiated for 120 minutes in a wetbox (anaerobic). After irradiation, 100 µL of the internal standard (10 mM) 1,3,5-trimethoxybenzene (TMB) in ACN was added to the reactions. Samples were filtered through a 0.2 µm filter plate prior to analysis by achiral UHPLC.

Synthetic Procedures

General Synthetic Procedures for Ru Cofactors

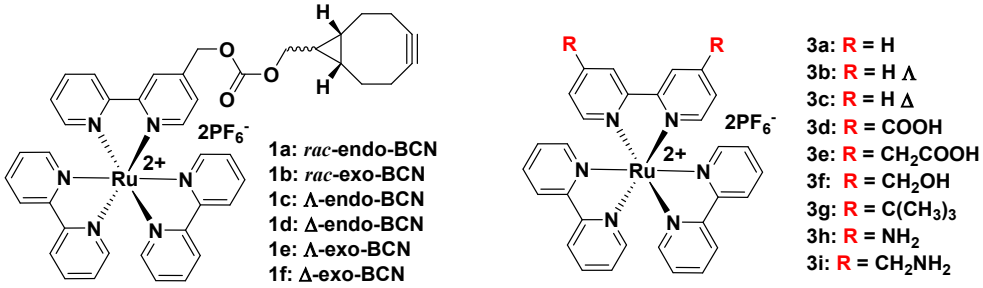

All chemicals and solvents were purchased from Fisher Scientific Co. and used as received unless otherwise noted. Silica gel (60 Å, 230−400 mesh) was purchased from Silicycle Inc. Several intermediates and cofactors, including 4,4'-diacetic acid-2,2'-bipyridine,[1] 4-(hydroxymethyl)-2,2'-bipyridine,[2] *cis*-$Ru(bpy)_2Cl_2$,[3] D-$[Ru(bpy)_2(py)_2]$[O,O'-dibenzoyl-D-tartrate]·$12H_2O$,[4] Λ-$[Ru(bpy)_2(py)_2]$ [O,O' -dibenzoyl-L-tartrate]·$12H_2O$,[4] **3a**,[5] **3b**,[6] **3c**,[6] **3d**,[7] **3f**,[8] **3h**,[9] and **3i**[10] were synthesized according to literature procedures. ^{1}H NMR spectra were recorded at room temperature on a Varian I500 (500 MHz) spectrometer. ^{13}C NMR spectra were recorded on a Varian I500 (125 MHz) spectrometer with complete proton decoupling. ESI mass spectra were obtained using an Agilent Technologies 1290/6135B quadrupole LC-MS.

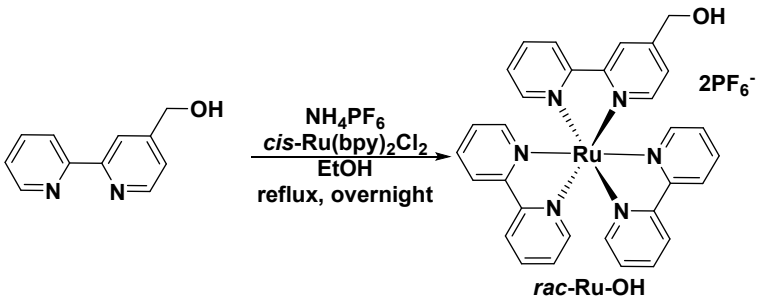

Synthesis of *rac*-Ru-OH:

The *cis*-$Ru(bpy)_2Cl_2$ (260 mg, 0.52 mmol) was added to a solution of 4-(hydroxymethyl)-2,2'-bipyridine (100 mg, 0.52 mmol) in EtOH (20 ml). The mixture was heated at reflux overnight under nitrogen atmosphere in the dark. After cooling to room temperature, 10 equiv. NH_4PF_6 in H_2O (50 mL) was added to precipitate an orange-red solid. The obtained crude product was purified by column chromatography on silica gel and eluted with dichloromethane/methanol (100/2, v/v) to afford the product as an orange-red solid (281 mg, 54 %). ^{1}H NMR (500 MHz, CD_3OD): δ 8.67 (dd, J = 8.2, 0.9 Hz, 5H), 8.62 (d, J = 1.6 Hz, 1H), 8.10 (td, J = 7.9, 1.6 Hz, 5H), 7.82 (dtt, J = 5.9, 3.7, 1.8 Hz, 5H), 7.72 (d, J = 5.7 Hz, 1H), 7.47 (tdd, J = 5.6, 2.7, 1.3 Hz, 6H), 4.84 (s, 2H). ^{13}C NMR (125 MHz, CD_3OD): δ 158.52, 158.09, 155.80, 154.37, 152.62, 152.06, 139.12, 128.92, 126.24, 125.55, 122.74, 62.94. ESI-MS: Calcd. $[C_{31}H_{26}N_6ORu]^{2+}$ for 300.06, found 300.03.

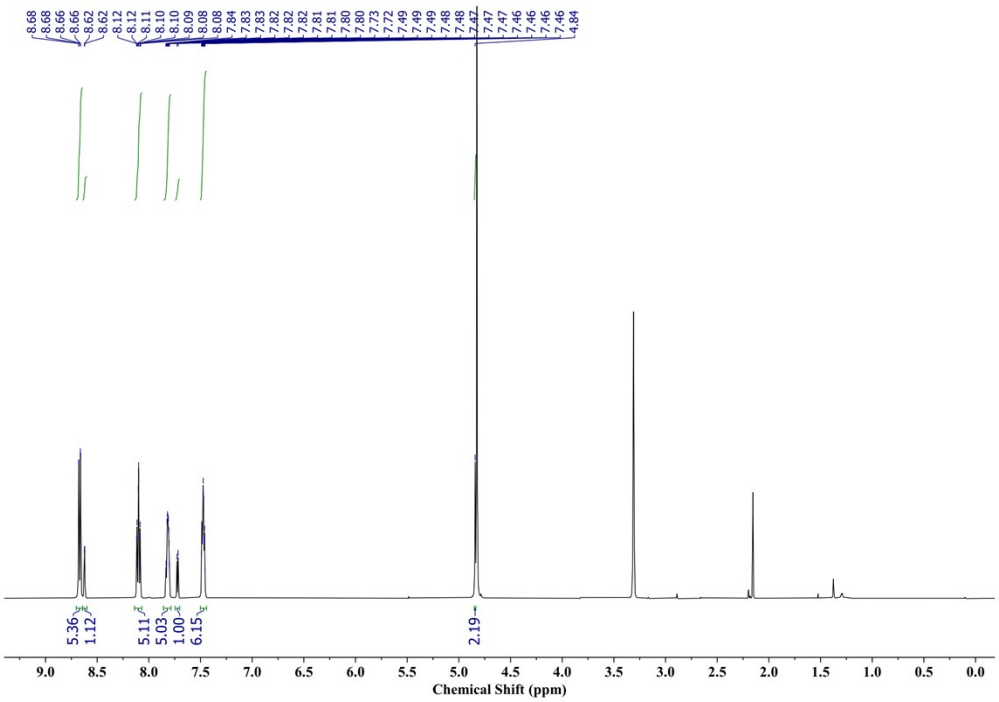

Supplementary Figure 22.
^{1}H NMR spectrum (500 MHz, CD_3OD) for ***rac*-Ru-OH**.

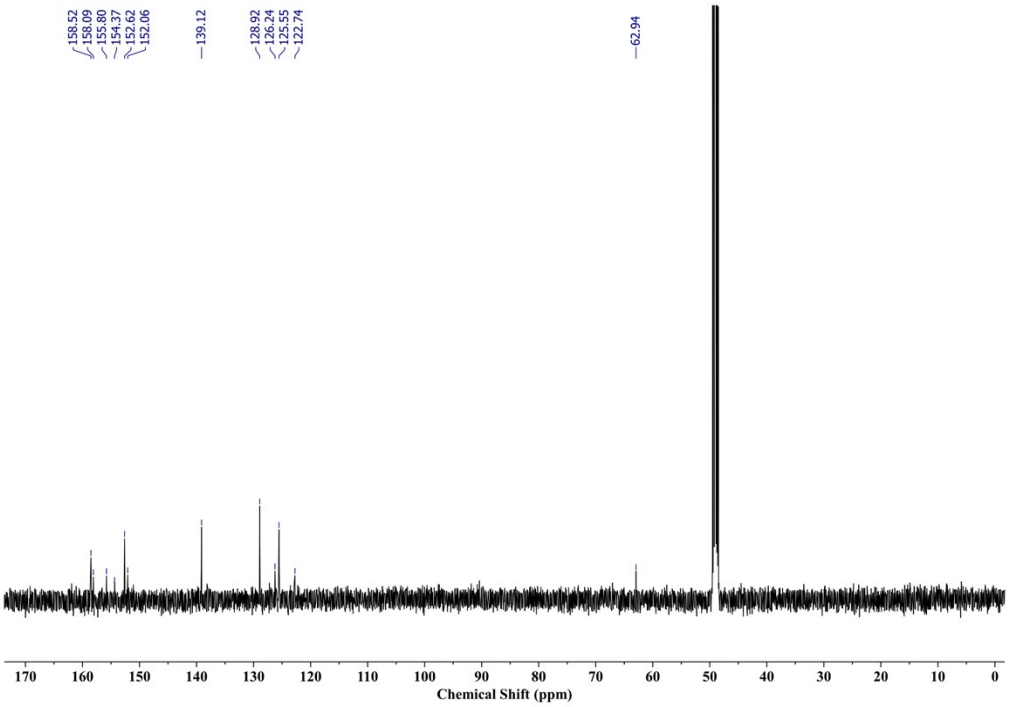

Supplementary Figure 23.
^{13}C NMR spectrum (125 MHz, CD_3OD) for ***rac*-Ru-OH**.

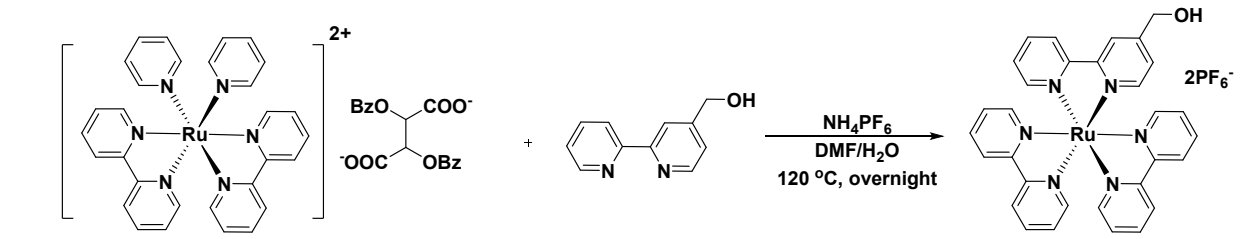

Δ-[Ru(bpy)$_2$(py)$_2$][(+)-O.O'-dibenzoyl-D-tartrate]·12H$_2$O
Λ-[Ru(bpy)$_2$(py)$_2$][(-)-O.O'-dibenzoyl-L-tartrate]·12H$_2$O

Δ-Ru-OH
Λ-Ru-OH

Synthesis of D-Ru-OH:

A mixture of D-[Ru(bpy)$_2$(py)$_2$][O,O'-dibenzoyl-D-tartrate]·12H$_2$O (450 mg, 0.39 mmol) and ligand (109 mg, 0.59 mmol) in 10 mL of 4:1 DMF/H$_2$O solution was heated at 120 °C overnight under nitrogen atmosphere. The dark reaction solution was then cooled to room temperature. After removing the volatiles via rotary evaporation, 20 mL water was added. The product was then precipitated by the addition of 10 eq NH_4PF_6 in H_2O (30 mL). The obtained solid was filtered out and further washed with acetone/ether to afford pure product as orange solid (274 mg, 79%). ^{1}H NMR (500 MHz, CD_3OD): δ 8.67 (dd, J = 8.2, 1.0 Hz, 5H), 8.62 (d, J = 1.1 Hz, 1H) 8.10 (tt, J = 7.8, 1.6 Hz, 5H), 7.82 (qt, J = 3.7, 2.0 Hz, 5H), 7.72 (d, J = 5.9 Hz, 1H), 7.48 (ddq, J = 7.1, 3.8, 1.3 Hz, 6H), 4.84 (s, 2H). ^{13}C NMR (125 MHz, CD_3OD): δ 158.53, 155.82, 152.62, 152.06, 142.03, 139.13, 128.92, 126.24, 125.56, 125.50, 122.74, 62.93. ESI-MS: Calcd. $[C_{31}H_{26}N_6ORu]^{2+}$ for 300.06, found 300.04.

Synthesis of L-Ru-OH:

A mixture of L-[Ru(bpy)$_2$(py)$_2$][O,O'-dibenzoyl-L-tartrate]·12H$_2$O (450 mg, 0.39 mmol) and ligand (109 mg, 0.59 mmol) in 10 mL of 4:1 DMF/H$_2$O solution was heated at 120 °C overnight under nitrogen atmosphere. The dark reaction solution was then cooled to room temperature. After removing the volatiles via rotary evaporation, 20 mL water was added. The product was then precipitated by the addition of 10 eq NH_4PF_6 in H_2O (30 mL). The obtained solid was filtered out and further washed with acetone/ether to afford pure product as orange solid (277 mg, 80%). ^{1}H NMR (500 MHz, CD_3OD): δ 8.68 (dt, J = 8.2, 1.1 Hz, 5H), 8.63 (d, J = 1.1 Hz, 1H), 8.11 (ddd, J = 7.9, 7.0, 1.5 Hz, 5H), 7.82 (qt, J = 3.7, 1.9 Hz, 5H), 7.72 (d, J = 5.9 Hz, 1H), 7.48 (ddq, J = 7.9, 5.6, 1.3 Hz, 6H), 4.84 (s, 2H). ^{13}C NMR (125 MHz, CD_3OD): δ 158.54, 158.11, 155.84, 152.63, 152.07, 139.14, 128.92, 126.24, 125.56, 122.75, 62.93. ESI-MS: Calcd. $[C_{31}H_{26}N_6ORu]^{2+}$ for 300.06, found 300.07.

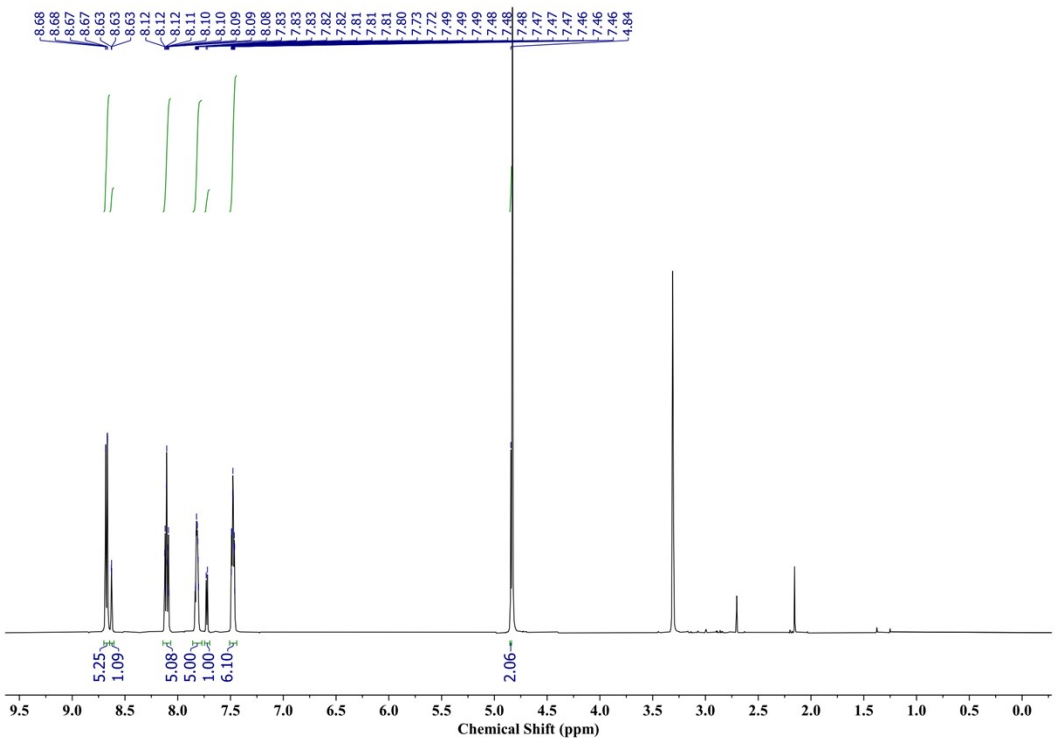

Supplementary Figure 24.
^{1}H NMR spectrum (500 MHz, CD_3OD) for **D-Ru-OH**.

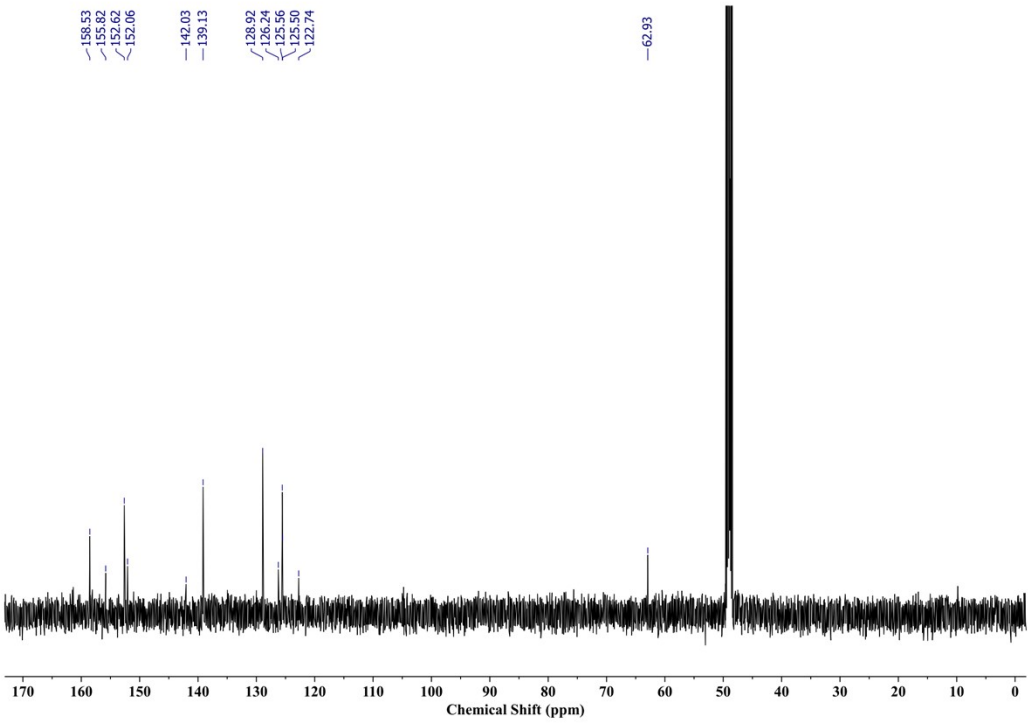

Supplementary Figure 25.
^{13}C NMR spectrum (125 MHz, CD_3OD) for **D-Ru-OH**.

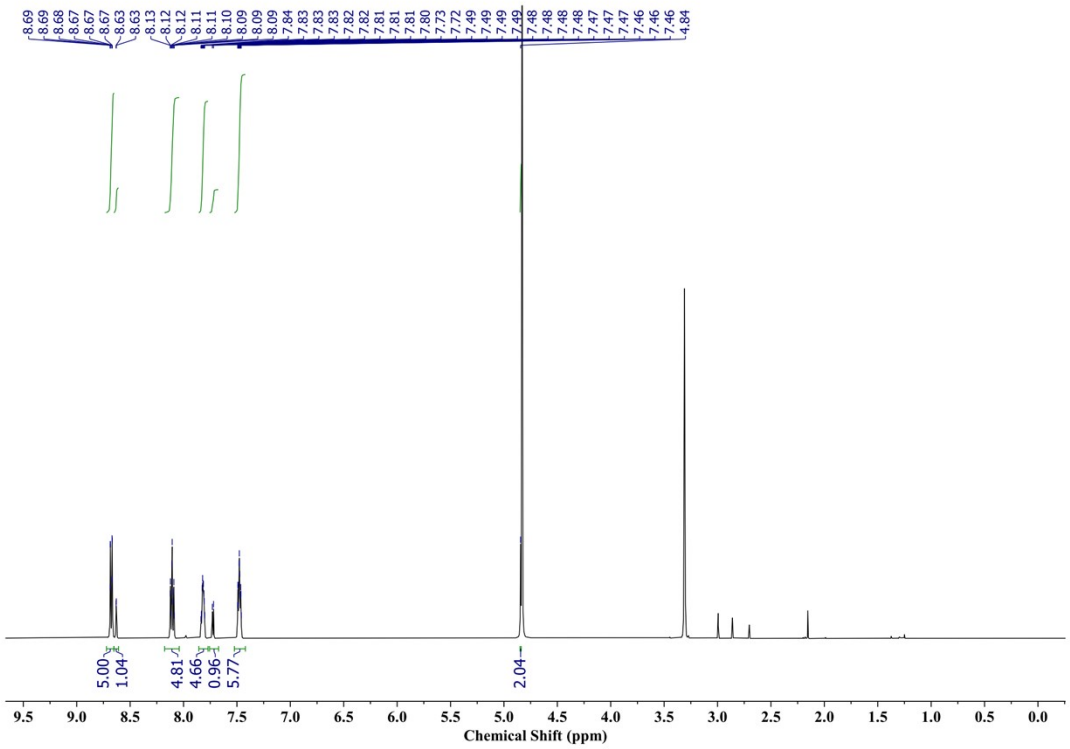

Supplementary Figure 26.
^{1}H NMR spectrum (500 MHz, CD_3OD) for **L-Ru-OH**.

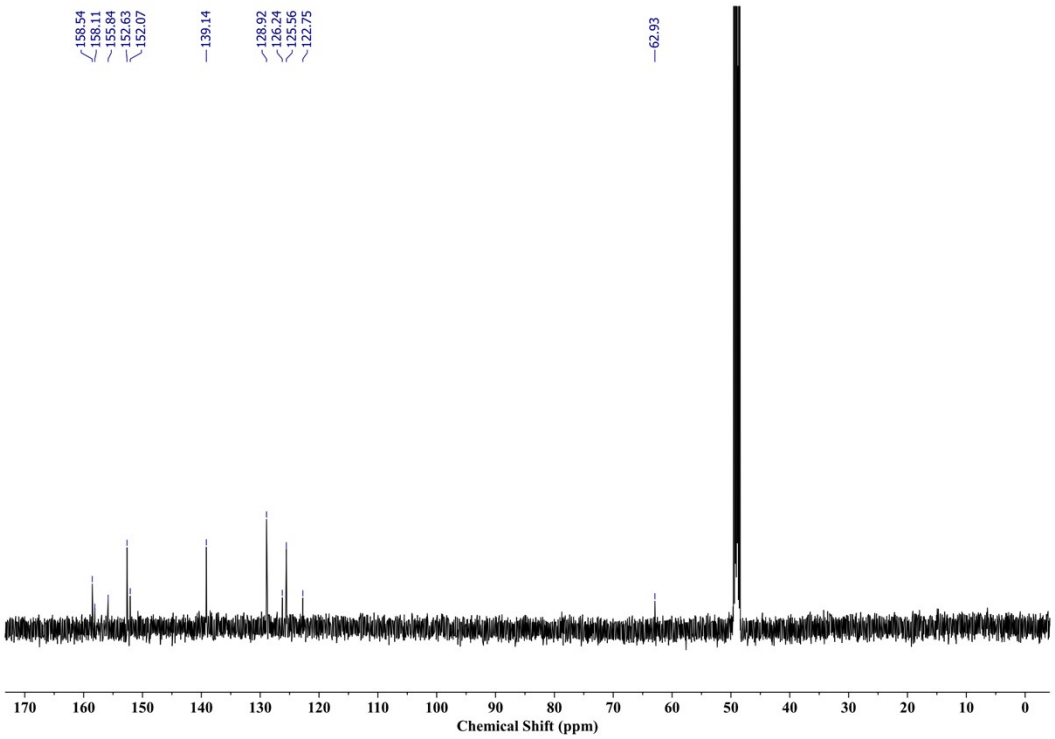

Supplementary Figure 27.
^{13}C NMR spectrum (125 MHz, CD_3OD) for **L-Ru-OH**.

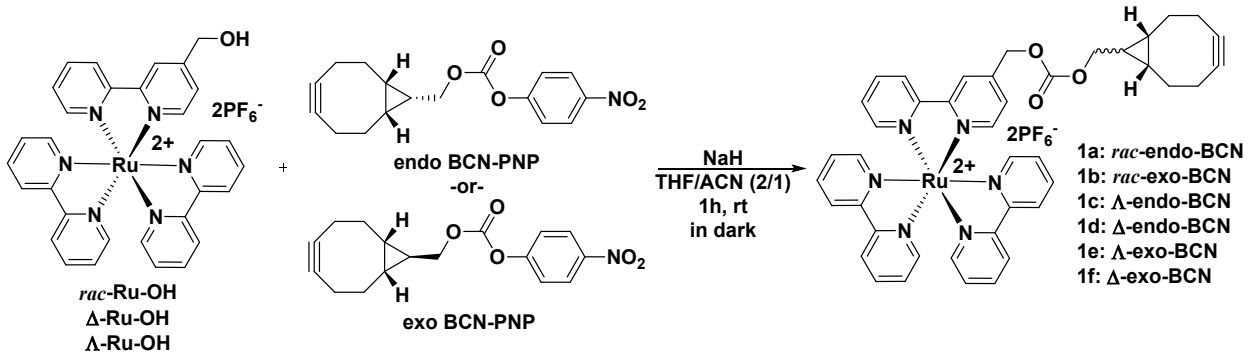

Synthesis of **1a-1f**:

NaH (3.5 mg, 0.09 mmol, 60% dispersion in mineral oil) was added to a solution of Ru-OH (35.6 mg, 0.04 mmol) in ACN (2 mL). The obtained suspension was stirred at r.t. for 5 min. Then, a solution of exo-BCN-PNP (13.8 mg, 0.044 mmol) in THF (4 mL) was added dropwise and the mixture was stirred at room temperature for 1h. After drying *in vacuo*, the obtained orange solid dissolved in a minimal amount of acetone, and the solution was added dropwise to a saturated aqueous solution of NH_4PF_6 (10 mL). The precipitate was further washed with acetone/ether to afford the pure product.

1a. Orange powder (36 mg, 84%). ^{1}H NMR (500 MHz, CD_2Cl_2): δ 8.46 – 8.38 (m, 6H), 8.07 (t, J = 7.9 Hz, 5H), 7.76 – 7.68 (m, 6H), 7.51 – 7.42 (m, 6H), 5.36 (s, 2H), 4.30 (d, J = 7.9 Hz, 2H), 2.31 – 2.14 (m, 6H), 1.54 (s, 2H), 1.45 – 1.41 (m, 1H), 1.05 – 0.92 (m, 2H). ^{13}C NMR (125 MHz, CD_2Cl_2): δ 157.12, 155.09, 151.69, 138.54, 128.50, 126.39, 124.61, 122.57, 99.01, 67.72, 66.80, 29.44, 21.60, 20.75, 17.69. ESI-MS: Calcd. $[C_{42}H_{38}N_6O_3Ru]^{2+}$ for 388.10, found 388.09.

1b. Orange powder (33 mg, 77%). ^{1}H NMR (500 MHz, CD_2Cl_2): δ 8.47 – 8.39 (m, 6H), 8.07 (td, J = 7.9, 1.6 Hz, 5H), 7.75 – 7.67 (m, 6H), 7.50 – 7.42 (m, 6H), 5.36 (d, J = 1.7 Hz, 2H), 4.10 (dd, J = 6.8, 2.0 Hz, 2H), 2.38 (d, J = 13.7 Hz, 2H), 2.28 – 2.22 (m, 2H), 2.12 (d, J = 2.6 Hz, 2H), 1.38 – 1.36 (m, 2H), 0.80 – 0.73 (m, 3H). ^{13}C NMR (125 MHz, CD_2Cl_2): δ 157.12, 155.13, 151.72, 148.24, 138.54, 128.52, 126.44, 124.61, 122.59, 98.95, 73.74, 66.78, 33.53, 23.51, 21.55. ESI-MS: Calcd. $[C_{42}H_{38}N_6O_3Ru]^{2+}$ for 388.10, found 388.10.

1c. Orange powder (36 mg, 84%). ^{1}H NMR (500 MHz, CD_2Cl_2): δ 8.47 – 8.39 (m, 6H), 8.07 (t, J = 8.1 Hz, 6H), 7.71 (tt, J = 12.0, 5.7 Hz, 6H), 7.50 – 7.42 (m, 6H), 5.36 (s, 1H), 4.29 (d, J = 8.2 Hz, 2H), 2.30 – 2.17 (m, 6H), 1.59 – 1.52 (m, 2H), 1.43 (p, J = 8.5 Hz, 1H), 1.00 (td, J = 8.6, 7.6, 3.1 Hz, 2H). ^{13}C NMR (125 MHz, CD_2Cl_2): δ 157.12, 155.10, 151.73, 138.54, 128.52, 126.42, 124.61, 122.56, 99.01, 67.74, 66.81, 29.44, 21.60, 20.77, 17.69. ESI-MS: Calcd. $[C_{42}H_{38}N_6O_3Ru]^{2+}$ for 388.10, found 388.10.

1d. Orange powder (37 mg, 87%). ^{1}H NMR (500 MHz, CD_2Cl_2): δ 8.46 – 8.39 (m, 6H), 8.07 (t, J = 8.2 Hz, 5H), 7.72 (tt, J = 12.0, 6.0 Hz, 6H), 7.50 – 7.42 (m, 6H), 5.36 (s, 2H), 4.30 (d, J = 8.2 Hz, 2H), 2.30 – 2.17 (m, 6H), 1.56 (d, J = 9.4 Hz, 2H), 1.44 – 1.41 (m, 1H), 1.00 (t, J = 10.2 Hz, 2H). ^{13}C NMR (125 MHz, CD_2Cl_2): δ 157.11, 151.72, 148.21, 138.53, 128.52, 126.43, 124.57, 122.55, 99.00, 67.73, 66.80, 29.45, 21.60, 20.76, 17.69. ESI-MS: Calcd. $[C_{42}H_{38}N_6O_3Ru]^{2+}$ for 388.10, found 388.09.

1e. Orange powder (35 mg, 84%). ^{1}H NMR (500 MHz, CD_2Cl_2): δ 8.47 – 8.39 (m, 6H), 8.06 (tq, J = 8.1, 1.6 Hz, 5H), 7.75 – 7.67 (m, 6H), 7.49 – 7.42 (m, 6H), 5.35 (s, 2H), 4.10 (d, J = 7.0 Hz, 2H), 2.38 (dq, J = 13.7, 3.1 Hz, 2H), 2.28 – 2.21 (m, 2H), 2.15 – 2.10 (m, 2H), 1.40 – 1.35 (m, 2H),

0.80 – 0.73 (m, 2H). ^{13}C NMR (125 MHz, CD_2Cl_2): *δ* 157.13, 155.12, 151.69, 148.23, 138.55, 128.51, 126.41, 124.63, 122.60, 98.96, 73.72, 66.78, 33.53, 23.50, 23.44, 21.55. ESI-MS: Calcd. $[C_{42}H_{38}N_6O_3Ru]^{2+}$ for 388.10, found 388.11.

1f. Orange powder (36 mg, 84%). ^{1}H NMR (500 MHz, CD_2Cl_2): *δ* 8.48 – 8.40 (m, 6H), 8.06 (t, *J* = 7.9 Hz, 5H), 7.71 (tt, *J* = 12.3, 5.6 Hz, 6H), 7.49 – 7.42 (m, 6H), 5.35 (s, 2H), 4.10 (d, *J* = 6.8 Hz, 2H), 2.38 (dd, *J* = 13.3, 2.9 Hz, 2H), 2.28 – 2.21 (m, 2H), 2.14 – 2.10 (m, 2H), 1.41 – 1.34 (m, 2H), 0.81 – 0.73 (m, 3H). ^{13}C NMR (125 MHz, CD_2Cl_2): *δ* 157.13, 155.12, 151.67, 148.21, 138.55, 128.49, 126.40, 124.64, 122.61, 98.96, 73.71, 66.78, 33.52, 23.49, 23.44, 21.54. ESI-MS: Calcd. $[C_{42}H_{38}N_6O_3Ru]^{2+}$ for 388.10, found 388.12.

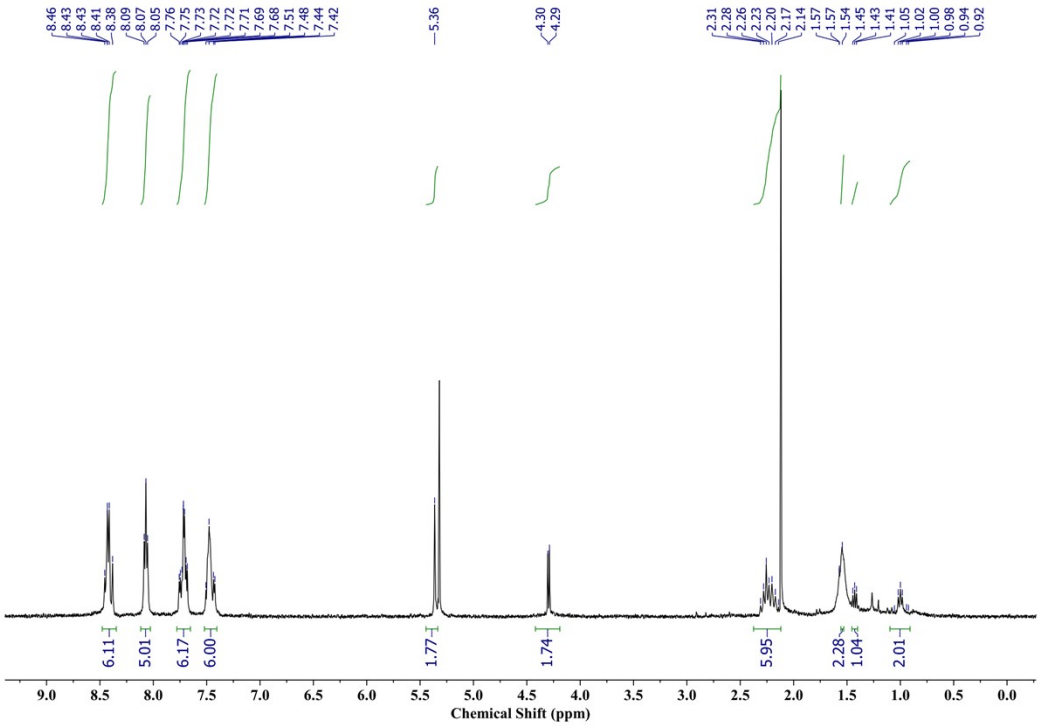

Supplementary Figure 28.
^{1}H NMR spectrum (500 MHz, CD_2Cl_2) for **1a**.

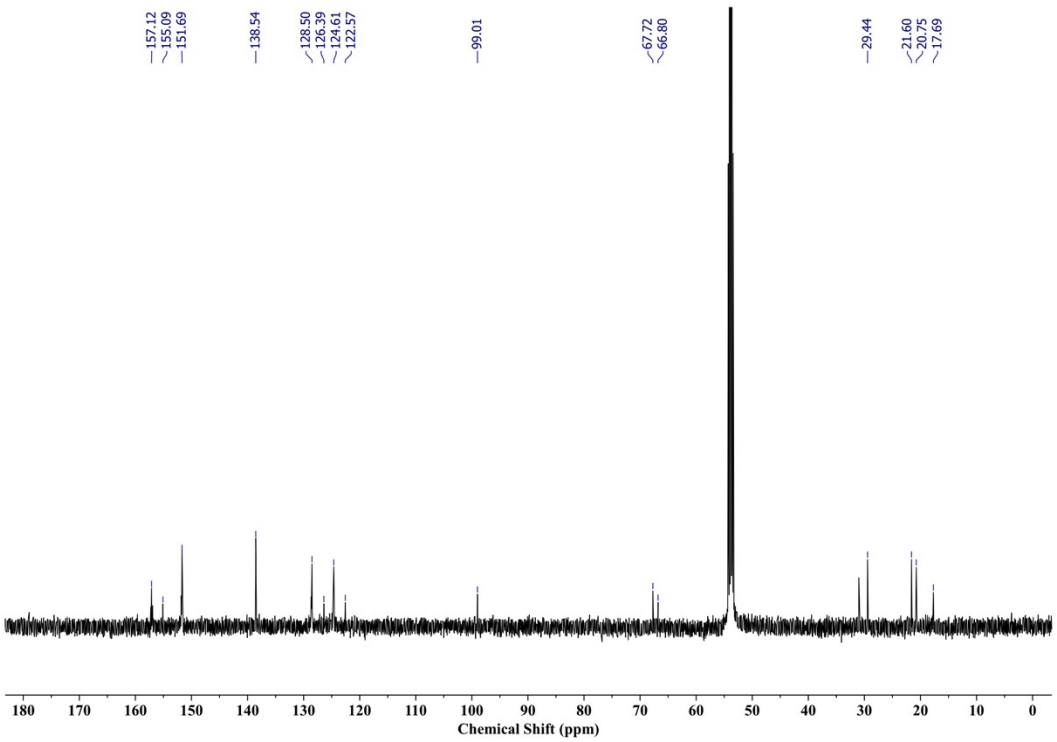

Supplementary Figure 29.
^{13}C NMR spectrum (125 MHz, CD_2Cl_2) for **1a**.

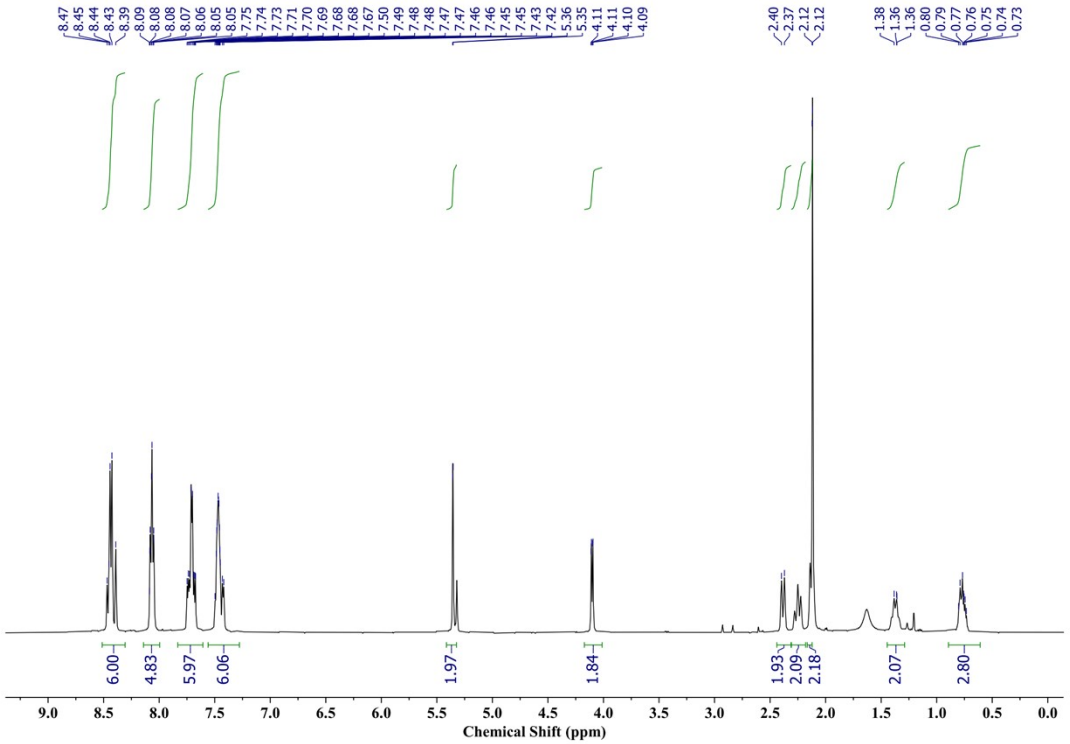

Supplementary Figure 30.
^{1}H NMR spectrum (500 MHz, CD_2Cl_2) for **1b**.

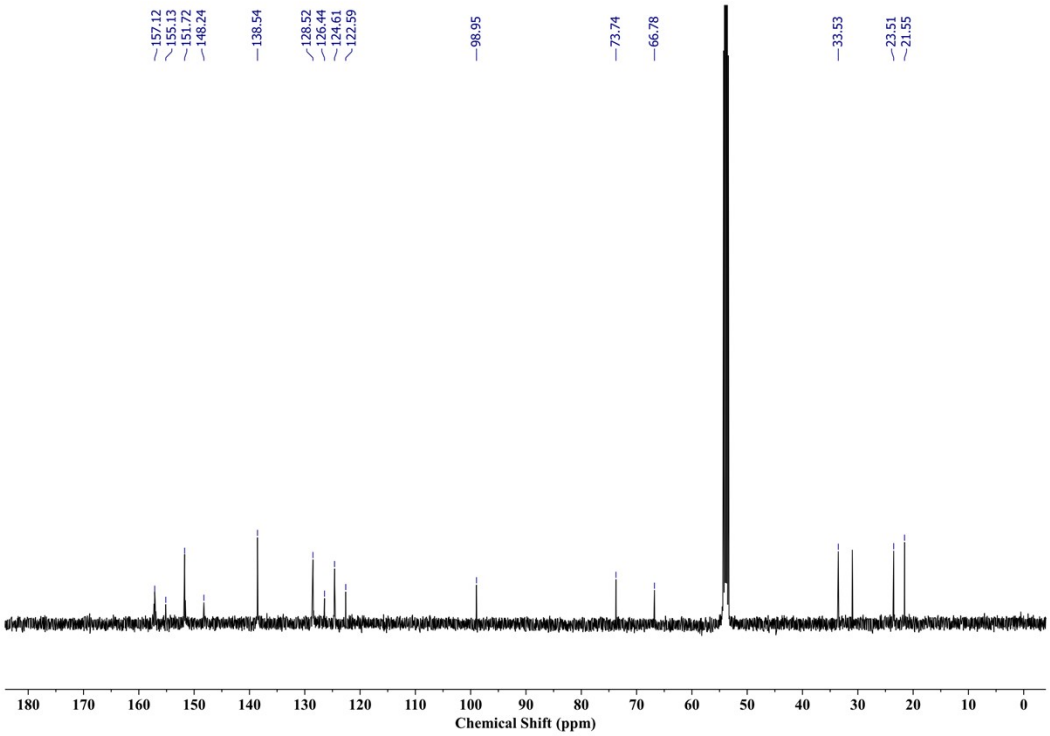

Supplementary Figure 31.
^{13}C NMR spectrum (125 MHz, CD_2Cl_2) for **1b**.

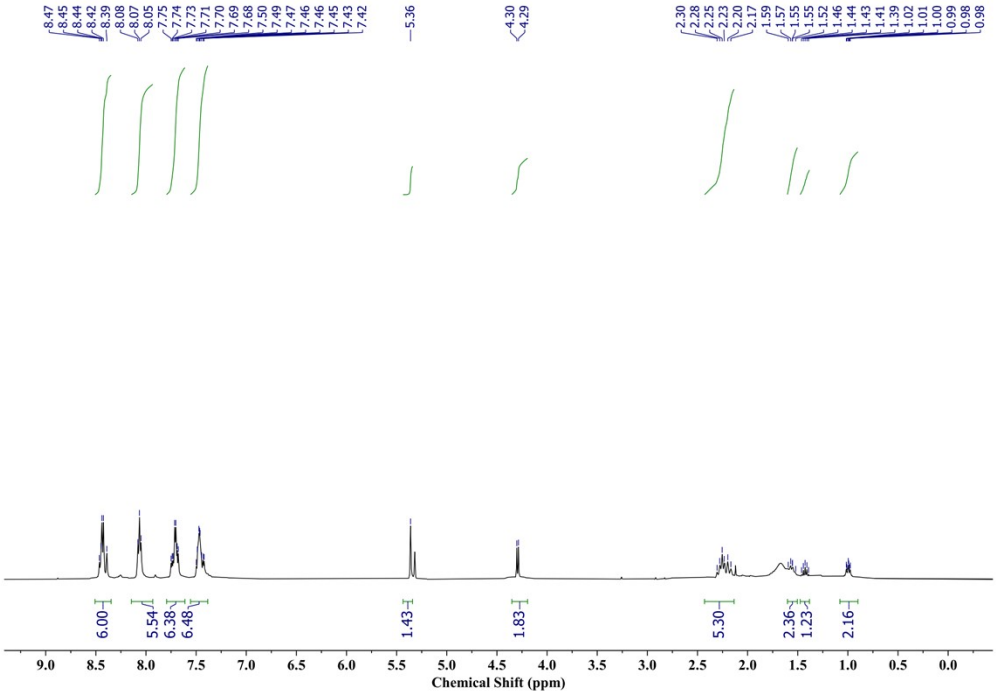

Supplementary Figure 32.
^{1}H NMR spectrum (500 MHz, CD_2Cl_2) for **1c**.

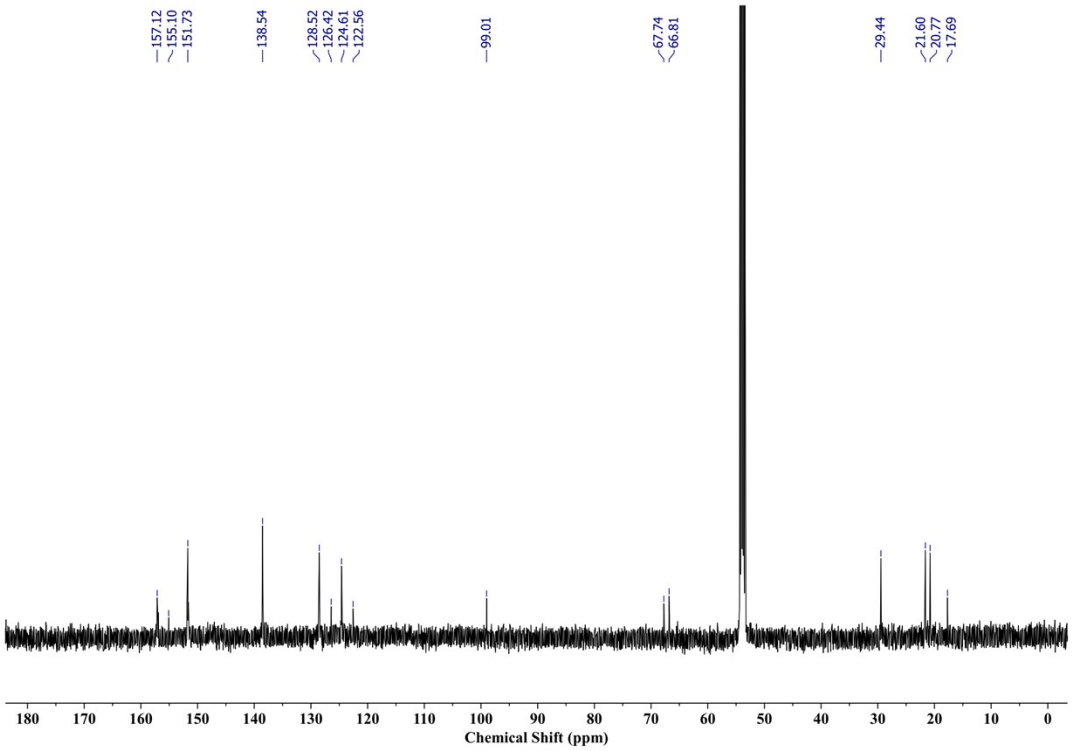

Supplementary Figure 33.
^{13}C NMR spectrum (125 MHz, CD_2Cl_2) for **1c**.

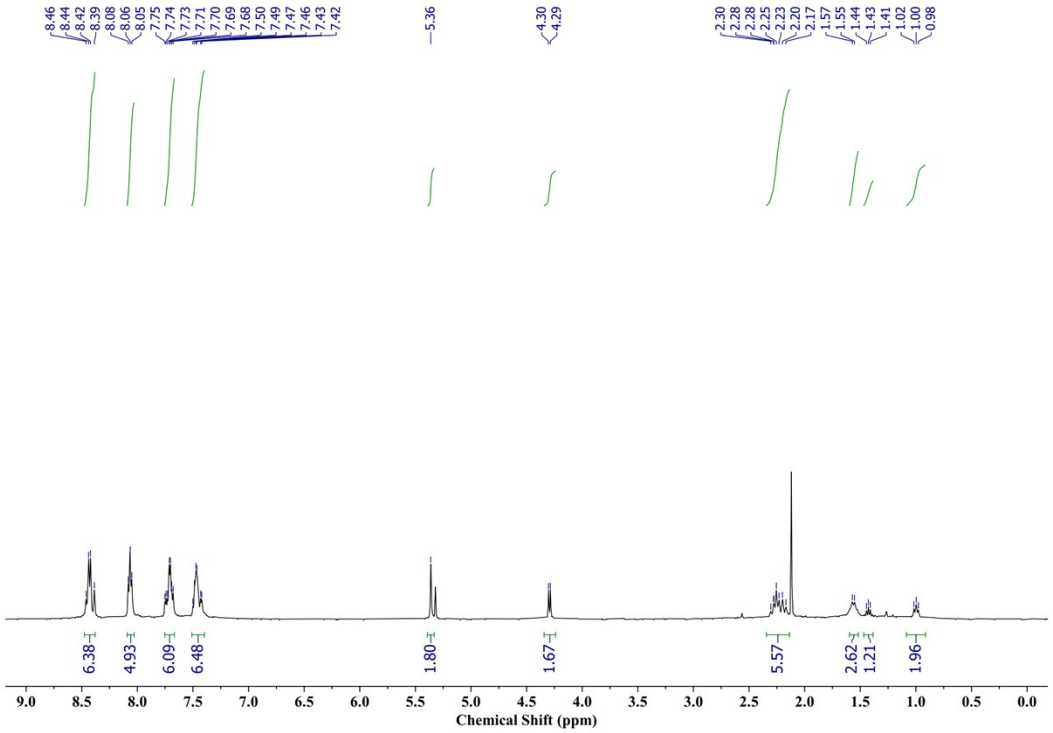

Supplementary Figure 34.
^{1}H NMR spectrum (500 MHz, CD_2Cl_2) for **1d**.

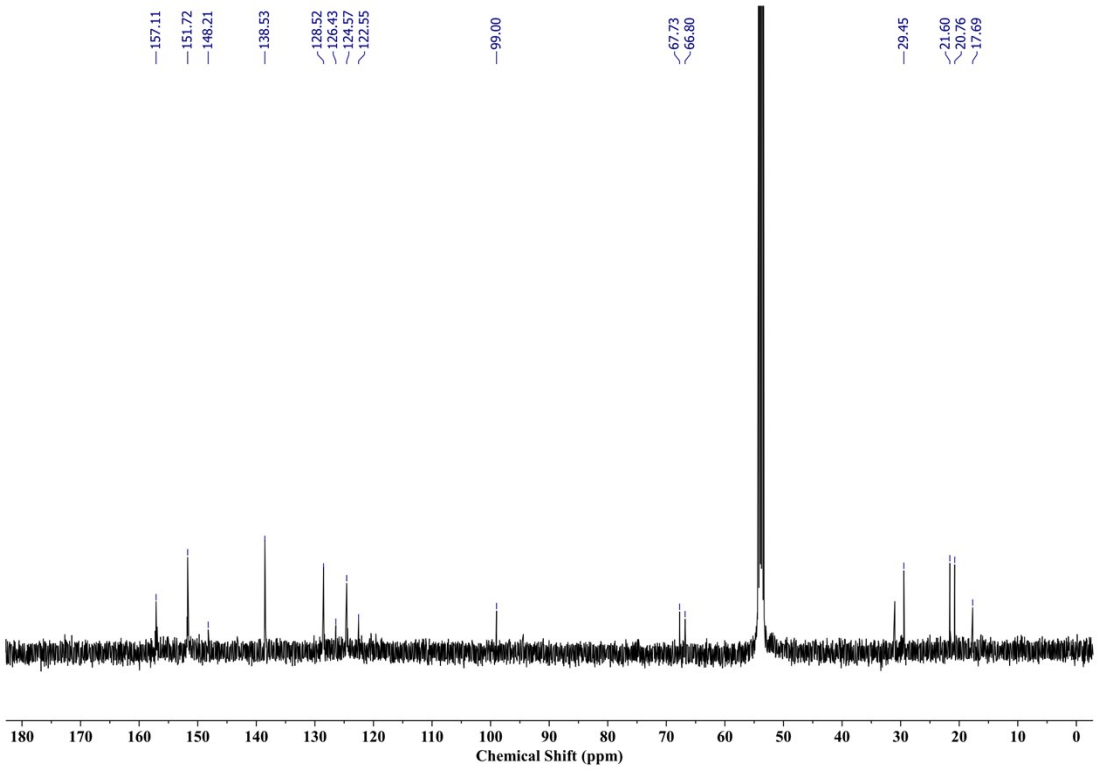

Supplementary Figure 35.
^{13}C NMR spectrum (125 MHz, CD_2Cl_2) for **1d**.

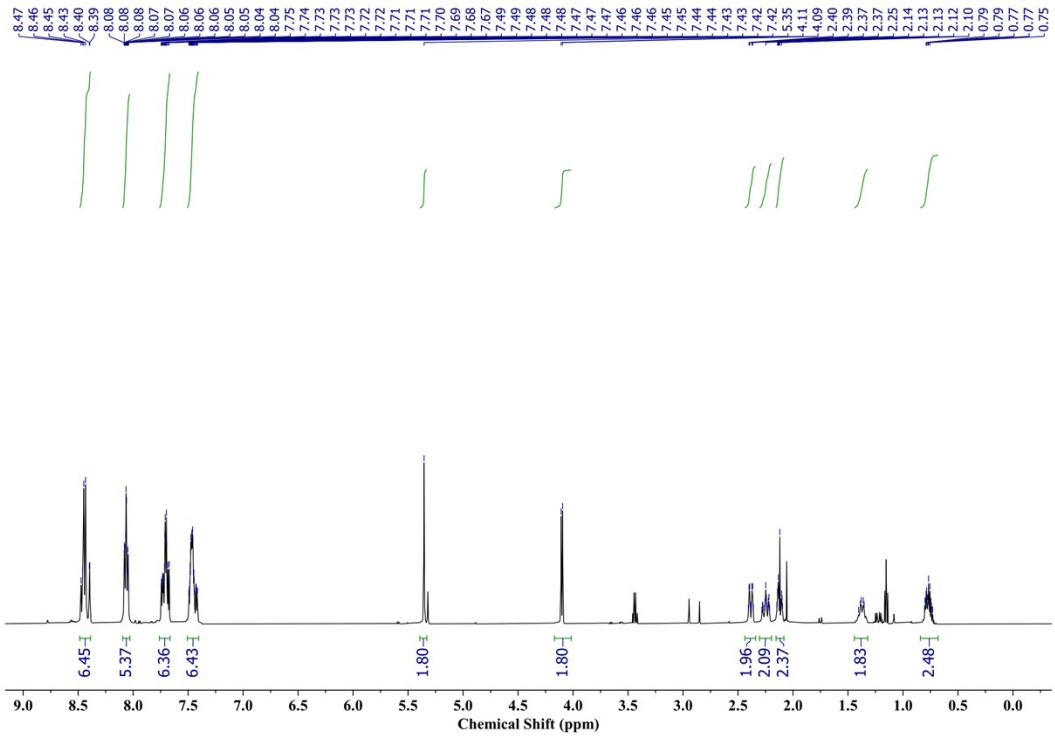

Supplementary Figure 36.
^{1}H NMR spectrum (500 MHz, CD_2Cl_2) for **1e**.

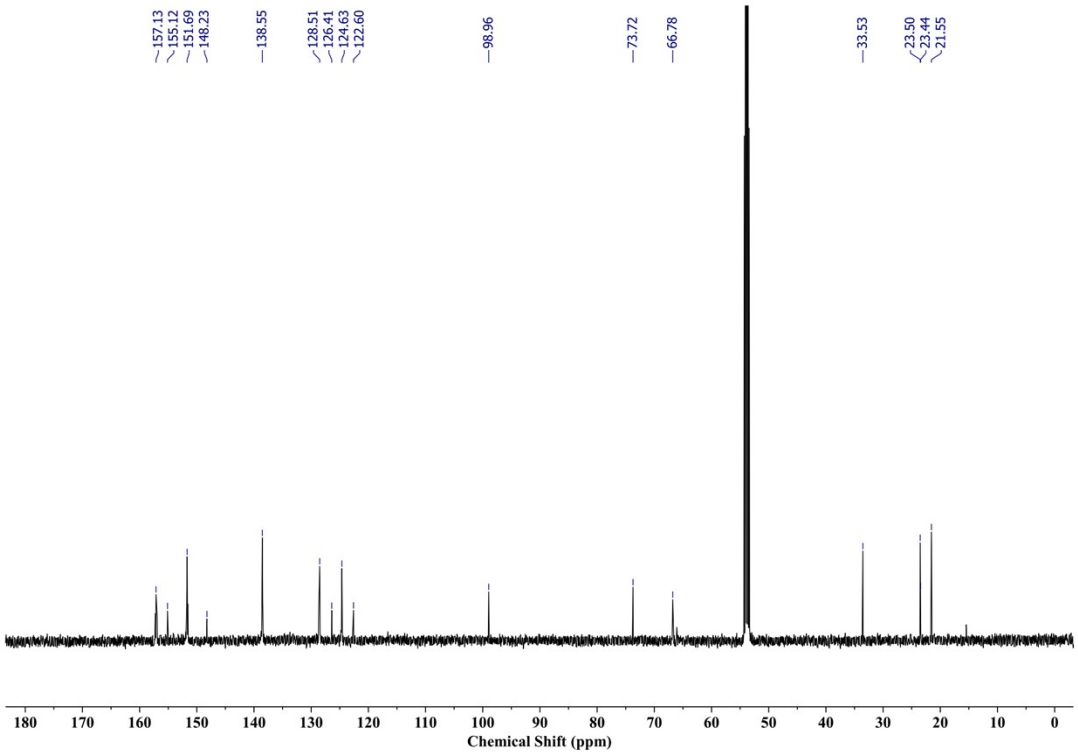

Supplementary Figure 37.
^{13}C NMR spectrum (125 MHz, CD_2Cl_2) for **1e**.

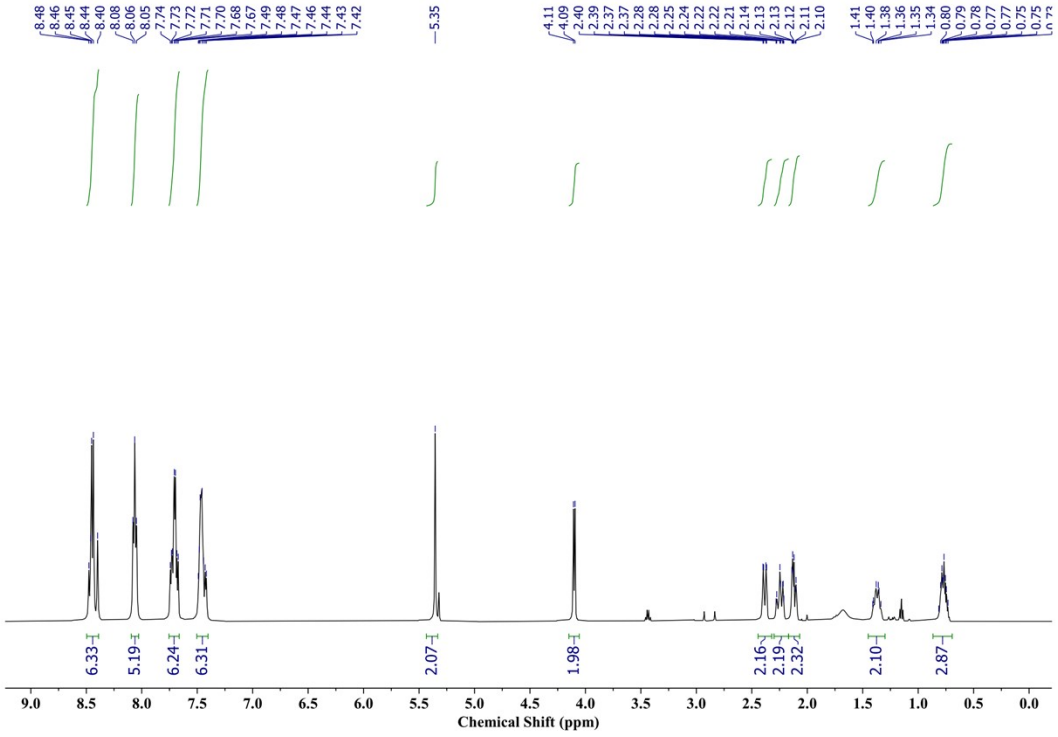

Supplementary Figure 38.
^{1}H NMR spectrum (500 MHz, CD_2Cl_2) for **1f**.

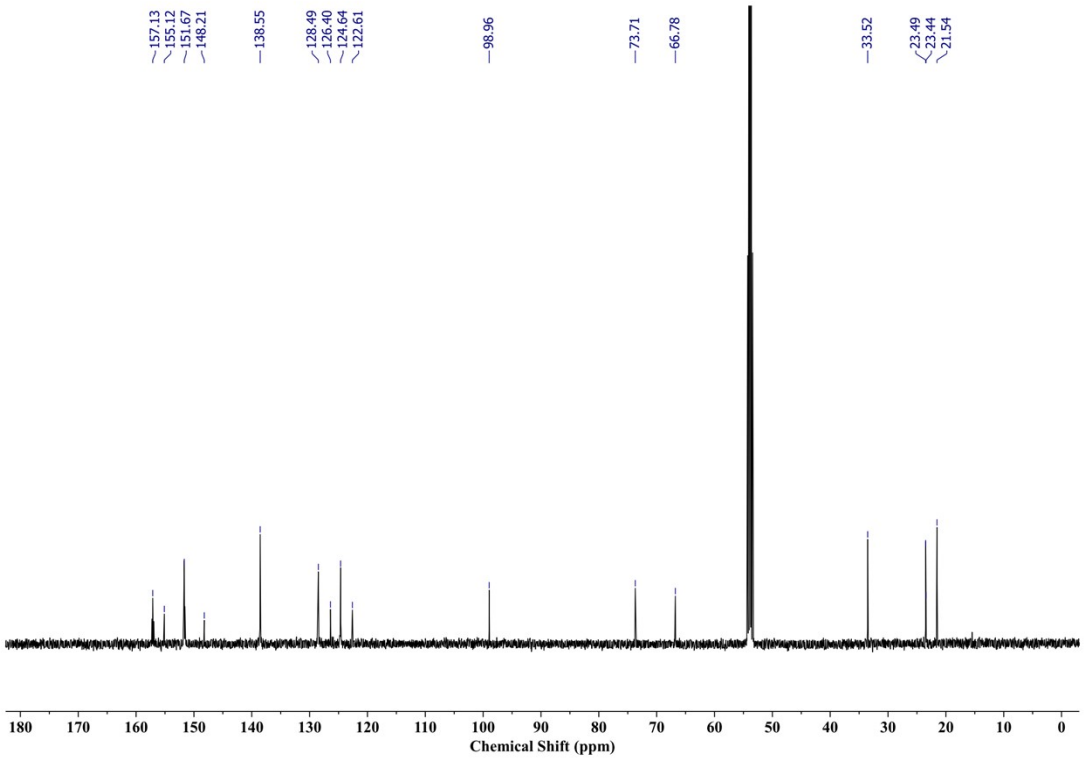

Supplementary Figure 39.
^{13}C NMR spectrum (125 MHz, CD_2Cl_2) for **1f**.

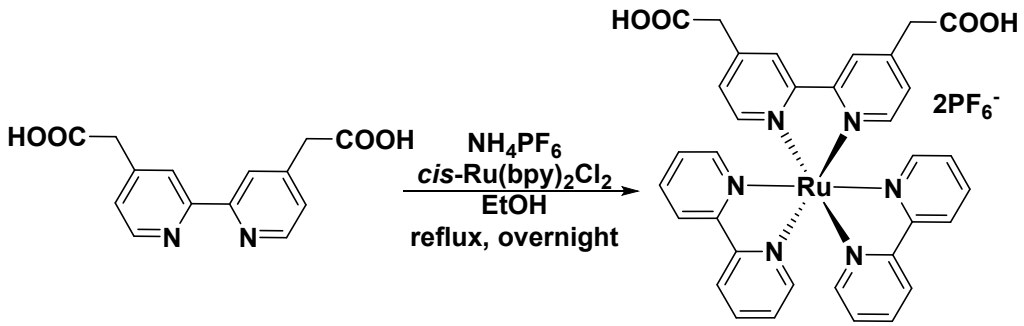

Synthesis of **3e**:
A mixture of bis(bipyridine)ruthenium dichloride (48.4 mg, 0.1 mmol), di-tert-butyl-bipyridine (27.3 mg, 0.10 mmol), and ethanol (10 mL) was degassed and heated to reflux overnight in the dark. After cooling to room temperature, H_2O (50 mL) and DCM (5 × 50 mL) were added. The aqueous layer was collected and concentrated to 10 mL *in vacuo*. Addition of excess amount of NH_4PF_6, the aqueous was washed with DCM/Acetone (5/1) to afford target compound as a red solid. ^1H NMR (500 MHz, CD_3OD): δ 8.68 (dd, J = 8.2, 3.1 Hz, 4H), 8.60 (d, J = 1.9 Hz, 2H), 8.10 (td, J = 7.9, 1.5 Hz, 4H), 7.94 – 7.93 (m, 2H), 7.82 – 7.80 (m, 2H), 7.61 (d, J = 5.8 Hz, 2H), 7.48 (dtd, J = 7.1, 5.6, 1.3 Hz, 4H), 7.36 (dd, J = 5.9, 1.8 Hz, 2H), 3.73 – 3.67 (m, 4H). ^{13}C NMR (125 MHz, CD_3OD): δ 158.74, 158.53, 158.09, 152.93, 152.56, 151.65, 151.46, 138.93, 129.82, 128.88, 128.77, 126.62, 125.48, 125.43, 45.40. ESI-MS: Calcd. $[C_{38}H_{40}N_6Ru]^{2+}$ for 343.0, found 343.0.

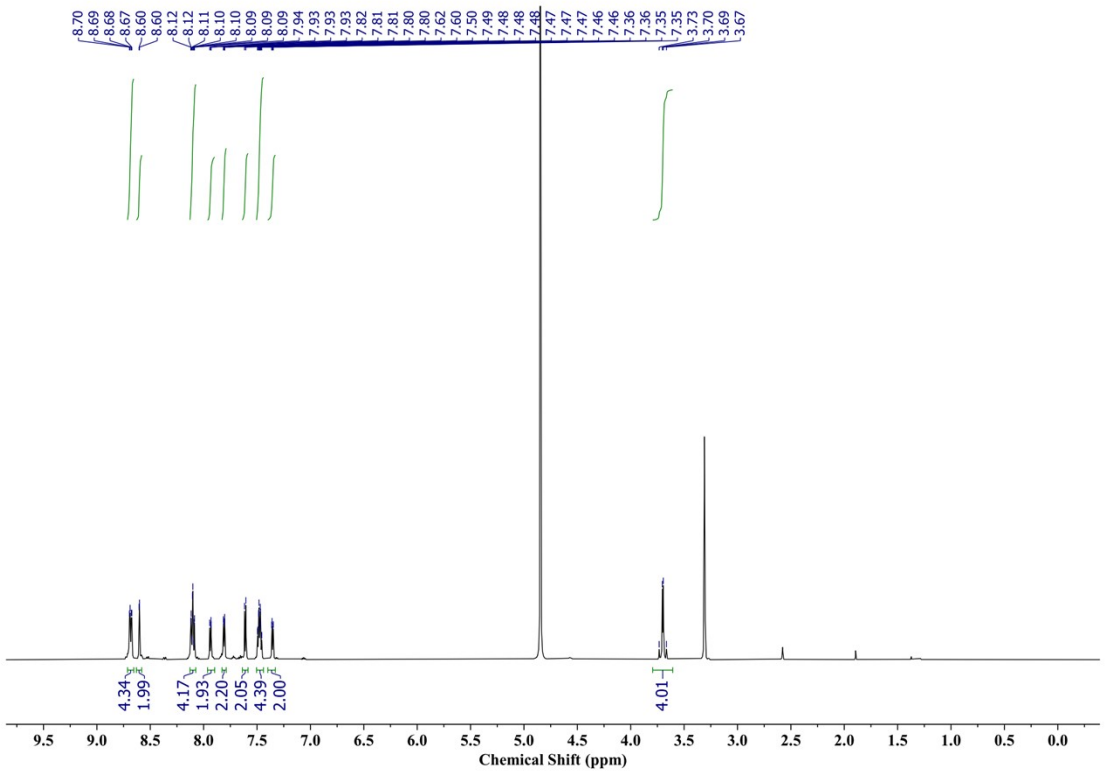

Supplementary Figure 40.
^{1}H NMR spectrum (500 MHz, CD_3OD) for **3e**.

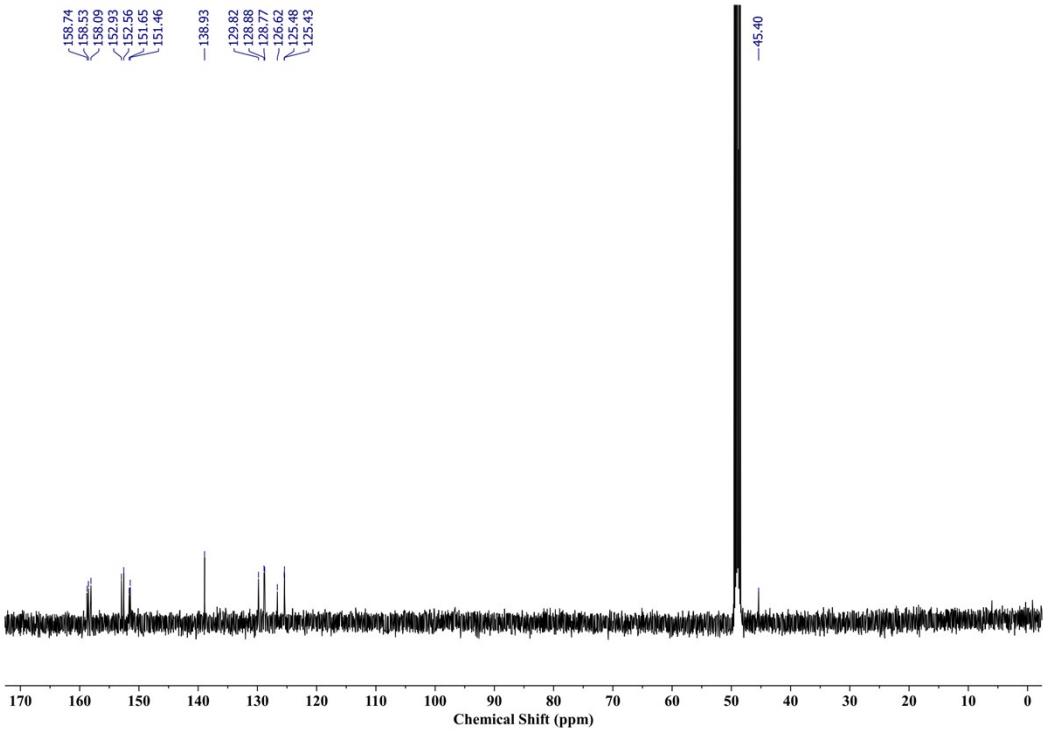

Supplementary Figure 41.
^{13}C NMR spectrum (125 MHz, CD_3OD) for **3e**.

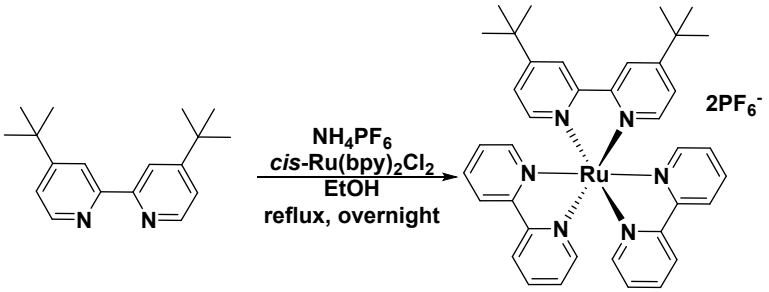

Synthesis of **3g**:

A mixture of bis(bipyridine)ruthenium dichloride (96.8 mg, 0.20 mmol), di-tert-butyl-bipyridine (54 mg, 0.20 mmol), and ethanol (20 mL) was degassed and heated to reflux for 24 h in the dark. After cooling to room temperature, NH_4PF_6 (10 equiv) was added, and the mixture was stirred for 2 h at room temperature. The resulting precipitate was filtered and purified by column chromatography on silica column eluted with DCM/MeOH (100/2, v/v) to obtain the pure complex as a red solid (133 mg, 81%). ^{1}H NMR (500 MHz, CD_3CN): *δ* 8.53 – 8.44 (m, 6H), 8.04 (tdd, *J* = 7.7, 5.6, 1.6 Hz, 4H), 7.71 (d, *J* = 5.7 Hz, 4H), 7.58 (d, *J* = 6.1 Hz, 2H), 7.45 – 7.29 (m, 6H), 1.40 (s, 18H). ^{13}C NMR (125 MHz, CD_3OD): *δ* 163.65, 158.04, 158.01, 157.70, 152.58, 152.46, 151.91, 138.61, 138.58, 128.50, 125.61, 125.16, 122.53, 30.43. ESI-MS: Calcd. $[C_{38}H_{40}N_6Ru]^{2+}$ for 341.1, found 341.1.

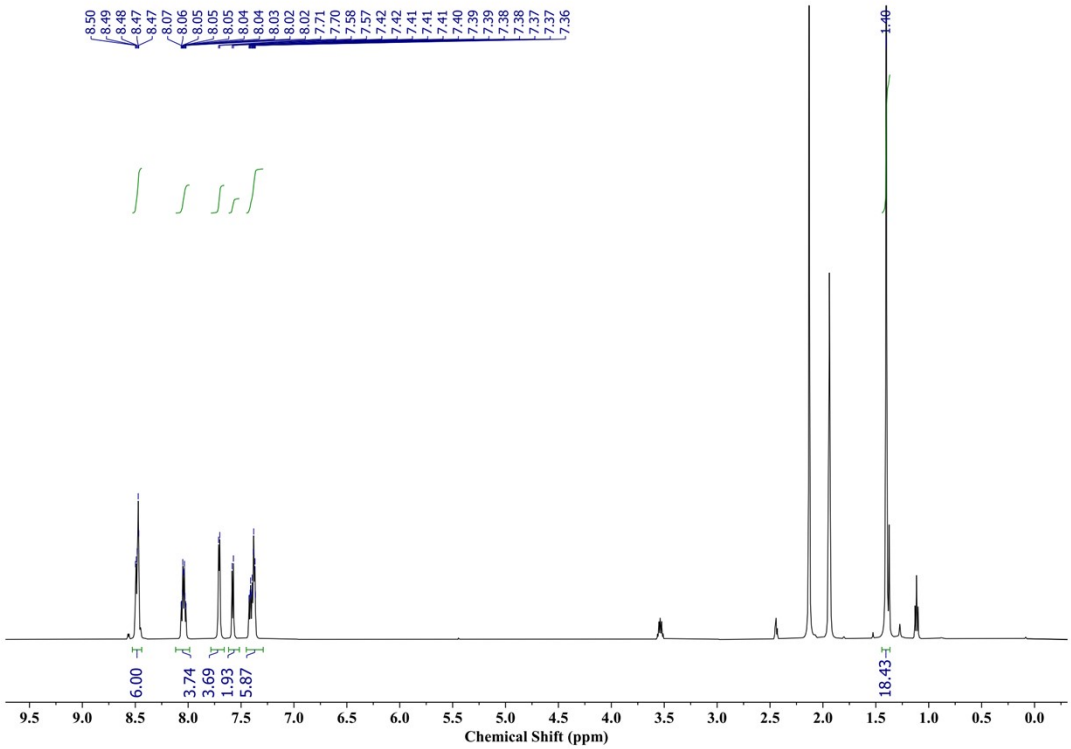

Supplementary Figure 42.

^{1}H NMR spectrum (500 MHz, CD_3CN) for **3g**.

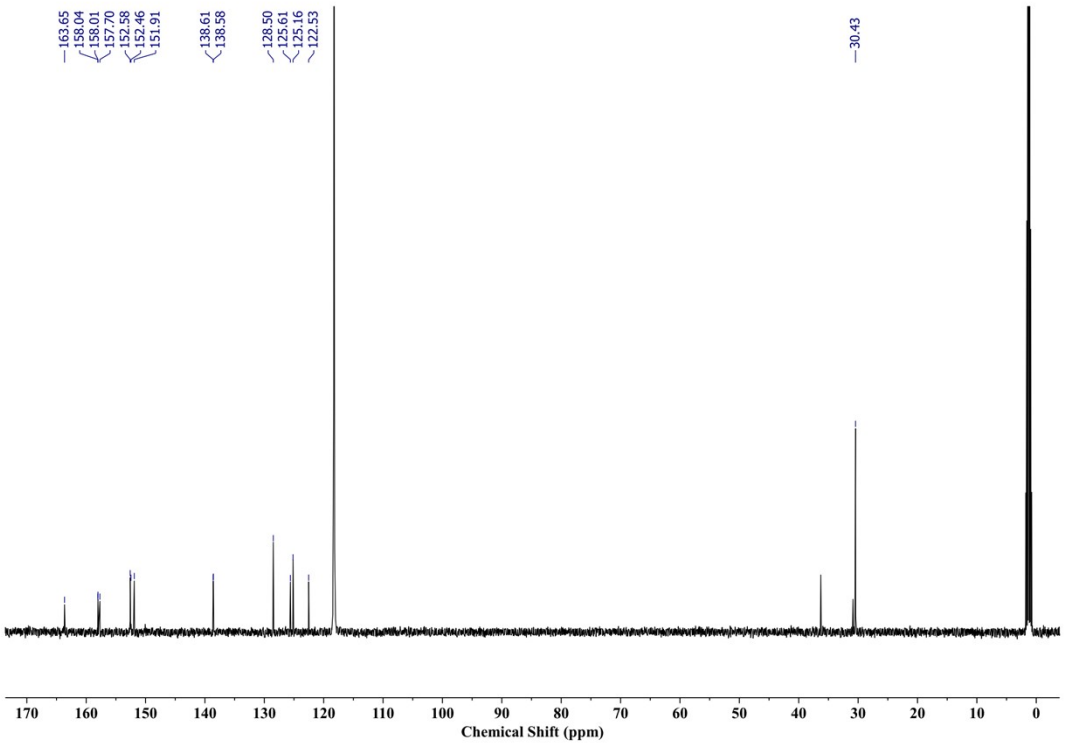

Supplementary Figure 43.
^{13}C NMR spectrum (125 MHz, CD_3CN) for **3g**.

General Synthetic Procedures for AzF, Substrates and Authentic Products

All chemicals and solvents were purchased from Fisher Scientific Co. and used as received unless otherwise noted. Silica gel (60 Å, 230−400 mesh) was purchased from Silicycle Inc. *p*-Azidophenylalanine,[9] **4**,[10] **5**,[10] and **6**[11] were synthesized according to the literature procedures. 4-methoxystyrene was purchased from Sigma Aldrich (St. Louis, MO), stored in the dark, and degassed before storage in an Inert wetbox.

Synthesis of **8**:

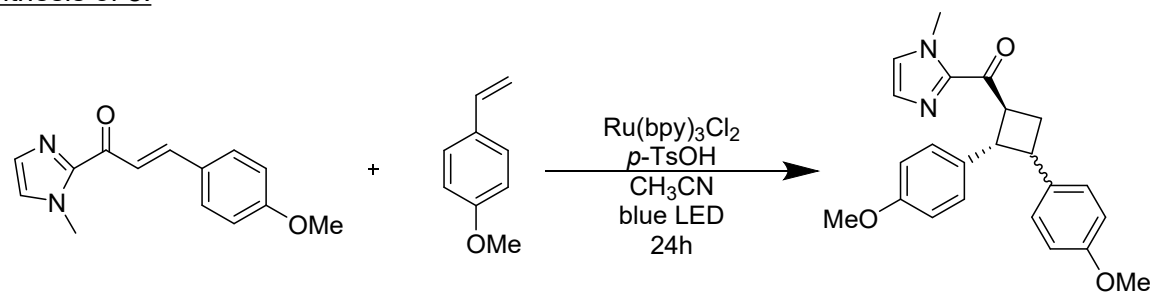

The target compound was synthesized based on a published procedure.[11] In a glovebox, a mixture of cinnamoyl imidazole (96.9 mg, 0.4 mmol), *p*-toluenesulfonic acid monohydrate (15.1 mg, 0.08 mmol), 4-vinylanisole (536 mg, 4.0 mmol), and $Ru(bpy)_3Cl_2$•$6H_2O$ (7.5 mg, 0.01 mmol) in dry MeCN (10 mL) was irradiated by blue LEDs (470 nm) at room temperature for 24 h. The solvent was removed *in vacuo*, and the resulting residue was purified by silica column eluted with Et_2O/hexane (1/1, v/v) to afford a mixture of diastereomers (1.8:1 d.r.) as colorless semisolid (93 mg, 62%). ^1H NMR (400 MHz, $CDCl_3$) *δ*: 7.24 – 7.13 (m, 3H), 7.06 – 6.96 (m, 2H), 6.90 (d, *J* = 8.5 Hz, 1H), 6.84 (d, *J* = 8.6 Hz, 1H), 6.80 (d, *J* = 8.6 Hz, 1H), 6.69 (d, *J* = 8.5 Hz, 1H), 6.61 (d, *J*

= 8.5 Hz, 1H), 4.96 (q, *J* = 8.9 Hz, 0H), 4.51 (q, *J* = 9.5 Hz, 1H), 4.34 (t, *J* = 9.1 Hz, 0H), 4.03 (s, 3H), 3.92 (q, *J* = 8.3, 6.7 Hz, 1H), 3.79 (s, 2H), 3.75 (s, 2H), 3.73 (s, 1H), 3.68 (s, 1H), 3.55 – 3.41 (m, 2H), 2.83 – 2.72 (m, 1H), 2.73 – 2.64 (m, 1H).^{13}C NMR (125 MHz, $CDCl_3$) *δ*: 193.27, 192.70, 158.35, 157.80, 142.76, 142.68, 135.95, 134.89, 133.04, 132.12, 129.35, 129.16, 128.10, 128.09, 127.38, 127.33, 113.92, 113.90, 113.46, 113.27, 55.40, 55.36, 55.26, 55.19, 48.83, 45.47, 45.24, 44.43, 43.46, 41.39, 36.36, 36.30, 32.03, 30.45, 29.83, 28.82. ESI-MS (m/z): calcd for $[C_{23}H_{25}N_2O_3]^+$, 377.18; found m/z 377.18.

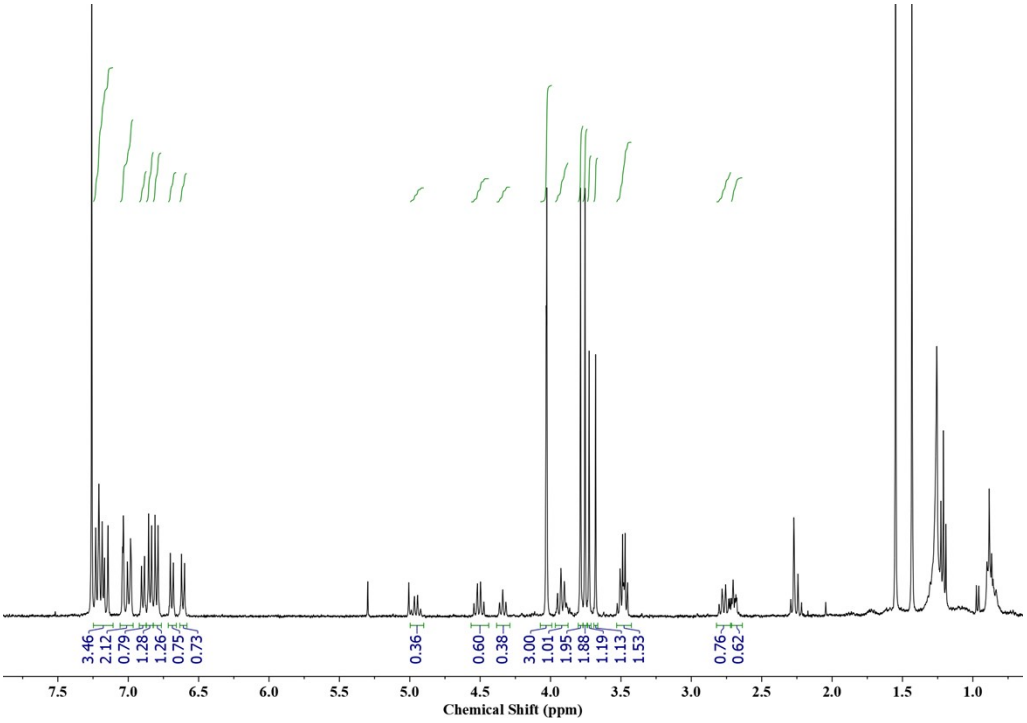

Supplementary Figure 44.
^{1}H NMR spectrum (500 MHz, $CDCl_3$) for **8**.

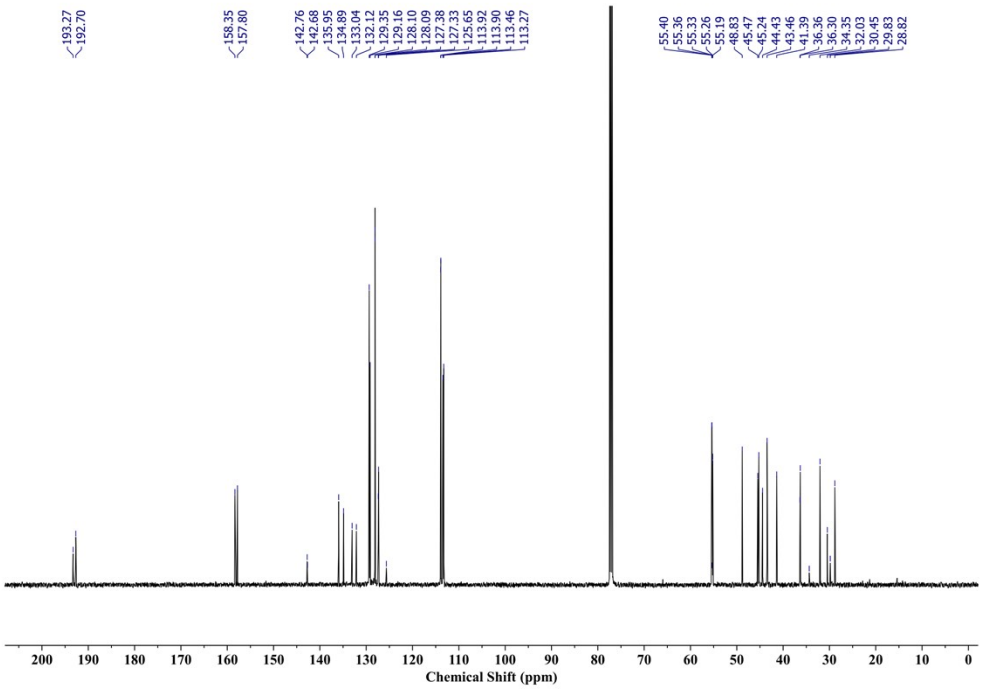

Supplementary Figure 45.
^{13}C NMR spectrum (125 MHz, CD_3CN) for **8**.

Computational Procedures

Docking Simulations

Molecular docking simulations were performed with Chimera AutoDock Vina,[12] and the results were visualized with PyMOL (2.5.0)[13]. Protein structures were prepared from a crystal structure of *Pfu* POP (PDB: 5t88),[14] and cofactor structures were prepared in Avogadro (1.2.0)[15] using existing crystal structures of Ru(II) diimine complexes (CSD: 1115194)[16]. The BCN fragment was built, and ground state geometry optimization of the fragment in the gas phase was performed in Spartan'20 (V1.0.0)[17] using density functional theory. The ωB97X-D functional[18] was employed along with the 6-31G* basis set[19]. Finally, the BCN fragment was fused to the Ru(II) crystal structure in Spartan'20 (V1.0.0)[17]. Since AutoDock Vina is unable to handle 4d metals like ruthenium, the identity of the metal was manually changed to Fe(II) prior to docking.

Preparation of Protein Scaffolds and ArMS

General Materials and Methods

Unless otherwise noted, all reagents were obtained from commercial suppliers and used without further purification. Aqueous solutions were prepared using Milli-Q water. PrimeSTAR Max DNA polymerase master mix was purchased from Takara Bio (Mountainview, CA). Quick Ligase kit, restriction enzymes and CutSmart buffer were purchased from New England Biolabs, Inc (Ipswitch, MA). Vivaspin 20 ultrafiltration units (20 mL volume, 30 kDa cutoff) from Sartorius (Goettingen, Germany) were used to concentrate protein scaffolds and perform diafiltration prior to bioconjugation. QIAquick Gel Extraction Kit and QIAprep Spin Miniprep Kit were purchased from QIAGEN Inc. (Valencia, CA) and used according to the manufacturer's instructions. Diafiltration of ArMs was performed with Amicon Ultra columns (0.5 mL volume, 30 kDa cutoff) from EMD Millipore (Billerica, MA) and used according to the manufacturer's suggestions. WHEATON 0.2 µm nylon syringe filters were purchased from DWK Life Sciences, LLC (Millville, NJ). 0.4 mL 96-well filter plates (0.2 µm, PVDF membrane) were purchased from Agilent Technologies (Santa Clara, Ca). Zeba desalting columns (0.5 mL, 40 kDa cutoff) were purchased

from Thermo-Fisher Scientific (Waltham, MA) and used to prepare samples for analysis by intact protein ESI-MS.

4-methoxystyrene was purchased from Sigma Aldrich (St. Louis, MO), stored in the dark, and degassed prior to storage in an Inert wetbox. All reagents for biocatalysis that were liquids at room temperature were degassed by sparging vigorously with N_2 prior to storing in an Inert wetbox. *p*-Azidophenylalanine was prepared according to protocol[9] described above (*vide supra*). Oligonucleotide primers were purchased from Sigma Aldrich (St. Louis, MO). pEVOL-pAzF[20] was generously provided by Peter Schultz of the Scripps Research Institute, CA. Luria broth (LB) and 2XYT broth were purchased from Research Products International, Corp (Mt. Prospect, IL). LB agar was purchased from BD (Franklin Lakes, NJ). Kanamycin monosulfate was purchased from Alfa Aesar (Ward Hills, MA) and prepared as a 50 mg/mL solution in water. Chloramphenicol (prepared as a 25 mg/mL solution in ethanol), isopropyl β-D-1-thiogalactopyranoside (IPTG, prepared as a 1 M solution in water), and L-arabinose (prepared as a 20% w/v solution in water) were purchased from Chem-Impex International (Wood Dale, IL). Azide agarose resin (cat: 1038-25) was purchased as a 50% slurry in 20% EtOH from Click Chemistry Tools (Scottsdale, AZ). *E. coli* BL21-Gold (DE3) cells were purchased from Agilent Technologies (Santa Clara, CA) and used to prepare electrocompetent cells. DNA Clean and Concentrator kit was purchased from Zymo Research (Irvine, CA) and used to purify DNA after PCR reactions and restriction digests according to the manufacturer's instructions. HisPur Ni-NTA resin and Pierce Coomassie (Bradford) Protein Assay Kit were purchased from Thermo-Fisher Scientific (Waltham, MA). $Ru(Bpy)_3Cl_2$ hexahydrate (cat: 544981-1G), KB_4, tetrabutylammonium chloride $N(C_4H_9)_4Cl$, and benzyltriethylammonium chloride $N(C_2H_5)_3(CH_2C_6H_5)Cl$ were purchased from Aldrich (St. Louis, MO). 1,3,5-trimethoxybenzene (TMB) and trifluoracetic acid (TFA) were purchased from Alfa Aesar (Ward Hills, MA). Tris base, monobasic potassium phosphate, $MgCl_2$, $CaCl_2$, $NaBF_4$, KBr, and HPLC grade ACN were purchased from Fisher Scientific (Waltham, MA). KI was purchased from Santa Cruz Biotechnology Inc. (Dallas, TX). KCl, LiCl, DMAP, pyridine, triethylamine, piperidine, butylamine, morpholine, DBU, aniline, 4-aminophenol, BSA, Z-pro-prolinal (ZPP), and (+)-sodium L-ascorbate were purchased from Sigma Aldrich (St. Louis, MO). NaCl was purchased from Macron Fine Chemicals (Center Valley, PA). NH_4Cl was purchased from VWR International (Radnor, PA). NaBr and CHES were purchased from Acros Organics (Morris Plains, NJ). KPF_6 was purchased from Strem Chemicals (Newburyport, MA). MES was purchased from Chem Impex International (Wood Dale, IL). Tricine was purchased from Research Products International, Corp (Mt. Prospect, IL).

All gene sequences were confirmed by DNA sequencing through QuintaraBio (Boston, MA). Electroporation was carried out on a Bio-Rad MicroPulser™ using method Ec2 (1 pulse; 2.5 kV) with 2mm gap electroporation cuvettes (Fisher Scientific). Aqueous media was prepared using Milli-Q water and sterilized either by autoclaving or by filtration. Antibiotics were prepared as 1,000x stocks and stored at -20°C. Final concentrations for antibiotics used were: Kanamycin at 50 µg/mL and Chloramphenicol at 25 µg/mL. *E. coli* cultures were handled using sterile technique under open flame. DNA was quantified by absorbance at 260 nm and purity was assessed by ratio of absorbance at 260nm/280nm using a Tecan Infinite M200 Pro plate reader with a NanoQuant plate. Protein concentrations were measured using the Pierce Coomassie (Bradford) Protein Assay Kit with a standard curve generated from standard BSA control samples and protein stocks were then flash frozen with liquid N_2 and stored at -80 °C until use. Lyophilization was performed using a LABCONCO benchtop FreeZone freeze dryer (2.5 L) according to the manufacturer's instructions. Standard molecular cloning procedures were followed. Gels were imaged with an Alpha Innotech AlphaImager EP and gel luminescence was visualized using a Typhoon FLA 9500 Imager using default settings for detecting SPYRO Ruby (exc: 450 nm and em: 610 nm; 473 nm laser; LPG/O575; 600 V PMT; 50 µm pixel size). Intact protein mass

spectrometry was performed using a Waters Synapt G2S HDMS using a C18 column. Protein samples were desalted using manufacturer specifications before MS analysis. UV-Vis spectroscopy was performed using a Cary 5000 UV-Vis-NIR spectrophotometer at room temperature after blanking with a solution containing just water using 10 mm pathlength quartz cuvettes. Circular dichroism (CD) spectra were obtained at room temperature on a JASCO J-1500 CD Spectrometer using 10 mm pathlength quartz cuvettes. UHPLC analysis was performed on an Agilent 1290 Infinity UHPLC. Excitation/emission spectra and luminescence lifetime measurements were performed in a low volume cuvette (Hellma Analytics High Precision Cell; 3x3 mm light path; 9,65 centre; Art. No. 105251005965-40) and data was acquired using a FLS1000 Spectrofluorometer (Edinburgh Instruments) with a 450 Xenon lamp or EPL-450 laser for excitation and a Hamamatsu R13456 PMT for detection.

Cloning Procedures

pET28a plasmid vector containing a codon optimized gene for *Pyrococcus furiosus* prolyl oligopeptidase (POP) (cloned using NcoI and XhoI restriction sites upstream of a C-terminal hexa-histidine tag for Ni-NTA affinity chromatography) was previously prepared[14] and used for cloning of all POP variants. POP_{Neut} was previously constructed in our lab using splicing by overlap extension (SOE) PCR[21] and restriction cloning techniques. POP_{Neut} includes the following mutations relative to POP_{WT}: R55A, G99A, W142A, R198A, K255A, Y326A, and R338A. POP_{Neg} was cloned from POP_{Neut} using SOE PCR[21] and restriction cloning techniques. POP_{Neg} includes the following mutations relative to POP_{Neut}: A99D, A142D, and A326D.

SOE PCR was used to introduce more than one mutation at once into a target sequence. Primers were designed as shown in Scheme 1 showing an example in which two mutations are introduced into a target sequence along with overhanging sequences corresponding to restriction enzyme recognition sites.

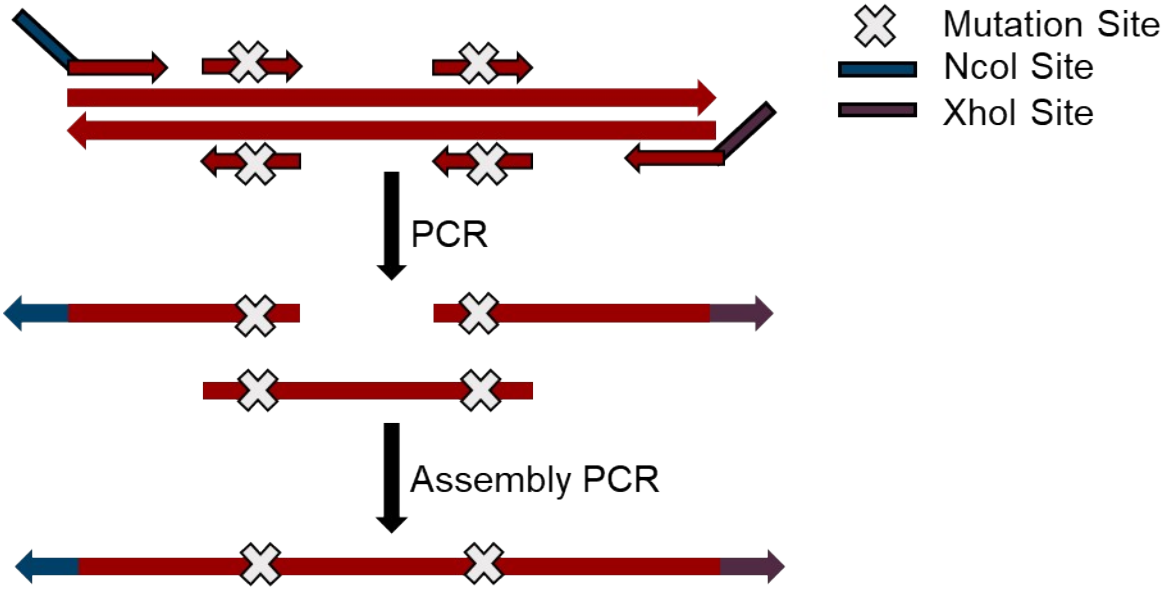

Scheme 1. General workflow and primer design for SOE PCR generation of POP variants containing more than one mutation.

Primers were 20-30 bp long, designed so they introduced NcoI and XhoI recognition sites at the 5' and 3' ends of the gene and did not possess any significant secondary structural elements. PCR was used first to generate fragments in individual reactions using 50 ng of template DNA, 400 nM of each primer, sterilized MQ water, and 2X Primestar Max premix. Thermal cycler was programmed using the following parameters:

1. 98 °C – 120 seconds (initial denaturation)
2. 98 °C – 10 seconds (denaturation)
3. 55 °C – 15 seconds (annealing)
4. 72 °C – variable (elongation) ~5 sec/kb
5. Repeat cycles #2 to #4 28 times
6. 72 °C – 5 minutes (final elongation)
7. 4 °C – hold

PCR fragment products were purified by gel extraction using a commercially available kit from Qiagen. Assembly PCR was set up with 50 ng of each fragment, 400 nM each of the global forward and reverse primers, sterilized MQ water, and 2X Primestar Max premix. Thermal cycler was programmed using the following parameters:

1. 98 °C – 120 seconds (initial denaturation)
2. 98 °C – 10 seconds (denaturation)
3. 55 °C – 15 seconds (annealing)
4. 72 °C – 20 seconds (elongation)
5. Repeat cycles #2 to #4 28 times
6. 72 °C – 5 minutes (final elongation)
7. 4 °C - hold

Assembly products were purified by gel extraction using a commercially available kit from Qiagen. Restriction digests with NcoI and XhoI were then performed according to the manufacturer's guidelines. Insert DNA and vector (pET28a) were digested separately and purified by a standard DNA cleanup kit. Ligations were setup using a Quick Ligase kit from NEB at a ratio of 1:7 vector:insert. Ligated DNA was then transformed directly into electrocompetent cells and colonies were analyzed by colony PCR prior to sequencing.

Supplementary Table 7. Primers used for POP_{Neg} Generation and Sequencing.

Primer name	Primer Sequence
A99D_F	5'- GAA GTC CTG CTG CAG GAC TTT ACC ACG GAC G -3'
A99D_R	5'- CGT CCG TGG TAA AGT CCT GCA GCA GGA CTT C -3'
A142D_F	5'- CAA ACC GTC CAT TGA CAA CAT CAC CTT C -3'
A142D_R	5'- GAA GGT GAT GTT GTC AAT GGA CGG TTT G -3'
A326D_F	5'- GGT TCA CTG GAT CCG CTG GAT AAA G -3'
A326D_R	5'- CTT TAT CCA GCG GAT CCA GTG AAC C -3'
T7-Promoter	5'- TAA TAC GAC TCA CTA TAG GG -3'
T7-Terminal	5'- GCT AGT TAT TGC TCA GCG G -3'

All other variants were constructed using Quikchange[22] mutagenesis to site-specifically introduce mutations. The following PCR conditions were used: 25 µL PrimeSTAR Max premix (2X), 0.8 µM forward primer, 0.8 µM reverse primer, >50 ng template plasmid, adjusted to a final volume of 50 µL with sterile DNase- and RNase-free water.

Thermal cycler was programmed as:
1. 98 °C -120 seconds
2. 98 °C - 10 seconds
3. 55 °C - 15 seconds
4. 72 °C - 150 seconds
5. Repeat cycles from steps #2 to #4 30 times
6. 72 °C - 5 mins
7. 4 °C – hold

An analytical gel (1% agarose) of the PCR reaction (5 µL) was run to confirm successful amplification of the product. The PCR product was then digested with DpnI to degrade template DNA for 2 hours at 37 °C and then stored at 4 °C until further use. The following digestion reaction conditions were used: 45 µL PCR product, 10 µL CutSmart buffer (10X), 2 µL DpnI, and 43 µL sterile DNase- and RNase-free water. The reaction mixture was cleaned using DNA purification kits and transformed into electrocompetent *E. coli* BL21-Gold (DE3) cells. Cells were recovered in LB medium for 1 hour at 37 °C (250 rpm) before spreading on LB agar plates with antibiotics (0.05 mg/mL kanamycin) and incubating at 37 °C overnight. To verify the genotype, individual colonies were inoculated in LB media (with 0.05 mg/mL kanamycin) and grown overnight at 37 °C (250 rpm). Plasmids from these overnight grown cultures were isolated using QiaPrep kits) and sequenced by QuintaraBio (Boston, MA). T7-Promoter and T7-Terminal primers (provided by QuintaraBio) were used for sequencing reactions. Once the genotype was confirmed with sequencing, the plasmid harboring the POP gene was transformed into electrocompetent *E. coli* BL21-Gold (DE3) cells containing pEVOL-pAZF plasmid in the same manner described above except that selection was performed in the presence of both kanamycin (0.05 mg/mL) and chloramphenicol (0.025 mg/mL). Glycerol stocks of cells were prepared with 0.5 mL overnight culture (inoculated from a single colony) and 0.5 mL sterile 50% (v/v) glycerol and stored at -80 °C. All other variants not covered in Supplementary Tables 5-6 (i.e. POP_{GSH}-Z_{477}, POP_{2PL}-Z_{477}, POP_{3H}-Z_{477}, POP_{3L}-Z_{477}, and POP_{5G}-Z_{477}) were generously provided by David Upp and Rui Huang (Indiana University, IN) and arose from directed evolution of dirhodium-POP ArMs[23,24].

Supplementary Table 8. Primers used for POP TAG variant generation.

Primer name	Primer Sequence
53TAG_F	5’- CCA TTG GCT AGG CAC GTA TCA CGA AAA AAG G-3’
53TAG_R	5’- GAT ACG TGC CTA GCC AAT GGT CGG TTG GGA G -3’
53NegTAG_F	5’- GAC CAT TGG CTA GGC AGC TAT CAC GAA AAA AG -3’
53NegTAG_R	5’- GAT AGC TGC CTA GCC AAT GGT CGG TTG GGA G -3’
99TAG_F	5’- CTG CTG CAG TAG TTT ACC ACG GAC GAG GAA GG -3’
99TAG_R	5’- CGT GGT AAA CTA CTG CAG CAG GAC TTC ATC -3’
326TAG_F	5’- GGT TCA CTG TAG CCG CTG GAT AAA GAC GAA G -3’
326TAG_R	5’- CCA GCG GCT ACA GTG AAC CCG GCA CAT CG -3’
338TAG_F	5’- GTT CTG CTG TAG TAC ACC TCG TTT ACG ATT CC -3’
338TAG_R	5’- CGA GGT GTA CTA CAG CAG AAC ACG TTC TTC -3’
399TAG_F	5’- GCG TGG GTT TAG GGC TAC GGC GGT TTC AAC -3’
399TAG_R	5’- GCC GTA GCC CTA AAC CCA CGC GCG TTT TTC -3’
401TAG_F	5’- GTT TTT GGC TAG GGC GGT TTC AAC ATC GCC -3’
401TAG_R	5’- GAA ACC GCC CTA GCC AAA AAC CCA CGC GCG -3’
411TAG_F	5’- CTG ACC CCG TAG TTT TTC CCG CAG GTC ATT C -3’
411TAG_R	5’- CGG GAA AAA CTA CGG GGT CAG GGC GAT GTT G -3’
413TAG_F	5’- CCG ATG TTT TAG CCG CAG GTC ATT CCG TTT C -3’
413TAG_R	5’- GAC CTG CGG CTA AAA CAT CGG GGT CAG GGC -3’

Protein Expression and Purification

Proteins for all applications were expressed in the same manner as described here. 5 mL of LB media (with 0.05 mg/mL kanamycin; 0.02 mg/mL chloramphenicol was also added if AzF was being incorporated) was inoculated from the appropriate glycerol stock and grown overnight at 37 °C (250 rpm). The following day, 5 mL of the O/N culture was used to inoculate 500 mL of 2XYT media with 0.05 mg/mL kanamycin (+ 0.02 mg/mL chloramphenicol if an UAA was to be incorporated) in a 2.8L Fernbach flask. The culture was grown at 37 °C (250 rpm) until the OD_{600} was between 0.6 and 1.0. To induce overexpression from the pEVOL plasmids (required for incorporation of ncAAs), pAzF (1-2 mM final concentration in 500 mL culture) dissolved in 2.5 mL 20% (w/v) L-arabinose and NaOH (~0.1 mL of concentrated base was added until solution became homogenous upon sonication) was added to the culture. To induce overexpression of POP, IPTG (1 mM final concentration) was added, and the cells were grown overnight at 37 °C (250 rpm). The cells were harvested by centrifugation at 3,600 rpm (4 °C) for 30 minutes. The supernatant was discarded, and the pellet was resuspended in 50 mL equilibration buffer (20 mM Na_2HPO_4, 300 mM NaCl, 10 mM imidazole, pH 7.4). The cells were split into 25 mL aliquots (in 50 mL conical tubes) and then stored at -80 °C until lysis.

Cells were lysed by sonication on ice with a cylindrical horn (40 W amplitude, 30 second bursts, 5 minutes 'on' time, 10 minutes total). The cells were then heated at 75 °C for 15 minutes as an initial purification step (since *Pfu* POP is hyperthermophilic), and the lysate was clarified by centrifugation at 12,000 rpm (4 °C) for 30 minutes. The soluble lysate fraction (supernatant) was immediately decanted into a new conical tube. The lysate was loaded onto Ni-NTA resin (5 mL) and the flow-through was discarded. The resin was washed with 10 CV of wash buffer (20 mM Na_2HPO_4, 300 mM NaCl, 20 mM imidazole, pH 7.4). The protein was eluted using 10 CV of elution buffer (20 mM Na_2HPO_4, 300 mM NaCl, 250 mM imidazole, pH 7.4). Diafiltration was then performed with MQ H_2O (for non-covalent ArM scaffolds) or 50 mm Tris, pH 7.4 (for covalent ArM scaffolds). Scaffolds were the aliquoted, flash frozen with liquid N_2, lyophilized, and stored at -80 °C until further use.

SPAAC Bioconjugation

General protocol: The bioconjugation of cofactors **1a-f** to POP was performed by adding 120 µL of the cofactor stock solution (825 µM or 0.88 mg/mL) in ACN to the scaffold solution (480 µL of 75 µM protein in 50 mM Tris, pH 7.4) while shaking at 4 °C, 750 rpm. The mixture was incubated at 4 °C, 750 rpm overnight (12-16) hours using a Thermo Scientific™ Thermal Mixer (with Blocks), at which point the shaking was stopped and 100 µL of a 50% suspension of N_3-agarose resin solution was added to scavenge the free cofactor. The mixture was agitated by end-over-end rotation at 4°C overnight (12-16 hours). After the resin purification was complete, the resin was pelleted by centrifugation at 5,000 rpm for 10 minutes and the supernatant was removed with a pipette. The resin was washed with 500 µL of 50 mM Tris (pH 7.4) and inverted several times. The resin was pelleted by centrifugation at 5,000 rpm for 10 minutes and the supernatant was removed with a pipette. The pooled supernatant fractions containing the ArMs were centrifuged for an additional 10 minutes at 5,000 rpm. The supernatant was removed by a pipette (~1 mL) and then concentrated to 50 µL. Diafiltration was performed using MQ H_2O. ArMs were flash frozen using liquid N_2, lyophilized, and stored at -80 °C until further use. A representative SDS-PAGE gel of proteins pre- and post-bioconjugation is shown in Figure 46. When samples were ready for further experiments, they were transferred into an Inert wetbox and redissolved in MQ H_2O.

Time-course SPAAC: The bioconjugation of cofactors **1a** to POP was performed by adding 120 µL of the cofactor stock solution (825 µM or 0.88 mg/mL in ACN) to the scaffold solution (480 µL of 75 µM protein in 50 mM Tris, pH 7.4) while shaking at 4 °C, 750 rpm. Aliquots of protein were

removed at specific times and diluted to a final concentration of 5 μM protein with MQ H_2O and immediately desalted using Zeba desalting columns (according to the manufacturer's instructions), and filtered through 0.2 μm nylon syringe filters, The mixture was incubated at 4 °C, 750 rpm overnight for 16 hours, at which point the shaking was stopped and a final time point sample was prepared for MS analysis.

Intact protein mass spectrometry was used to analyze the extent of bioconjugation and performed using a Waters Synapt G2S HDMS using a C18 column. A 10-minute LC method (A: H2O with 0.1% formic acid, B = acetonitrile with 0.1% formic acid) with a linear gradient from 95% A to 1% A over 6 minutes followed by a 4-minute flush at 95% A was used with the mass spectrometer recording between 400-2000 Da, providing an LC trace like the representative one in Supplementary Figure 47 (protein retention time = 4.38 mins). Deconvolution of the mass spectrum was performed using a 700-900 M/Z window with a deconvoluted mass range of 70-75 kDa.

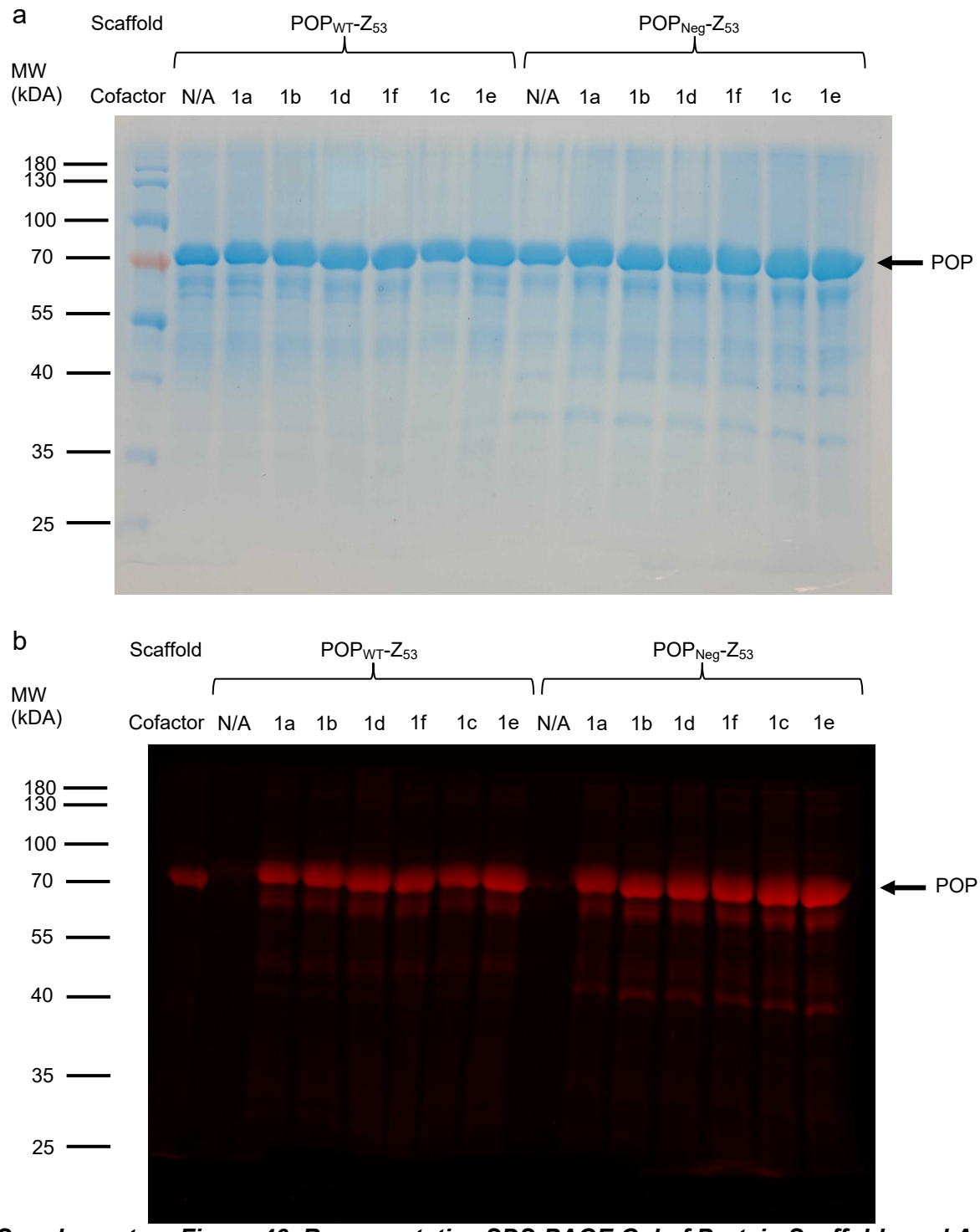

Supplementary Figure 46. Representative SDS-PAGE Gel of Protein Scaffolds and ArMs. SDS-PAGE analysis POP$_{WT}$-Z$_{53}$ and POP$_{Neg}$-Z$_{53}$ before and after bioconjugation to cofactors **1a**-**1f**. PageRuler™ Prestained Protein Ladder (Thermo Fisher), 10 to 180 kDa, was used for reference. 4 µg of each protein sample was loaded onto the gel. Prior to staining with Coomassie Blue, gels were scanned using a Typhoon FLA 9500 Imager using default settings for detecting SPYRO Ruby (exc: 450 nm and em: 610 nm; 473 nm laser; LPG/O575; 600 V PMT; 50 µm pixel size). Only protein that had been bioconjugated to a Ru(II) cofactor luminesced.

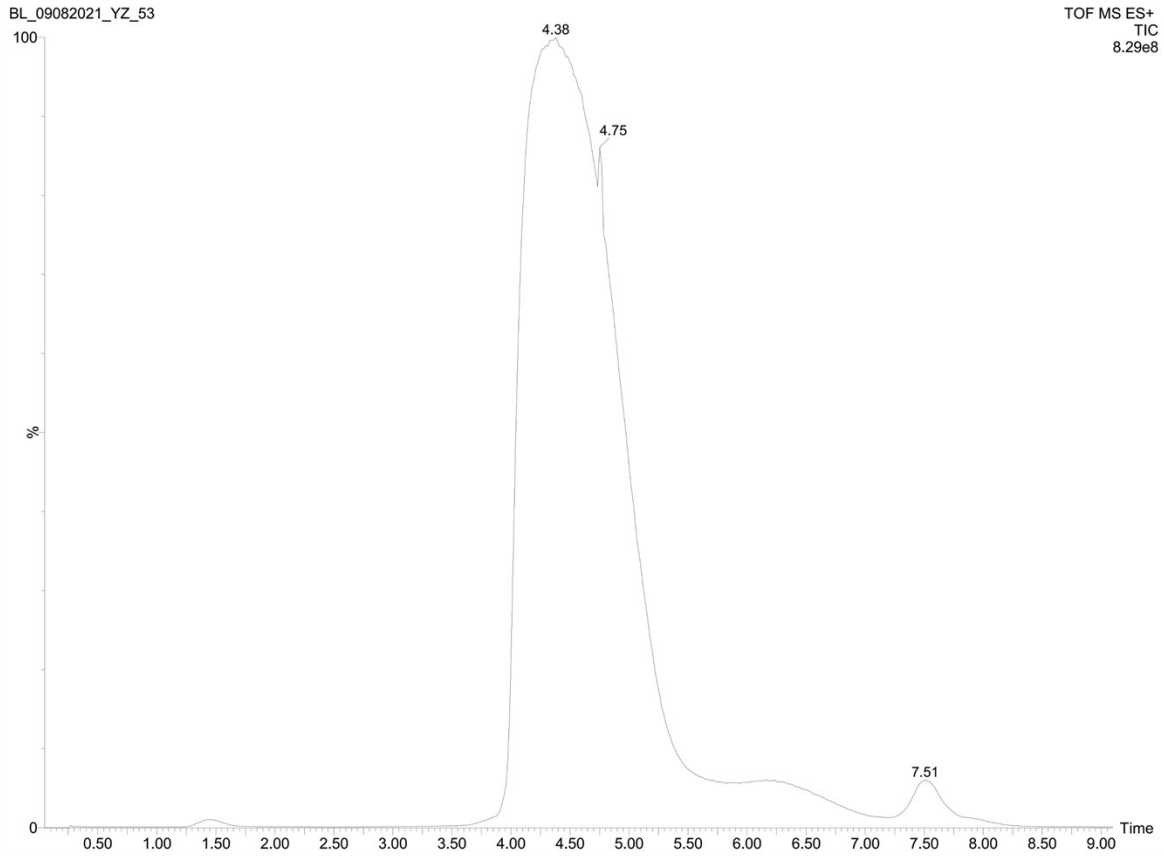

Supplementary Figure 47. Representative LC Trace of POP Variant.
The chromatograms obtained from LC separation of different POP samples were nearly identical. Shown here, is a selected LC trace for POP_{WT}-Z_{53}. In all cases, POP elutes at approximately 4.3 minutes.

Non-Covalent ArM Formation

General Protocol: After lyophilization of protein, samples were transferred into a wetbox and bioconjugated under anaerobic conditions. Protein samples were diluted to approximately 500 µM using MQ H_2O and stock solutions (1 mM) of the Ru(II) cofactor were prepared in MQ H_2O; cofactors that were poorly soluble in water (i.e. those with PF_6^- counterions) were prepared in 10% ACN. Variable amounts of protein (0-300 µM) were added to cofactor so that the final concentration of the metal complex was 5 µM (+/- 0.5% ACN). Samples were incubated for 15 minutes at room temperature prior to measurements unless otherwise notes.

Physical Characterization of ArMs

Intact Protein ESI-MS

Intact protein mass spectrometry was used to analyze the extent of bioconjugation and performed using a Waters Synapt G2S HDMS using a C18 column. A 10-minute LC method (A: H2O with 0.1% formic acid, B = acetonitrile with 0.1% formic acid) with a linear gradient from 95% A to 1% A over 6 minutes followed by a 4-minute flush at 95% A was used with the mass spectrometer recording between 400-2000 Da, providing an LC trace like the representative one in Supplementary Figure 47 (protein retention time = 4.38 mins). Deconvolution of the mass

spectrum was performed using a 700-900 M/Z window with a deconvoluted mass range of 70-75 kDa.

UV-Vis Spectroscopy

ArM samples were diluted to 50 µM with MQ H_2O and free cofactor samples were diluted to 50 µM in 5% ACN/MQ H_2O. UV-Vis spectra were collected at room temperature using a Cary 5000 UV-Vis-NIR spectrophotometer. A spectrum of a blank solution was collected first, and then subtracted from all spectra. 1 scan from 750-300 nm (1 nm step) was performed in a 10 mm pathlength quartz cuvette.

Circular Dichroism Spectroscopy

Circular dichroism (CD) spectra were obtained at room temperature on a JASCO J-1500 CD Spectrometer. CD of cofactors **1a-1f** (0.1 mg/mL) was performed in ACN. CD spectra of ArMs (20 µM) were collected in MQ H_2O. 5 accumulations from 600-170 nm were performed in a 10 mm pathlength quartz cuvette and the following parameters were utilized: 1.0 nm band width, 100 nm/min scan rate, and 0.1 nm data pitch. 20 µM was required to clearly see the features at ~300 nm in ArM samples, but at these high concentrations, the absorbance at wavelengths >280 nm was too high, leading to noisy data. To visualize the secondary structures of the proteins, samples were diluted to 5 µM, where a characteristic peak for POP was observed around 220 nm (Supplementary Fig. 48), matching previously reported spectra[25].

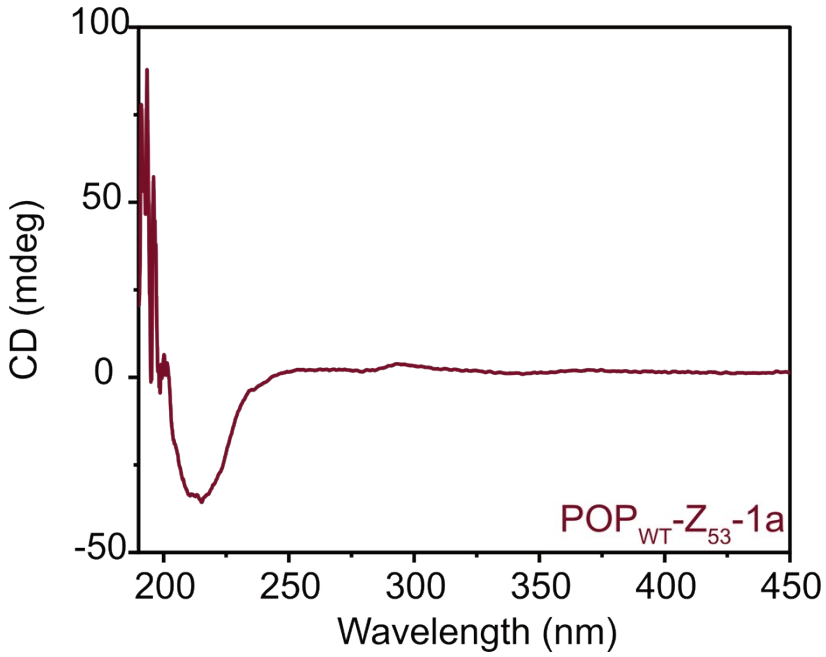

Supplementary Figure 48. Representative CD Spectrum of an ArM Diluted to 5 µM.
CD spectrum of the ArM POP_{WT}-Z_{53}-1a diluted to 5 µM. At the higher concentrations (50 µM) necessary to visualize certain features associated with the Ru(II) cofactor (i.e. Cotton effects near 300 nm), the signal was too high to clearly see secondary structural elements of the protein present in the far-UV region, thus spectra were collected at lower concentrations as well. A deep peak around 220 nm, characteristic of folded *Pfu* POP was observed[25].

Steady-State Luminescence Measurements of ArMs

After preparing ArMs for analysis under anaerobic conditions, the samples were transferred to a low volume cuvette (Hellma Analytics High Precision Cell; 3x3 mm light path; 9,65 centre; Art. No.

105251005965-40). The sample was protected from light, tightly capped with a PFTE stopper, and wrapped with PTFE tape to minimize exposure to air once the sample was removed from the wetbox. Since the photocatalysts form triplet excited states, protection from O_2 was important in minimizing quenching.[26] Luminescence excitation and emission scans were recorded on a FLS1000 Spectrofluorometer (Edinburgh Instruments). The FLS1000 utilizes a 450 Xenon lamp for excitation and a Hamamatsu R13456 PMT for detection. Spectra are corrected for lamp intensity using a silicone reference detector and the emission spectral response was corrected for intensity and wavelength from calibrated lamps. An excitation wavelength of 450 nm (3.00 nm bandwidth) and emission wavelengths of 460-900 nm (3.00 nm bandwidth) were used for emission spectra. Excitation wavelengths of 260-610 nm (3.00 nm bandwidth) and an emission wavelength of 620 nm (3.00 nm bandwidth) were used for excitation spectra. 1.00 nm step sizes and 0.3 s dwell times were used. A total of 3 repeat scans were performed. Steady-state luminescence measurements were performed for covalent ArMs at 50 μM. For non-covalent ArMs, measurements were collected for the respective cofactors at 5 μM +/- 300 μM POP (to compare difference between cofactors before and after binding to the target protein scaffold).

Luminescence Lifetime Measurements of ArMs

General Protocol: Time-correlated single photon counting (TCSPC) luminescence lifetimes were recorded on the FLS1000 using an Edinburgh Instruments EPL-450 laser, with max signal no greater than 5% of the repetition rate to avoid pulse-pileup. Monoexponential tail-fit analysis on a time range of 700 – 3000 ns was performed with the Fluoracle software to determine luminescence lifetimes (an example of this fitting is shown in Supplementary Figure 49). Samples were excited with the EPL-450 laser and emission at 620 nm (8.00 nm bandwidth) was collected unless otherwise noted. ArM samples prepared with cofactors **3e** and **3i** were analyzed at 630 nm and 650 nm, respectively. Covalent ArM measurements were performed with 50 μM samples. Other experiments are described in detail below (*vide infra*). After preparing ArMs for analysis under anaerobic conditions, the samples were transferred to a low volume cuvette (Hellma Analytics High Precision Cell; 3x3 mm light path; 9,65 centre; Art. No. 105251005965-40). The sample was protected from light, tightly capped with a PFTE stopper, and wrapped with PTFE tape to minimize exposure to air once the sample was removed from the wetbox. Since the photocatalysts form triplet excited states, protection from O_2 was important in minimizing quenching.[26]

Free cofactor: 3c

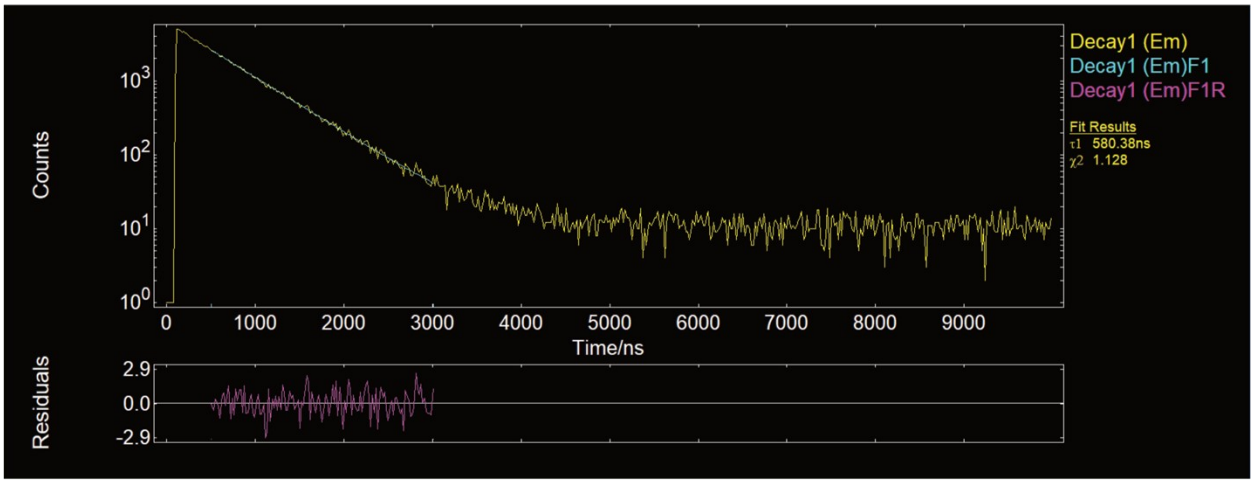

Covalent ArM: POP_{WT}-Z_{53}-1a

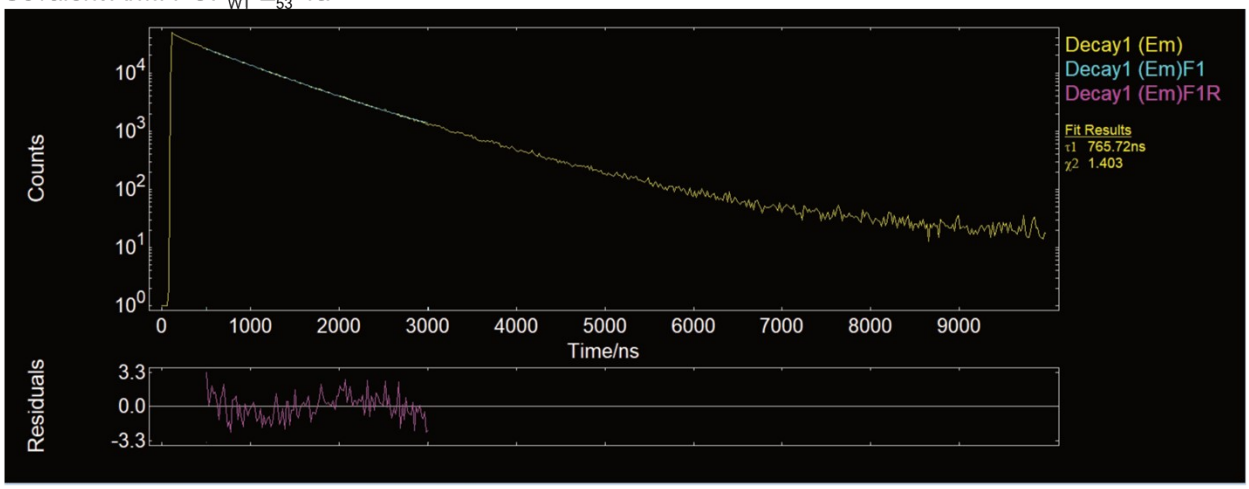

Non-covalent ArM: 200 μM POP_{WT} + 5 μM 3a

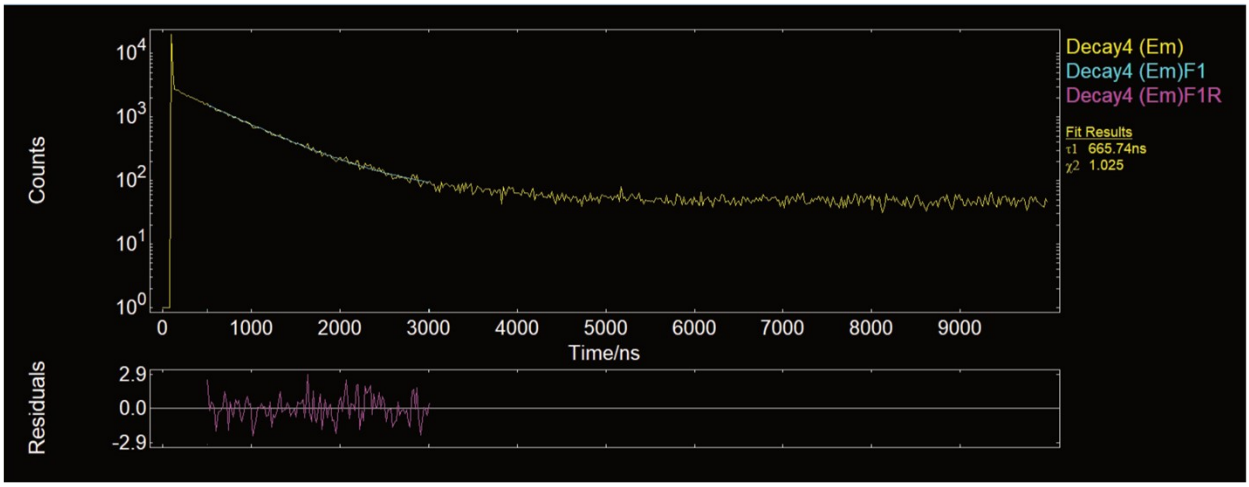

Supplementary Figure 49. Fitting of Representative Luminescence Decays.
Representative luminescence decays (yellow curves) of a free cofactor, a covalent ArM, and a non-covalent ArM. Fits with a monoexponential function (blue) and corresponding residual plots (in pink) are also shown.

Titration Experiments with POP: 0-300 μM of the POP variant of interest was incubated with 5 μM of the cofactor of interest for 15 minutes prior to analysis. Samples were prepared in MQ H_2O; 0.5% ACN was added in cases of poor solubility due to PF_6^- counterions. Triplet excited state luminescence lifetimes were plotted vs. protein concentration, and K_d was determined from nonlinear least-squares fit[27,28] of the binding isotherms assuming a 1:1 binding stoichiometry using the single-site quadratic binding equation, ***Eq. 1*** adapted from Heyduk and Lee[29]:

$Eq.1$:

$$S_i = S_0 + (S_{complex} - S_0) * \left[\left\{K_a * Ru_{tot} + K_a * POP_{tot} + 1 - \sqrt{((K_a * Ru_{tot} + K_a * POP_{tot} + 1}\right.\right.$$
$$(2 * K_a * Ru_{tot})$$

where S_i = luminescence lifetime at any given concentration of POP; S_0 = luminescence lifetime of the free cofactor; $S_{complex}$ = luminescence lifetime of the protein-cofactor complex; K_a = association constant; Ru_{tot} = total concentration of cofactor (5 μM); and POP_{tot} = total concentration of POP in sample (0-300 μM). The quadratic equation was used because the total concentration of the ligand (5 μM) was empirically determined to be within range of K_d (~ an order of magnitude) for the majority of receptor/ligand pairs, meaning that a significant portion of POP would be bound to cofactor, making use of a simpler binding equation inappropriate[30]. Data were plotted in OriginPro 2021 (64-bit) 9.8.0.200 (Academic) and fit with ***Eq.1*** (unweighted) using the SimpleFit function. Variable S_i (y) and POP_{tot} (x) were the dependent and independent variables, respectively. For all other variables except Ru_{tot}, which was known and fixed to 5 μM, optimized values were solved for (i.e. S_0, $S_{complex}$, and K_a). K_d was then determined by taking the inverse of K_a.

For the majority of samples, data was consistent with being in either the 'binding' or 'intermediate' regimes[31] and fitting of data yielded reasonable values for binding affinity. Data obtained for POP_{Neg} was consistent with being in a 'titration' regime, where the concentration of the cofactor was significantly higher than the apparent binding affinity (see work by Jarmoskaite *et al.*[31] for a more detailed discussion) as is apparent by the sharp nature of the titration data. Unfortunately, the concentration of the Ru(II) cofactor could not be reduced enough to where this behavior was not observed due to the inherently low quantum yields of these polypyridyl complexes[26], precluding accurate determination of K_d values. As such, these affinity constants only represent upper-bounds and the actual K_d values might be significantly lower. Simulations have shown that using a constant ligand concentration in ~200-fold excess compared to K_d values resulted in an overestimation of the K_d value by 100-fold,[31] suggesting that POP_{Neg} could be binding the Ru(II) cofactors even tighter compared to POP_{Neut}.

Titration Experiments with BSA: 0-575 μM of BSA (CAS: A2153-100G) was incubated with 5 μM **3a** for 15 minutes prior to analysis. Samples were prepared in MQ H_2O. Measurements were collected as was described above (*vide supra*).

Luminescence Lifetime Time-Course Experiments: 300 μM of either BSA (CAS: A2153-100G) or POP_{Neg} was incubated with 5 μM **3a** for either 15 minutes or 6 hours prior to analysis. Samples were prepared in MQ H_2O. Measurements were collected as was described above (*vide supra*). There was no significant change in lifetime between samples, suggesting that 15 minutes was sufficient for reaching equilibrium (Supplementary Figure 50).

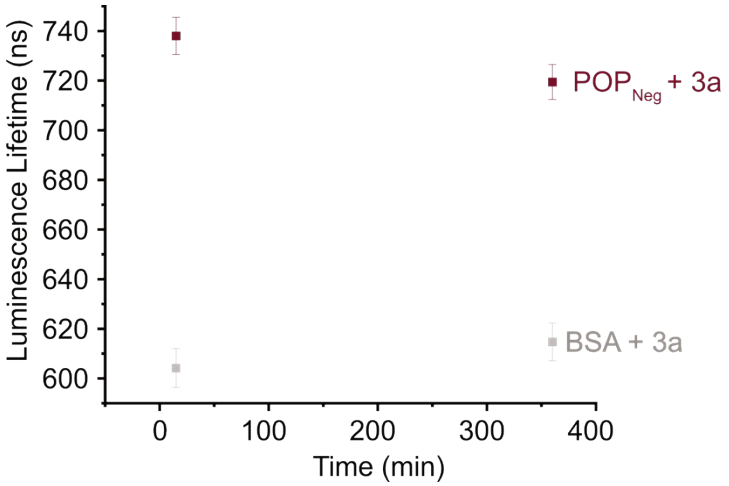

Supplementary Figure 50. Incubation Time vs. Luminescence Lifetime.
The luminescence lifetime of **3a** (5 μM) + POP_{Neg} (300 μM) or BSA (300 μM) did not significantly change between measurements collected after 15 minutes or 6 hours of incubation at room temperature, suggesting that samples reach an equilibrium state within 15 minutes. Plotted data points represent single measurements and error bars represent standard deviations resulting from single exponential tail fitting of decay data.

Titration Experiments with POP and Different Buffers/Salts: 0-300 μM POP_{Neg} was incubated with 5 μM of **3a** for 15 minutes prior to analysis. Samples were prepared either 50 mM KCl, KI, potassium phosphate buffer (pH 7.4), or Tris buffer (pH 7.4). Measurements were collected and data was analyzed as was described above (*vide supra*).

Titration Experiments with POP and Increasing KCl: 100 μM POP_{Neg} was incubated with 5 μM of **3a** for 15 minutes prior to analysis. Samples were prepared in 0-1 M KCl. Measurements were collected and data was analyzed as was described above (*vide supra*). Control samples showed that the luminescence lifetime of **3a** was similar in the absence of POP_{Neg} and presence of either 0 M KCl (588 ns) or 1 M KCl (572 ns).

Competition Assays Between POP and Inhibitor ZPP: 300 μM POP_{Neg} was preincubated with 0-1000 μM ZPP (SML0205-5MG). Then, the samples were incubated with 5 μM **3a** for 15 minutes prior to analysis. Samples were prepared in 10% ACN/MQ H_2O. Measurements were collected and data was analyzed as was described above (*vide supra*). Control experiments without POP_{Neg} showed that increasing concentrations of ZPP did not significantly affect the luminescence lifetime of **3a** (Supplementary Figure 51).

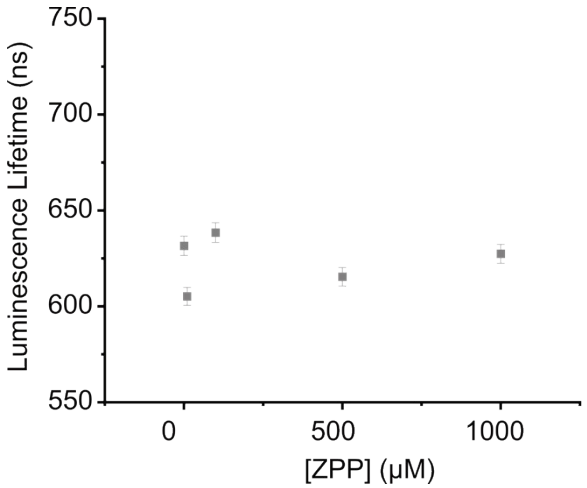

Supplementary Figure 51. Luminescence Lifetime of 3a vs. ZPP Concentration.
The luminescence lifetime of **3a** (5 μM) without POP_{Neg} did not significantly change with increasing concentrations of ZPP. Plotted data points represent single measurements and error bars represent standard deviations resulting from single exponential tail fitting of decay data.

Centrifugal Wash Experiments with Varying Ionic Strength

The following wash experiments were performed under ambient conditions. 400 μL samples of POP_{Neg} (95 μM) and **3a** (5 μM) were prepared in MQ H_2O. 10 mL of either MQ H_2O, 50 mM salt solution (LiCl, NaCl, $MgCl_2$, $CaCl_2$, NH_4Cl, KBr, KBF_4, or KPF_6), 10 mM salt solution (LiCl, NaCl, $MgCl_2$, $CaCl_2$, NH_4Cl, $N(C_4H_9)_4Cl$, $N(C_2H_5)_3(CH_2C_6H_5)Cl$, KBr, KBF_4, or KPF_6), 25 mM MES (pH 6.0), or 50 mM sodium ascorbate was used to dilute the non-covalent ArM samples. Samples were then concentrated to 1 mL in a 30 kDa MWCO spin filter. The luminescence intensities (λ_{exc} = 450 nm, λ_{em} = 620 nm) of the samples were determined using a Tecan Infinite M200 Pro plate reader. A control sample was prepared in 1 mL and not subjected to the wash (i.e. 38 μM POP_{Neg} and 2 μM **3a**).

Catalytic Characterization of ArMS

General Protocol for Reductive Cyclization of Dienone **4**

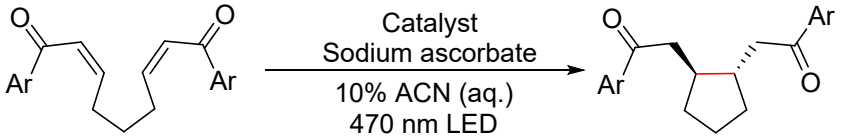

4 (25 μM) **5**

The reductive cyclization reactions were prepared in a wetbox under inert N_2 atmosphere using black 96 well plates with transparent and flat bottoms, unless otherwise noted. A typical 100 μL reaction was set up using stock solutions of the dienone **4** (250 μM in ACN), 100 mM sodium ascorbate (in MQ H_2O), and catalyst (either **3a** or an ArM dissolved in MQ H_2O). The final concentrations of each component are as follows: 25 μM **4**, 50 mM ascorbate, 25 nM catalyst, and 10% ACN. Reactions were irradiated on the custom LED photoreactor for 60 minutes in the wetbox without agitation. Typically, reactions were run in triplicate (n=3) and yields are reported as averages and standard deviations. After incubation, 100 μL of 3 mM TMB in ACN was added to the reaction under aerobic conditions. Samples were centrifuged at 3,600 rpm for 10 minutes. The supernatant was filtered through a 0.2 μm filter plate prior to analysis by achiral UHPLC. Yields were determined by a calibration curve prepared using isolated authentic product **5** and TMB (Supplementary Figure 52).

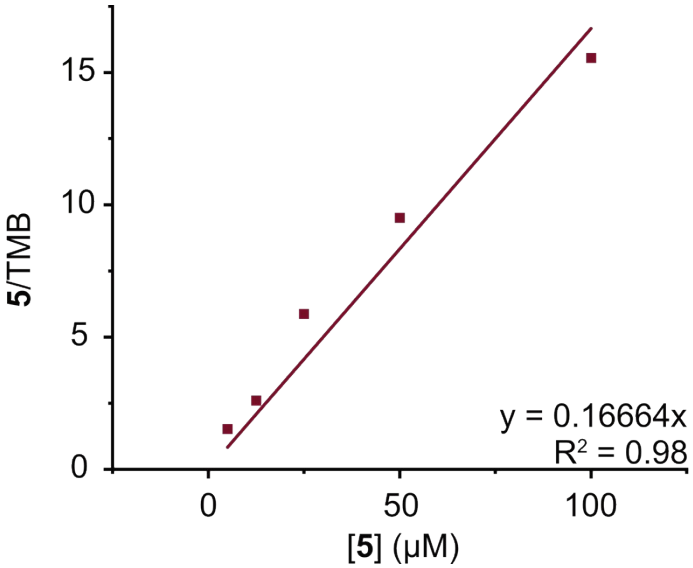

Supplementary Figure 52. Calibration Curve of 5 and TMB.

A calibration curve was generated to determine the yield of desired product **5** from UHPLC analysis. Samples were prepared by mixing 5 - 100 μM of **5** with 1.5 mM TMB in 30% ACN. Samples were filtered through a 0.2 μm filter prior to analysis. Each data represents the integration of the product peak divided by the integration of the IS peak (Pdt/IS) at different concentration of **5**. Each data point was collected in singlicate and data were fit with a linear regression.

For UHPLC analysis, a 5 cm Eclipse Plus C18 column was used with a guard column. The mobile phase consisted of A: H_2O + 0.1% TFA, B: ACN + 0.1% TFA. Method: 10% B to 100% B over 3.3 minutes, 1 minute at 100% B, 100% B to 10% B over 0.05 minutes, and 1-minute post-time. A flow rate of 0.3 μL per minute was used. 5.0 μL of each sample was injected and elution of compounds was followed by monitoring absorbance at 280 nm. Representative traces of from reaction mixtures are shown below (Supplementary Figure 53).

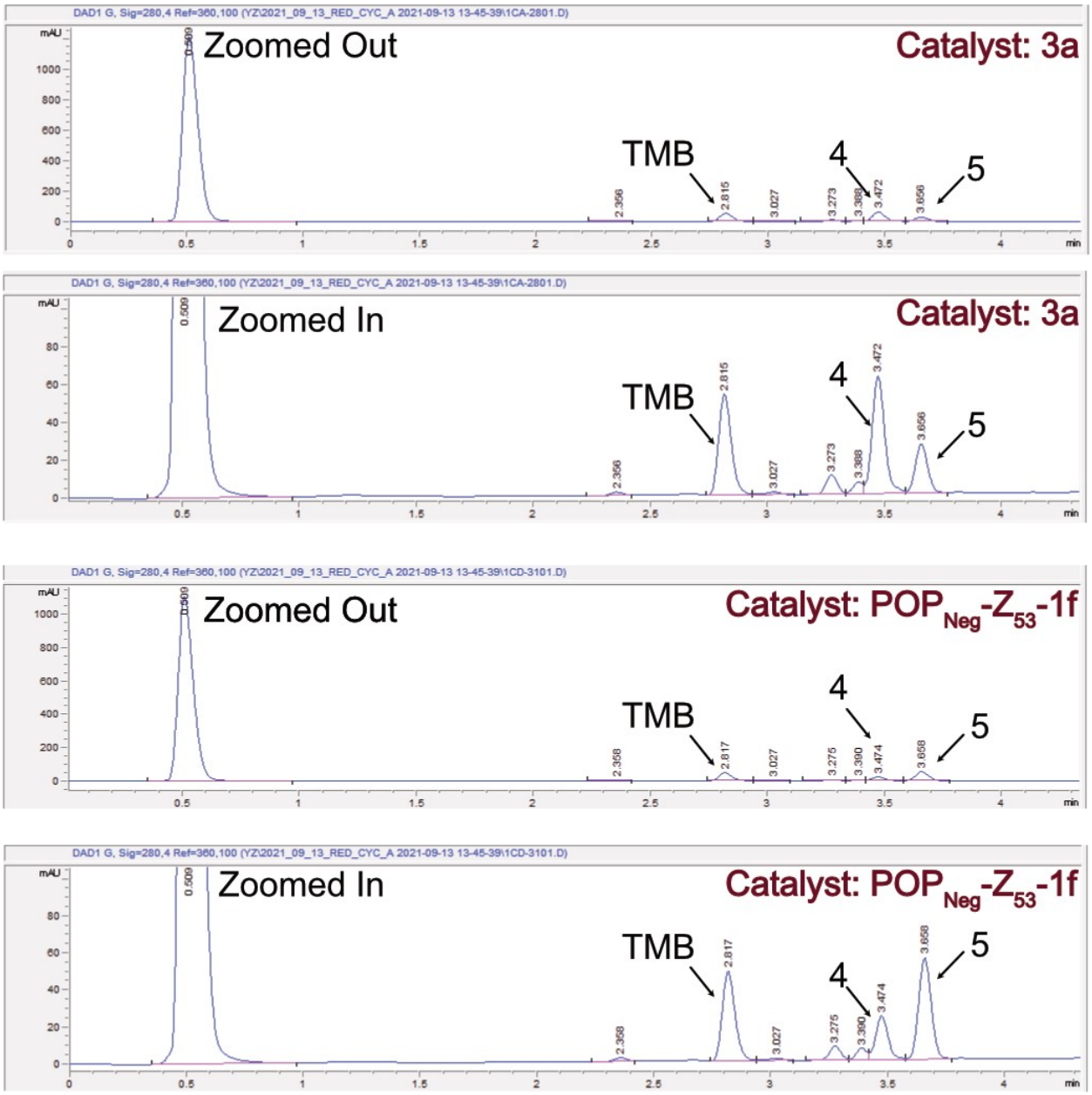

Supplementary Figure 53. Representative UHPLC Traces for Reductive Cyclization Reactions.

Chromatograms of 30-minute reactions from time course experiments (see Supplementary Figure 19). Both 'zoomed out' and 'in' views are shown. At around 0.5 minutes, a large signal associated with ascorbate is seen. The internal standard TMB, substrate **4**, and product **5** are labeled on each trace.

General Protocol for [2+2] Photocycloaddition of Substrates **6** and **7**

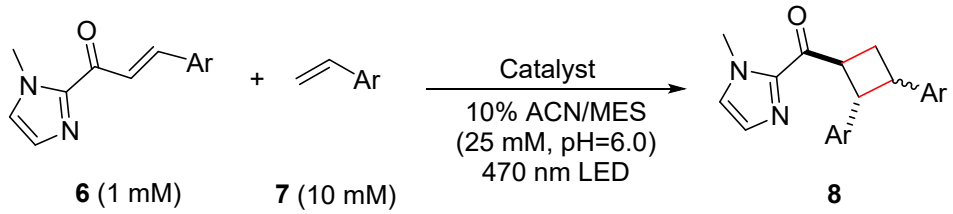

6 (1 mM) **7** (10 mM) **8**

The [2+2] photocycloaddition reactions were prepared in a wetbox under inert N_2 atmosphere using glass vials with a PE screw cap (12x35 mm), unless otherwise noted. A typical 100 µL reaction was set up using stock solutions of the *C*-cinnamoyl imidazole **6** (20 mM in ACN), 4-methoxystyrene **7** (200 mM in ACN), 50 mM MES (pH 6.0), and catalyst (either **3a** or an ArM dissolved in MQ H_2O). The final concentrations of each component are as follows: 1 mM **6**, 10 mM **7**, 25 mM MES (pH 7.4), 10 µM catalyst, and 10% ACN. Reactions were irradiated on the custom LED photoreactor for 2 hours in the wetbox without agitation. Typically, reactions were run in triplicate (n=3) and yields are reported as averages and standard deviations. After incubation, 100 µL of 10 mM TMB in ACN was added to the reaction under aerobic conditions. Samples were centrifuged at 10,000 rpm for 10 minutes. The supernatant was filtered through a 0.2 µm filter plate prior to analysis by achiral UHPLC. Yields were determined by a calibration curve prepared using isolated authentic product **8** and TMB (Supplementary Figure 54).

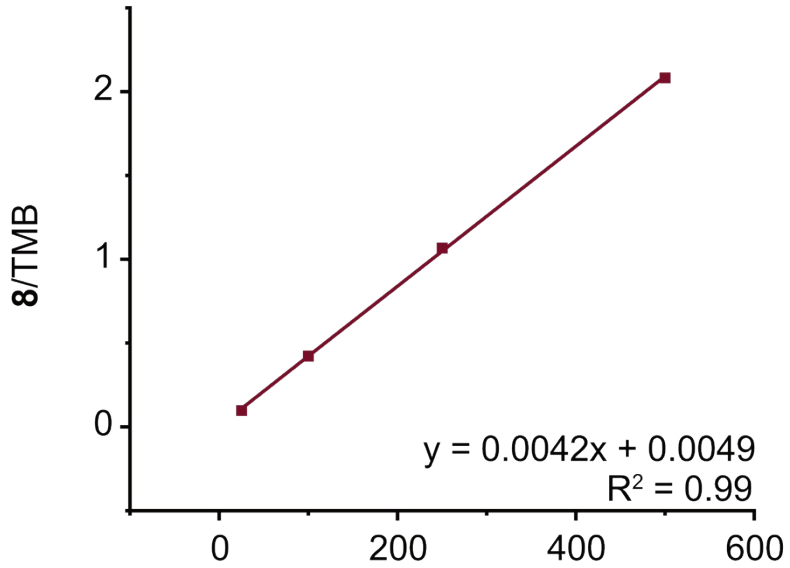

Supplementary Figure 54. Calibration Curve of 8 and TMB.
A calibration curve was generated to determine the yield of desired product **8** from UHPLC analysis. Samples were prepared by mixing 0.025 – 0.5 mM of **8** with 5 mM TMB in 30% ACN. Samples were filtered through a 0.2 µm filter prior to analysis. Each data represents the integration of the product peak divided by the integration of the IS peak (Pdt/IS) at different concentration of **8**. Each data point was collected in singlicate and data were fit with a linear regression.

For UHPLC analysis, a 5cm Eclipse Plus C18 column was used with a guard column. The mobile phase consisted of A: H_2O + 0.1% TFA, B: ACN + 0.1% TFA. Method: 10% B to 45% B over 3 minutes, 45% B to 55% B 2.5 minutes, 55% B to 100% B over 1.5 minutes, 1.5 minutes at 100% B, 100% B to 10% B over 0.01 minutes, and 1-minute post-time. A flow rate of 0.4 µL per minute was used. 5.0 µL of each sample was injected and elution of compounds was followed by

monitoring absorbance at 254 nm. Representative traces of **6**, **7**, **8**, TMB, and reaction mixtures are shown below (Supplementary Figure 55).

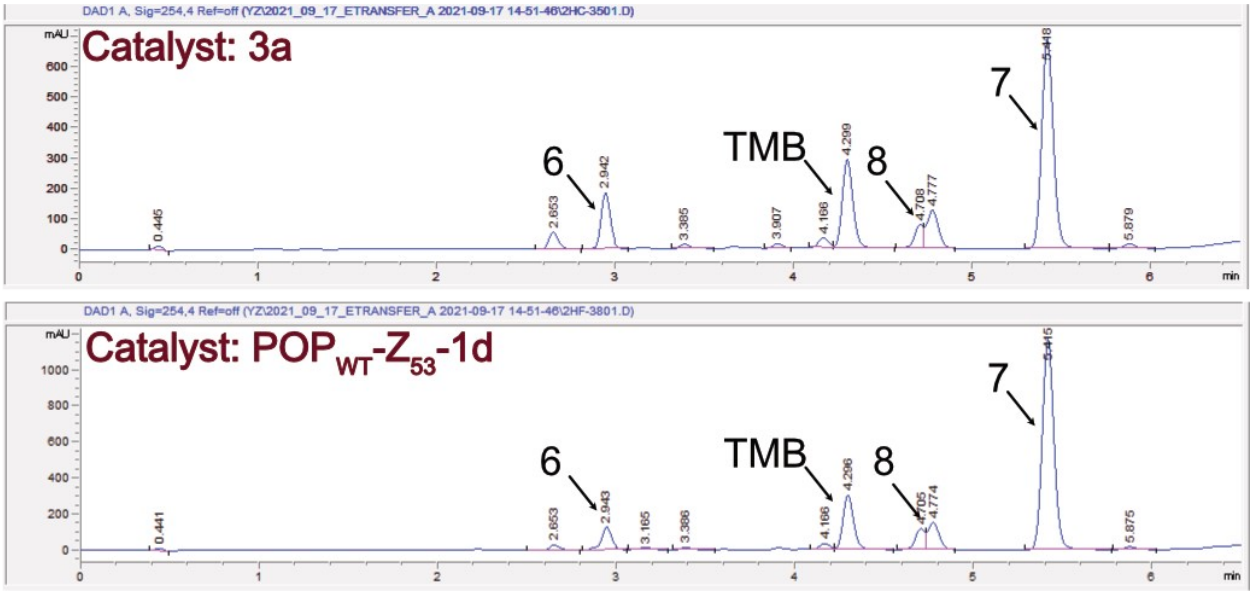

Supplementary Figure 55. Representative UHPLC Traces for [2+2] Cycloaddition Reactions.
Chromatograms of 240-minute reactions from time course experiments (see Supplementary Figure 20). The internal standard TMB, substrate **6**, substrate **7**, and product **8** are labeled on each trace. Product **8** eluted as a mixture of diastereomers with overlapping peaks. The integrations of both peaks were combined to determine total yield using this shorter method.

Since product **8** eluted as overlapping diastereomeric peaks, a longer method was developed to determine the d.r. of reactions more accurately. For longer UHPLC analysis, a 15cm Eclipse Plus C18 column was used. The mobile phase consisted of A: H_2O + 0.1% TFA, B: ACN + 0.1% TFA. Method: 1 minute at 10% B, 10% B to 90% B over 34 minutes, 5 minutes at 90% B, and a 3-minute post-time. A flow rate of 1.0 µL per minute was used. 5.0 µL of each sample was injected and elution of compounds was followed by monitoring absorbance at 254 nm (Supplementary Figure 21).

Plans for Custom Photoreactor
General Information
The custom photoreactor described here was built using 470 nm blue LEDS (VAOL-5GSBY4). Here, the schematics for the basic circuitry on the boards (Supplementary Figure 56), board layout (Supplementary Figure 57), and board layout with dimensions (Supplementary Figure 58) are shown.

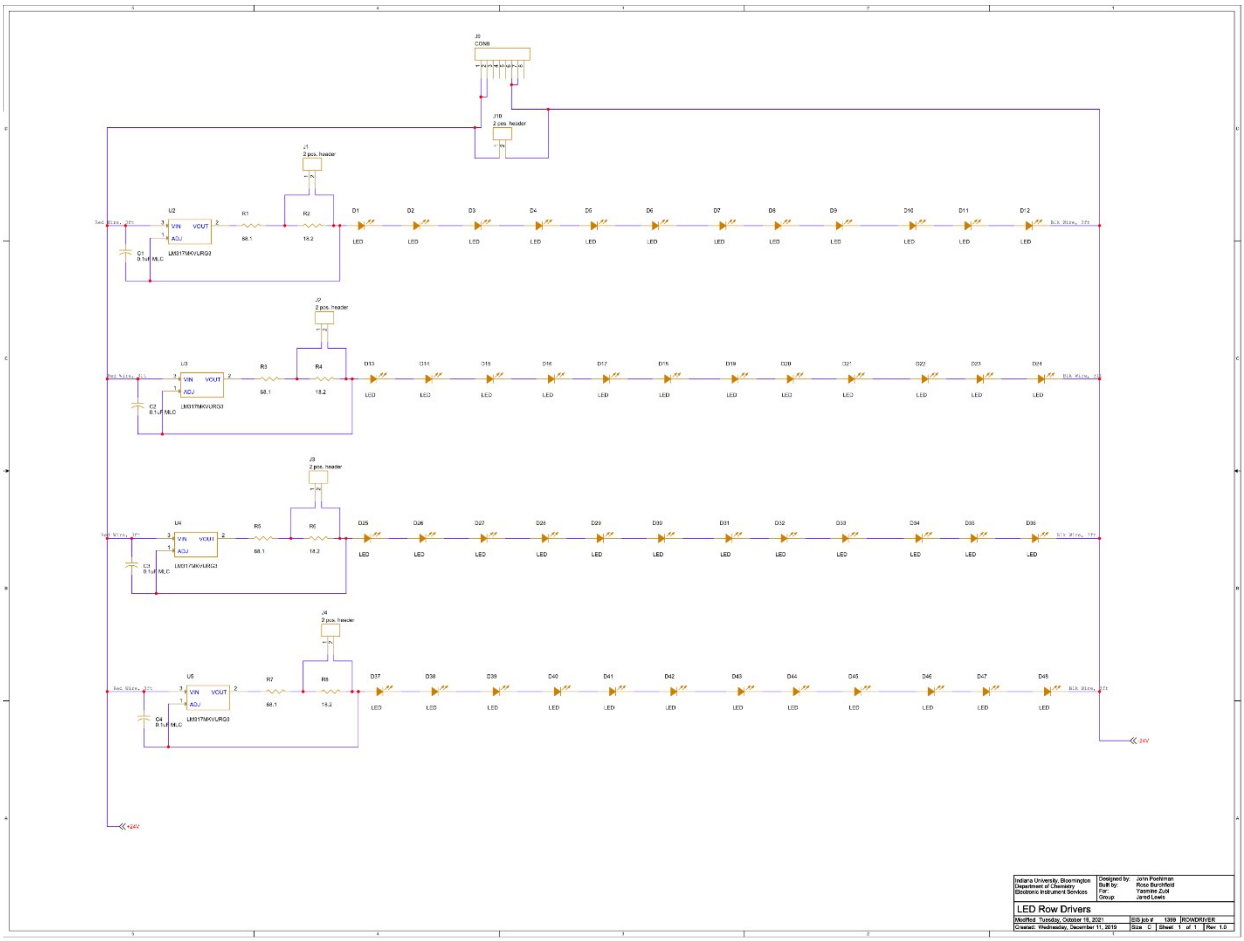

Supplementary Figure 56. Schematic for Basic Circuitry of LED Boards.

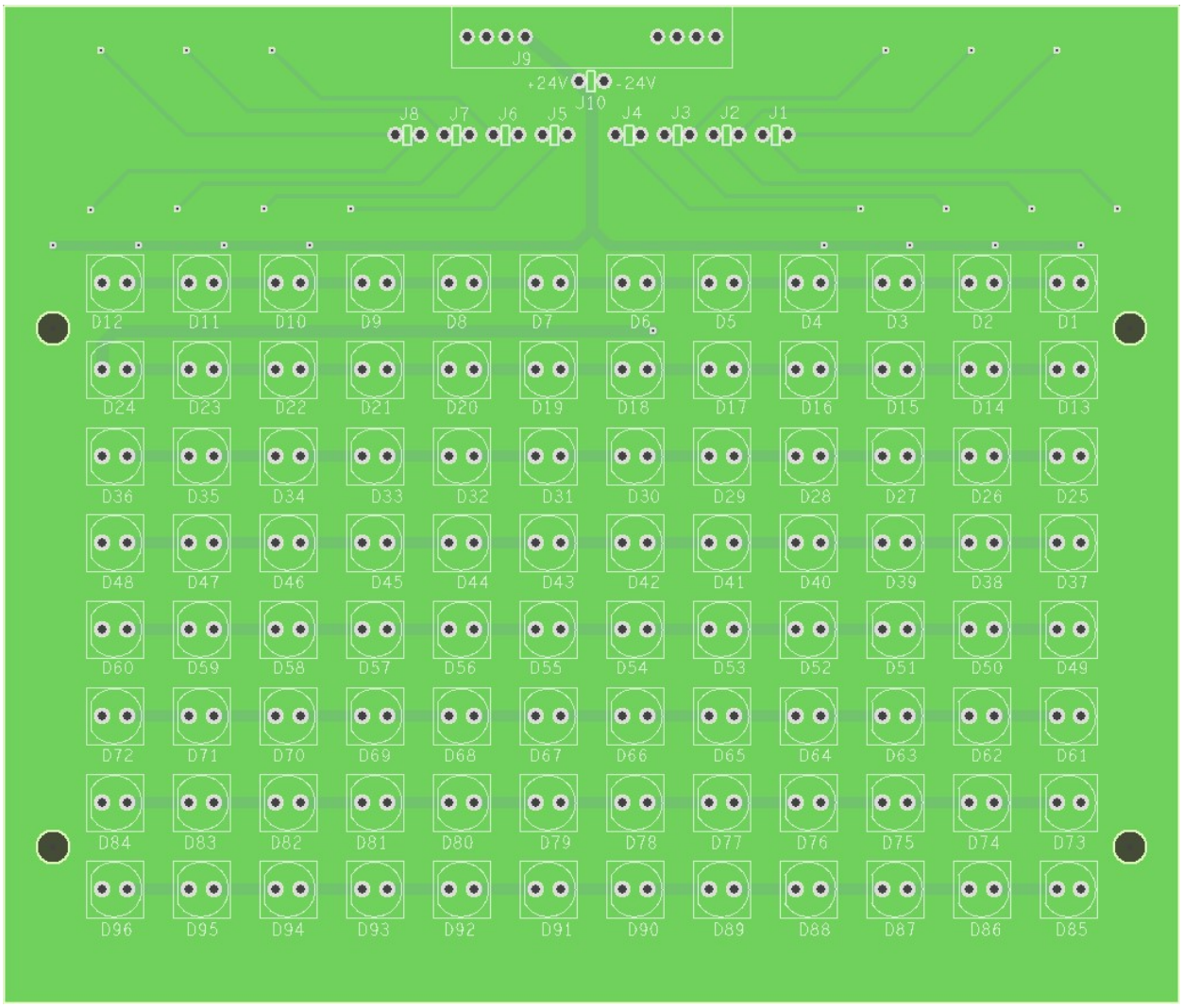

Supplementary Figure 57. LED Board Layout.

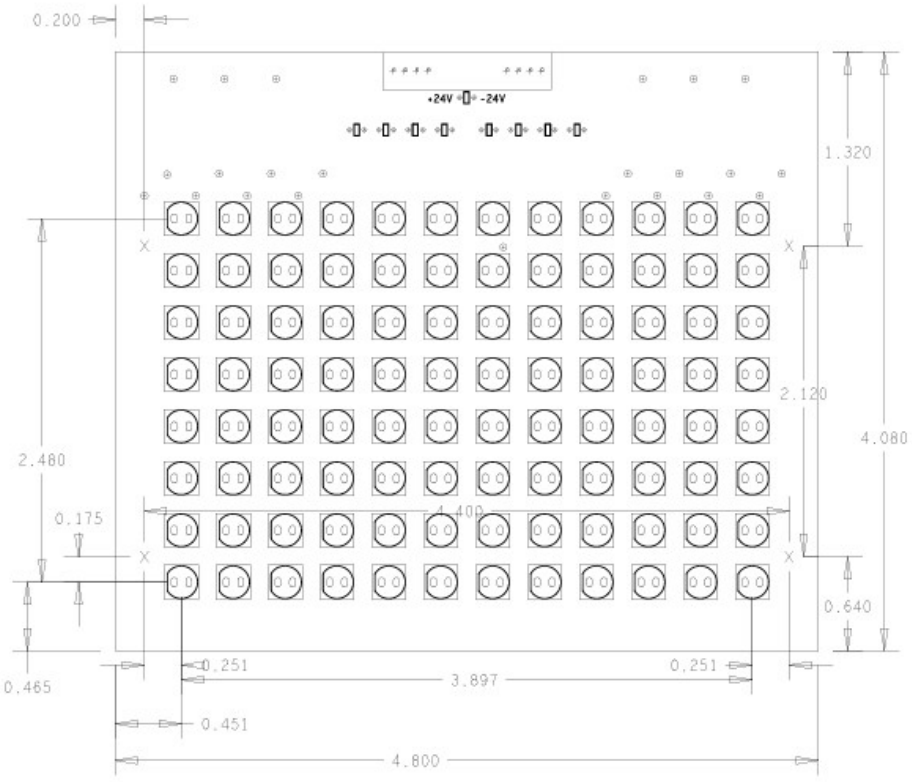

DRILL CHART: TOP to BOTTOM			
ALL UNITS ARE IN INCHES			
FIGURE	FINISHED_SIZE	PLATED	QTY
⊕	0.015	PLATED	23
○	0.035	PLATED	192
⊕	0.038	PLATED	18
⊕	0.038	PLATED	8
X	0.125	NON-PLATED	4
		TOTAL HOLES:	245

Supplementary Figure 58. LED Board Layout with Dimensions.

References

1 S. A. Archer, T. Keane, M. Delor, E. Bevon, A. J. Auty, D. Chekulaev, I. V. Sazanovich, M. Towrie, A. J. H. M. Meijer and J. A. Weinstein, *Chem. – A Eur. J.*, 2017, **23**, 18239–18251.

2 Y. Kobayashi, M. Hoshino, T. Kameda, K. Kobayashi, K. Akaji, S. Inuki, H. Ohno and S. Oishi, *Inorg. Chem.*, 2018, **57**, 5475–5485.

3 L. Wang, H. Yin, M. A. Jabed, M. Hetu, C. Wang, S. Monro, X. Zhu, S. Kilina, S. A. McFarland and W. Sun, *Inorg. Chem.*, 2017, **56**, 3245–3259.

4 J. Yin and R. L. Elsenbaumer, *Inorg. Chem.*, 2007, **46**, 6891–6901.

5 W. Zhang, B. Li, H. Ma, L. Zhang, Y. Guan, Y. Zhang, X. Zhang, P. Jing and S. Yue, *ACS Appl. Mater. Interfaces*, 2016, **8**, 21465–21471.

6 D. Tzalis and Y. Tor, *J. Am. Chem. Soc.*, 1997, **119**, 852–853.

7 E. E. Beauvilliers and G. J. Meyer, *Inorg. Chem.*, 2016, **55**, 7517–7526.

8 J. E. Collins, J. J. S. Lamba, J. Christopher Love, J. E. McAlvin, C. Ng, B. P. Peters, X. Wu and C. L. Fraser, *Inorg. Chem.*, 1999, **38**, 2020–2024.

9 M. B. Richardson, D. B. Brown, C. A. Vasquez, J. W. Ziller, K. M. Johnston and G. A. Weiss, *J. Org. Chem.*, 2018, **83**, 4525–4536.
10 J. Du, L. R. Espelt, I. A. Guzei and T. P. Yoon, *Chem. Sci.*, 2011, **2**, 2115–2119.
11 E. M. Sherbrook, H. Jung, D. Cho, M.-H. Baik and T. P. Yoon, *Chem. Sci.*, 2020, **11**, 856–861.
12 O. Trott and A. J. Olson, *J. Comput. Chem.*, 2009, **31**, 455-461.
13 The PyMOL Molecular Graphics System, Version 2.5.0 Schrödinger, LLC.
14 K. Ellis-Guardiola, H. Rui, R. L. Beckner, P. Srivastava, N. Sukumar, B. Roux and J. C. Lewis, *Biochemistry*, 2019, **58**, 1616–1626.
15 M. D. Hanwell, D. E. Curtis, D. C. Lonie, T. Vandermeersch, E. Zurek and G. R. Hutchison, *J. Cheminformatics,* 2012, **4**, 17.
16 M. Biner, H. B. Buergi, A. Ludi and C. Roehr, *J. Am. Chem. Soc.*, 2002, **114**, 5197–5203.
17 Y. Shao, L. F. Molnar, Y. Jung, J. Kussmann, C. Ochsenfeld, S. T. Brown, A. T. B. Gilbert, L. V. Slipchenko, S. V. Levchenko, D. P. O'Neill, R. A. D. Jr, R. C. Lochan, T. Wang, G. J. O. Beran, N. A. Besley, J. M. Herbert, C. Y. Lin, T. Van Voorhis, S. H. Chien, A. Sodt, R. P. Steele, V. A. Rassolov, P. E. Maslen, P. P. Korambath, R. D. Adamson, B. Austin, J. Baker, E. F. C. Byrd, H. Dachsel, R. J. Doerksen, A. Dreuw, B. D. Dunietz, A. D. Dutoi, T. R. Furlani, S. R. Gwaltney, A. Heyden, S. Hirata, C.-P. Hsu, G. Kedziora, R. Z. Khalliulin, P. Klunzinger, A. M. Lee, M. S. Lee, W. Liang, I. Lotan, N. Nair, B. Peters, E. I. Proynov, P. A. Pieniazek, Y. M. Rhee, J. Ritchie, E. Rosta, C. D. Sherrill, A. C. Simmonett, J. E. Subotnik, H. L. W. III, W. Zhang, A. T. Bell, A. K. Chakraborty, D. M. Chipman, F. J. Keil, A. Warshel, W. J. Hehre, H. F. S. III, J. Kong, A. I. Krylov, P. M. W. Gill and M. Head-Gordon, *Phys. Chem. Chem. Phys.*, 2006, **8**, 3172–3191.
18 J. D. Chai and M. Head-Gordon, *Phys. Chem. Chem. Phys.*, 2008, **10**, 6615–6620.
19 V. A. Rassolov, J. A. Pople, M. A. Ratner and T. L. Windus, *J. Chem. Phys.*, 1998, **109**, 1223.
20 T. S. Young, I. Ahmad, J. A. Yin and P. G. Schultz, *J. Mol. Biol.*, 2010, **395**, 361–374.
21 K. L. Heckman and L. R. Pease, *Nat. Protoc.*, 2007, **2**, 924–932.
22 H. Liu and J. H. Naismith, *BMC Biotechnol.* 2008, **8**, 91.
23 H. Yang, A. M. Swartz, H. June Park, P. Srivastava, K. Ellis-Guardiola, D. M. Upp, G. Lee, K. Belsare, Y. Gu, C. Zhang, R. E. Moellering and J. C. Lewis, *Nat. Chem.*, 2018, **10**, 318-324.
24 D. M. Upp, R. Huang, Y. Li, M. J. Bultman, B. Roux and J. C. Lewis, *Angew. Chemie Int. Ed.*, 2021, DOI:10.1002/anie.202107982.
25 P. Srivastava, H. Yang, K. Ellis-Guardiola and J. C. Lewis, *Nat. Commun.*, 2015, **6**, 7789.
26 D. M. Arias-Rotondo and J. K. McCusker, *Chem. Soc. Rev.*, 2016, **45**, 5803–5820.
27 C. J. Breen, M. Raverdeau and H. P. Voorheis, *Sci. Reports*, 2016, **6**, 25769.
28 X. Chen, A. Agarwal and D. P. Giedroc, *Biochemistry*, 1998, **37**, 11152–11161.
29 T. Heuduk and J.C. Lee, *Proc. Natl. Acad. Sci. U. S. A.*, 1990, **87**, 1744–1748.
30 T. D. Pollard, *Mol. Biol. Cell*, 2010, **21**, 4061.
31 I. Jarmoskaite, I. Alsadhan, P. P. Vaidyanathan and D. Herschlag, *Elife*, 2020, **9**, 1–34.